THE *S. CEREVISIAE* TELOMERASE RNP: FROM ASSEMBLY TO ACTION

By
Evan P. Hass

A dissertation submitted to Johns Hopkins University in conformity with the requirements for the degree Doctor of Philosophy

Baltimore, Maryland
July 2017

Abstract

Telomeres, the protective end-caps of linear eukaryotic chromosomes, progressively shorten as cells divide and, in most eukaryotes, are lengthened by the ribonucleoprotein enzyme telomerase. The telomerase RNA — one of the two core subunits of telomerase — contains the template for reverse transcription of new telomeric repeats and serves as a scaffold for the telomerase RNP. In *Saccharomyces cerevisiae*, the telomerase RNA (TLC1) tolerates repositioning of several of its protein-binding sites and deletion of the sequences in between, suggesting that TLC1 acts as an organizationally flexible scaffold that need only tether together the various subunits of telomerase.

In *Saccharomyces cerevisiae*, telomerase is recruited to telomeres through two pathways. While the primary recruitment pathway has been studied extensively, the secondary pathway, which involves the Ku70/Ku80 heterodimer bound to TLC1, has remained poorly understood. I found that TLC1-bound Ku recruits telomerase to telomeres by binding to the telomeric silent chromatin protein Sir4. I also found that this pathway is inhibited by the negative regulators of telomerase, Rif1 and Rif2, which compete with Sir4 for binding to the telomere-binding protein Rap1. My research suggests that the Ku-mediated recruitment pathway serves a regulatory function and connects the Rif proteins with the primary telomerase-recruitment pathway.

TLC1 is also bound by the Sm_7 complex, which stabilizes the major isoform of TLC1. While the other TLC1-bound holoenzyme subunits, Est1 and Ku, retain their functions when repositioned in full-length TLC1, this has not been tested for Sm_7. By repositioning the Sm-site via circular permutation, I found that Sm_7 retains function at diverse positions within TLC1, suggesting that all RNA-bound subunits of telomerase are organizationally flexible modules. I also used Sm-site repositioning without circular permutation to show that Sm_7 defines the mature 3′ end of the major TLC1 isoform.

Lastly, I developed a novel technique, CRISPR-assisted RNA/RBP yeast (CARRY) two-hybrid, which combines the yeast two-hybrid assay with the *Streptococcus pyogenes* CRISPR machinery to study RNA-protein interactions. I found that CARRY two-hybrid can detect RNA-protein interactions with high specificity and sensitivity, and I used this assay to investigate regions of the TLC1 core required for binding TERT, the catalytic subunit of telomerase.

Thesis Advisor:	**Dr. David Zappulla**
Thesis Committee:	**Dr. Karen Beemon**
	Dr. Carol Greider
	Dr. John Kim
	Dr. Robert Schleif

Acknowledgements

First, I would like to thank my thesis advisor David Zappulla. Your lab has proved to be an ideal place for me to do my graduate training. Beyond the uncountable skills that I have learned under your mentorship, you have been incredibly supportive of me throughout my time here. Whether I was buried in time-sensitive reviewer experiments, having a rough week for personal reasons, or having just a normal week in lab, you have always struck an ideal balance of encouraging me but not pushing me harder than I needed, and I cannot thank you enough for that.

I would also like to thank my thesis committee: Professors Karen Beemon, Carol Greider, John Kim, and Bob Schleif. All four of you have helped mentor me in different ways throughout my graduate training and have given me invaluable advice on my career that I have no doubt will have a lasting impact on my trajectory as a scientist.

Next, I would like to thank my lab mates – Kevin, Rachel, Melissa, and Karen – for their kindness and support, both as scientists and as friends. Since I became the lone member of this lab in the final year of my PhD, I have become intimately aware of the fact that science is more fun when done together, in large part because of what wonderful lab mates you were while you were here. I learned so much from your mentorship and support, which has continued even after many of you have left the lab, and I look forward to our friendships lasting for years to come. I would also like to extend special thanks to members of the Beemon, Schleif, Cunningham, Kim, and DiRuggiero labs, who have often served as surrogate lab mates during my final year here.

Thank you also to my friends in the Biology Department and CMDB Program, especially Matt Brown, who have made my time living in Baltimore incredibly enjoyable. From CMDB Game Nights to department happy hours to just plain hanging out, you have all been wonderful companions throughout this process. I would also like to thank my a cappella group Boh Re Mi for providing me with both support and an outlet for the non-scientific passions that are such a big part of my life. I will miss you all dearly when I move on to my postdoc. Thank you also to

Mark Soloski and Mary Blue, two longtime friends from Baltimore, whose hospitality and support made moving to a new city so much easier on me than it otherwise would have been.

Most of all, however, I must thank my family: my sisters Robin and Julia, my brother-in-law Jason, my edibly adorable nephew Noah, and my wonderful-beyond-measure parents. Even as I venture far away from our home base of Boston, often coming back with confusing, jargon-filled scientific stories, I can always count on you to answer when I call and make time for me when I come home. I hate that my career has taken me away from home, but I plan to return as soon as I can. To my mom and dad: I literally cannot thank you enough for all your love and support. As a kid with ADHD, many parts of academics didn't always come easy to me, but you saw my love for science and understood what I needed to succeed. You nagged me when I was clearly dropping the ball, comforted me when I had convinced myself I was stupid, and tirelessly encouraged me to fulfill my potential. There is no question in my mind that, without your unconditional support and encouragement, I would not have the budding scientific career that I have now. So, thank you. I love you more than I can say.

Table of Contents

List of Figures and Tables

Chapter 1: Introduction to telomeres and telomerase

1.1: Telomeres, telomerase, and counteracting the end-replication problem

Telomeres are DNA-protein structures located at the ends of linear eukaryotic chromosomes. These regions contain repetitive DNA sequence – the specific repeat sequence varies between species – which, along with associated proteins, serves two principal functions. The first of these functions is to protect the natural ends of chromosomes from being recognized as broken DNA ends resulting from DNA damage, which the cell normally ligates together. This repair-resistant characteristic of telomeres is critical for genome stability. If two telomeres from different chromosomes are fused together, the resulting ligated chromosome can be torn apart in the subsequent round of cell division if its two centromeres are pulled to opposite poles of the dividing cell. This, in turn, sets off "breakage-fusion-bridge" cycles in which these broken chromosomes are fused to yet other chromosomes which themselves are torn apart by mitosis, resulting in runaway genomic instability (McClintock, 1942). Telomere-binding proteins prevent this from happening by shielding the DNA from double-strand break repair machinery, maintaining genome stability (Cervantes and Lundblad, 2002).

The second, and arguably more important, function of telomeres is to protect against the so-called "end-replication problem", an unavoidable loss of DNA sequence at the ends of linear chromosomes which, if left unchecked, can compromise the end-protection function of telomeres (Watson, 1972; Olovnikov, 1973). The end-replication problem stems from the fact that replicative DNA-dependent DNA polymerases can only lengthen existing nucleic acid strands with available 3′ hydroxyl groups, meaning that strand synthesis must be initiated with RNA primers, which can be polymerized *de novo*. While most of these primers are eventually replaced with DNA sequence by DNA polymerases starting further 5′ (with respect to the replicated strand) on the chromosome, the RNA primer at the 5′-most end of a newly synthesized DNA strand cannot be replaced, resulting in a small gap where the parent DNA strand remains uncopied. These gaps caused by the end-replication problem add up through multiple rounds of DNA replication, causing chromosomes to progressively shorten from the ends as cells divide.

Because telomeres only consist of repeated sequence and do not contain any genes, they serve as buffer regions where small amounts of sequence can be lost without any deleterious effects.

Despite the ability of telomeres to act as buffer zones for chromosome shortening, if lost telomeric sequence is not somehow regenerated, telomere length places a strict limit on how many times a cell can divide (Levy et al., 1992). After too many rounds of DNA replication, telomeres will eventually erode away almost entirely. This compromises the end-protection function of telomeres, causing natural chromosome ends to be recognized as damaged DNA and triggering a cell-cycle arrest known as senescence (Weinert and Hartwell, 1988; Abdallah et al., 2009). Thus, to counteract this problem, most eukaryotes use the enzyme telomerase to add new sequence onto the ends of telomeres (Greider and Blackburn, 1985). The telomerase core enzyme consists of two subunits: the catalytic protein subunit telomerase reverse transcriptase (TERT) and the noncoding telomerase RNA (Greider and Blackburn, 1989; Lingner et al., 1997). The telomerase RNA contains, among other features, a short single-stranded region that TERT uses to template the addition of new telomeric DNA repeats onto the 3′ ends of telomeres (Shippen-Lentz and Blackburn, 1990). The telomeric 5′ end is filled in by replicative DNA polymerases, and a small gap is again left at the end by the final RNA primer.

This unique relationship between telomerase and the proliferative capacity of cells makes the enzyme highly relevant to human health. Telomerase upregulation is found in over 90% of cancers (Shay and Bacchetti, 1997), and mutations in telomere maintenance machinery that result in telomere shortening underlie a family of degenerative genetic diseases collectively known as "telomere syndromes" (Armanios and Blackburn, 2012). To avoid these outcomes, cells must precisely regulate telomerase action at telomeres and maintain telomeres within a narrow range of lengths. Underpinning this process of telomere-length homeostasis is a complex molecular interplay between the subunits of the telomerase holoenzyme and the factors associated with telomeric DNA.

1.2: Telomeric silent chromatin and the Rif1 and Rif2 proteins

In order to protect telomeric DNA from degradation or from being recognized as damaged, cells package telomeric and subtelomeric regions with specialized chromatin complexes that can also help regulate telomerase recruitment and action at telomeres. In the budding yeast *Saccharomyces cerevisiae*, which has been the focus of my thesis research, telomere repeat tracts are ~300 base pairs long on average and consist of the irregular repeat sequence $C_{1\text{-}3}A/TG_{1\text{-}3}$ (Shampay et al., 1984), with the G-rich strand terminating in a 3′ overhang. This telomeric DNA is bound directly by three different factors: the protein Rap1 (Conrad et al., 1990; Wright et al., 1992), the Ku70/Ku80 heterodimer (Yku70/Yku80 in yeast or simply "Ku") (Martin et al., 1999; Roy et al., 2004), and the protein Cdc13 (Lin and Zakian, 1996; Nugent et al., 1996) (Figure 1-1). Rap1 binds specifically to double-stranded telomeric repeat DNA and Cdc13 to the single-stranded telomeric overhang. Ku plays a highly-conserved DNA end-binding function in the canonical non-homologous end-joining (c-NHEJ) pathway for double-strand break repair (Fisher and Zakian, 2005) but paradoxically does not initiate repair when bound to telomeric DNA. All three of these factors contribute to the end-protection (or "capping") function of telomeres in different ways (Weinert and Hartwell, 1988; Nugent et al., 1996; Gravel et al., 1998; Polotnianka et al., 1998; Bertuch and Lundblad, 2004; Marcand et al., 2008; Bonetti et al., 2010). Cdc13 also plays an important role in recruiting telomerase to telomeres (discussed below), while Rap1 and Ku recruit other factors that protect telomeres and regulate telomerase.

One complex recruited to telomeres by Rap1 and Ku is the Sir2/3/4 transcriptional silencing complex. The structural components of the complex, Sir3 and Sir4, both interact with the Rap1 C-terminal domain (CTD), while Sir4 also binds Ku (Moretti et al., 1994; Tsukamoto et al., 1997; Roy et al., 2004). Once this complex is recruited to telomeres, it has been proposed that Sir3 and Sir4 dimerization recruits more Sir2/3/4 complexes, which then spread into subtelomeric regions by binding to histone tails, which Sir2 deacetylates (Luo et al., 2002), causing transcriptional silencing of telomere-proximal genes (Gottschling et al., 1990). Despite the fact

that the initial recruitment of the Sir2/3/4 complex to telomeres can occur through the Rap1 CTD or through Ku, both are required for telomeric silencing (Moretti et al., 1994; Boulton and Jackson, 1998).

In addition to Sir3 and Sir4, the Rap1 CTD also binds to the proteins Rif1 and Rif2 at telomeres. These four proteins have been shown to compete for binding to Rap1 (Hardy et al., 1992; Moretti et al., 1994; Wotton and Shore, 1997), though crystallographic data show that Rif2 can also bind the Rap1 CTD through a second, non-competitive interface (Shi et al., 2013). A large body of data suggests that, unlike the Sir2/3/4 complex, the major function of Rif1 and Rif2 at telomeres is to negatively regulate telomere lengthening (Hardy et al., 1992; Wotton and Shore, 1997). Of the 32 telomeres present in haploid yeast, only a small fraction are lengthened in a given cell cycle, and telomerase is preferentially recruited to and preferentially lengthens those which are among the shortest telomeres in a given cell (Teixeira et al., 2004; Bianchi and Shore, 2007; Sabourin et al., 2007). Though the detailed molecular mechanism for how cells sense telomere length and direct telomerase to shorter telomeres remains unclear, Rif1 and Rif2 have been heavily implicated in this process. Both *rif1*Δ and *rif2*Δ cells display telomere hyper-elongation phenotypes (Hardy et al., 1992; Wotton and Shore, 1997), and telomerase elongates telomeres more frequently in these cells than in wild type (Teixeira et al., 2004). Additionally, artificial tethering of Rif1, Rif2, or the Rap1 CTD to a telomere limits lengthening of said telomere proportional to the number of molecules tethered (Levy and Blackburn, 2004), and Rif2 and Rap1 have been shown to be depleted from short telomeres (Sabourin et al., 2007; McGee et al., 2010). Together, these data suggest a model in which telomere length is sensed by "counting" the number of Rif proteins bound to a telomere (Marcand et al., 1997; Levy and Blackburn, 2004; Teixeira et al., 2004; Bianchi and Shore, 2007). While it is clear why a shorter telomeric tract would bind fewer molecules of Rap1 and in turn bind fewer Rif proteins, the mechanism by which the Rif proteins negatively regulate telomere lengthening remains to be elucidated. It has, however, been shown that telomeres are more hyper-elongated in *rif1*Δ cells than in *rif2*Δ cells

and even more so in the *rif1*Δ *rif2*Δ double mutant than either single mutant (Wotton and Shore, 1997), suggesting that the two proteins do not negatively regulate telomere lengthening in precisely the same manner.

1.3: Structure and composition of the *S. cerevisiae* telomerase ribonucleoprotein complex

The largest subunit of the budding-yeast telomerase ribonucleoprotein (RNP) complex is the 1157-nucleotide telomerase RNA TLC1. TLC1 forms a Y-shaped secondary structure with three largely helical arms extending out from a conserved core region, with each arm containing a core-distal binding site for a protein subunit or subcomplex of the telomerase holoenzyme (Figure 1-1) (Dandjinou et al., 2004; Zappulla and Cech, 2004). The central core region contains four secondary-structure elements that are nearly universally conserved among telomerase RNAs: the core-enclosing helix (CEH), the template-boundary element (TBE), the single-stranded template, and the pseudoknot (Lin et al., 2004). The template and template-boundary element are directly involved in telomere-repeat addition (Singer and Gottschling, 1994; Tzfati et al., 2000), while the pseudoknot and core-enclosing helix have been implicated in binding TERT (Est2 in budding yeast) (Livengood et al., 2002; Chappell and Lundblad, 2004; Lin et al., 2004). These four secondary-structure elements are always found in the same conserved 5′-to-3′ order, and this arrangement is required for telomerase activity (Mefford et al., 2013). Connecting these four elements in the TLC1 core are four single-stranded junction regions. Junctions 1, 2, and 4 are part of an area of required connectivity (ARC) in the telomerase RNA core; disrupting RNA connectivity in these regions by repositioning the RNA 5′ and 3′ ends (also called circular permutation) abolishes telomerase activity *in vitro* and causes senescence *in vivo* (Mefford et al., 2013). Junction 4, which consists of only two nucleotides connecting the pseudoknot with the core-enclosing helix, seems to be especially important for telomerase activity, since deleting these two nucleotides causes a complete loss in telomerase function (Mefford et al., 2013). Though junction 4 is positioned directly between the two core elements implicated in TERT binding, it

remains unclear whether this junction is also required for TERT binding or whether it plays a role in function of the core enzyme once it is assembled.

In addition to its functions in the core telomerase enzyme, the telomerase RNA also acts as a flexible scaffold for the telomerase holoenzyme complex (Zappulla and Cech, 2006). However, unlike other noncoding RNAs that act as the central subunits of RNPs (e.g., ribosomal RNAs), telomerase RNAs are highly divergent, varying greatly in both size and sequence between species (Chen and Greider, 2004). Though secondary structure elements in the TLC1 RNA core are conserved, the sequences of these regions are only conserved among closely related yeast species (Tzfati et al., 2003; Dandjinou et al., 2004; Zappulla and Cech, 2004). Furthermore, while there are islands of conservation surrounding the protein-binding sites in the arms of TLC1, there is very little sequence conservation at all in the intervening regions of the arms (Zappulla and Cech, 2004). Indeed, it has been shown that these non-protein-binding parts of the arms — making up over half of TLC1 — are dispensable for telomerase function *in vivo* and *in vitro* (Zappulla et al., 2005). It has additionally been shown that these holoenzyme protein subunits that bind the arms of TLC1 retain their functions even when their binding sites are repositioned to dramatically different locations within the RNA (Zappulla and Cech, 2004; Zappulla et al., 2011; Mefford et al., 2013). These and other findings (Lebo and Zappulla, 2012) suggest strongly that TLC1 acts a flexible scaffold that, rather than holding its binding partners in a specific three-dimensional arrangement, need only tether the various RNA-bound holoenzyme protein subunits of telomerase to the catalytic core (Zappulla and Cech, 2006).

Of the telomerase holoenzyme subunits that are known to bind directly to TLC1, two play roles in recruitment of telomerase to telomeres (Est1 and Ku, discussed below), and one is involved in processing and stabilization of TLC1 RNA (Sm_7, also discussed below). The telomerase RNP also includes the protein Est3 (Hughes et al., 2000), which binds to TLC1 indirectly through interactions with Est2 and Est1 (Friedman et al., 2003; Talley et al., 2011; Tuzon et al., 2011), and the essential Pop1/6/7 complex has been reported to bind TLC1 at a

conserved sequence of previously unknown function (Lemieux et al., 2016). Although deleting *EST3* and the proposed Pop1/6/7 binding site in TLC1 both cause senescence (Lendvay et al., 1996; Laterreur et al., 2013; Lebo et al., 2015), it remains unclear what roles these proteins play in promoting lengthening of telomeres by telomerase.

1.4: *S. cerevisiae* telomerase is recruited to telomeres through two pathways

Of the several holoenzyme protein subunits of *S. cerevisiae* telomerase, two mediate recruitment of telomerase to telomeres. One of these two subunits is the protein Est1, the first telomerase subunit to be discovered in yeast (Lundblad and Szostak, 1989). Est1 mediates recruitment of telomerase to telomeres by binding to Cdc13 on the single-stranded telomeric overhang (Evans and Lundblad, 1999; Qi and Zakian, 2000). This recruitment pathway is essential for telomerase function *in vivo*; disrupting the pathway in any way results in a senescent phenotype that can be rescued by fusing Est2 directly to Cdc13 (Evans and Lundblad, 1999).

The second TLC1-bound factor that promotes recruitment to telomeres is the Ku heterodimer. In addition to, and independent of, the functions performed by DNA-bound Ku, the heterodimer binds specifically to a bulged hairpin structure in the TLC1 RNA, and deletion of this hairpin causes telomeres to initially shorten and then stabilize at a length ~70 base pairs shorter than wild type (Peterson et al., 2001; Stellwagen et al., 2003; Dalby et al., 2013). Additionally, it has been shown that TLC1 RNAs containing extra Ku-binding sites cause progressive telomere hyper-lengthening (Zappulla et al., 2011). Cells in which the Ku-binding site in TLC1 has been deleted also show greatly reduced Est2 enrichment at telomeres (Fisher et al., 2004) as well as decreased abundance (Zappulla et al., 2011) and nuclear localization of TLC1 RNA (Gallardo et al., 2008; Mozdy et al., 2008). However, increasing TLC1 RNA abundance in cells lacking the Ku-TLC1 interaction does not restore telomeres to wild-type length (Zappulla et al., 2011), and TLC1 nuclear localization can also be disrupted by deleting *EST1*, *EST2*, or *EST3* (Gallardo et al., 2008), implying that nuclear localization of TLC1 requires,

more generally, complete assembly of the telomerase RNP. This suggests that the primary function of TLC1-bound Ku is to recruit telomerase to telomeres. However, it has remained unclear how Ku promotes recruitment of telomerase to telomeres, especially given that DNA-bound Ku cannot also bind TLC1 RNA at the same time (Pfingsten et al., 2012).

In my thesis work, I discovered that Ku recruits telomerase to telomeres by binding to the telomere-associated protein Sir4. As stated above, Sir4 is a major component of telomeric silent chromatin previously reported to bind Ku (Tsukamoto et al., 1997; Roy et al., 2004), and though *sir4*Δ cells have been shown to have shortened telomeres, the cause of this phenotype had remained unclear prior to my work (Palladino et al., 1993; Askree et al., 2004; Gatbonton et al., 2006). My experiments show that Sir4 is required for TLC1-bound Ku to perform both its telomere-lengthening and telomerase-recruitment functions, and that tethering Sir4 directly to Ku-binding-defective TLC1 RNA restores telomeres to wild-type length. After having elucidated this mechanism, the purpose of the Ku-mediated recruitment pathway still remained unclear. Though this pathway has been suggested to increase the efficiency of the essential Est1-mediated recruitment pathway (Fisher et al., 2004; Williams et al., 2014), Ku-mediated recruitment is nonetheless neither necessary nor sufficient for telomerase function *in vivo*. In addressing this question, I found that the proteins Rif1 and Rif2 inhibit the Ku-Sir4-mediated recruitment pathway through their competition with Sir4 for binding to the Rap1 CTD. Taken together with what is known about the roles of Rif1 and Rif2 in telomere-length regulation, my findings suggest that the Ku-Sir4-mediated recruitment pathway acts as a regulatory intermediary that connects the telomere length-sensing Rif proteins with the essential Est1-mediated recruitment pathway, likely helping to direct telomerase recruitment to shorter telomeres.

1.5: The Sm_7 complex is required for proper biogenesis of TLC1 RNA

Though the majority of TLC1 RNA is 1157 nucleotides long, this is not the only form of TLC1 present in yeast cells. In addition to this major isoform of TLC1(poly(A)–), which is

present at ~30 molecules per cell in haploid yeast, there is also a polyadenylated form of TLC1 (poly(A)+), which is present at only ~1 molecule per cell on average (Chapon et al., 1997; Mozdy and Cech, 2006). Poly(A)+ TLC1 contains ~100 nucleotides more templated sequence beyond the 3′ end of poly(A)- TLC1 as well as a poly(A) tail (Chapon et al., 1997). Just six nucleotides 5′ of the poly(A)- TLC1 3′ end is the binding site for the Sm_7 complex (Seto et al., 1999), a conserved heteroheptameric complex that stabilizes many spliceosomal snRNAs and is required for several steps of snRNP biogenesis (Jones and Guthrie, 1990; Will and Luhrmann, 2001). Similar to its role in snRNPs, Sm_7 binding to TLC1 is required for stabilization of the poly(A)– isoform; mutating the Sm site in TLC1 (tlc1-Sm^-) results in complete loss of poly(A)– TLC1, leaving only the low-abundance poly(A)+ TLC1 RNA (Seto et al., 1999). Additionally, while senescent yeast strains start with normal growth and then progress through a small/mixed-colony-size phenotype before ceasing growth entirely, *tlc1-Sm*$^-$ cells do not completely stop growing, instead continuing to exhibit a small/mixed colony size phenotype (Seto et al., 1999). This unique "near-senescent" phenotype is likely due to the fact that there is, on average, only one molecule of poly(A)+ TLC1 RNA per cell. While some *tlc1-Sm*$^-$ cells will have fewer TLC1 molecules than average (i.e., zero) and senesce, other cells in the population will have just enough telomerase present to lengthen their critically short telomeres and make it through another cell division.

Since the discovery of Sm_7 binding to TLC1, several questions surrounding the function of Sm_7 in telomerase have remained unanswered. Firstly, of the three major TLC1-bound holoenzyme subunits, Sm_7 is the only one for which the aforementioned flexible scaffold model has not been fully tested. While it has been shown that Ku and Est1 both retain function when their binding sites are repositioned in full-length TLC1 (Zappulla and Cech, 2004; Zappulla et al., 2011), this has only been done for Sm_7 in the context of the Mini-T(460) allele of TLC1, in which all sequence in the bulk of the arms of TLC1 (i.e., other than the protein-binding sites) has been deleted (Mefford et al., 2013). Additionally, it remains unclear how Sm_7 stabilizes poly(A)-TLC1. It has been proposed that TLC1 is transcribed as the poly(A)+ form and undergoes

exosomal 3′-to-5′ degradation, which is stopped when the exosome encounters the Sm_7 complex, resulting in the formation of poly(A)- TLC1 (Seto et al., 1999; Coy et al., 2013). While nuclear exosome mutants have been shown to have increased abundance of poly(A)+ TLC1 (Coy et al., 2013), several aspects of this model, namely the idea that Sm_7 defines the 3′ end of poly(A)- TLC1, remain to be tested. This proposed model also reveals a larger unanswered question regarding the identity of the poly(A)- TLC1 precursor. While there is some evidence consistent with a model in which poly(A)+ is the precursor (Chapon et al., 1997), this is not the only possible precursor. TLC1 transcription can be terminated by the polyadenylation machinery to yield poly(A)+ TLC1 (Chapon et al., 1997), but it has been shown more recently that TLC1 transcription can also be terminated ~50 base pairs upstream of the polyadenylation signal by the Nrd1-Nab3-Sen1 (NNS) complex, resulting in unstable oligoadenylated TLC1 transcripts shorter than poly(A)+ TLC1 but still longer than poly(A)- TLC1 (Jamonnak et al., 2011; Noel et al., 2012). Both poly(A)+ TLC1 and these NNS-terminated TLC1 transcripts could in principle be processed to generate poly(A)- TLC1, but it remains unclear from which transcripts poly(A)- TLC1 is actually derived.

In my thesis work, I sought to answer these questions regarding both the nature of Sm_7 as an organizationally flexible module in the telomerase RNP and its function in biogenesis of TLC1. I found that Sm_7 retains its function of stabilizing poly(A)- TLC1 when the Sm site is repositioned in full-length TLC1 via circular permutation. This, along with the repositioning experiments performed previously with Est1 and Ku, demonstrates that all TLC1-bound holoenzyme protein subunits of telomerase behave as modules that can function irrespective of their position in the RNP. By repositioning the Sm site (without circular permutation of TLC1) to positions 5′ of its natural position, I also found that Sm_7 binding to TLC1 directs formation of the poly(A)- 3′ end. Lastly, I also sought to elucidate whether poly(A)+ TLC1 or NNS-terminated TLC1 transcripts are the unprocessed precursors of poly(A)- TLC1 by repositioning the Sm site further 3′, beyond the sites of NNS-mediated termination. While this experiment yielded results

consistent with a model in which only NNS-terminated TLC1 transcripts, not poly(A)+ TLC1, are processed to form poly(A)- TLC1, it is also possible that the repositioned Sm site was simply not functional at this position in the RNA due to improper folding of the site, ultimately leaving this question unanswered for now.

1.6: Inventing the "CARRY two-hybrid" method: a CRISPR-based yeast two-hybrid assay for RNA-protein interactions

RNA-binding proteins are critical for proper biogenesis and function of RNAs such as TLC1. While there are likely myriad RNA-protein interactions yet to be discovered, the techniques available for identifying such interactions are relatively few. The most commonly used techniques for identifying novel RNA-protein interactions do so in a protein-centric manner (i.e., asking the question "what RNAs bind to my protein of interest?") by pulling down a protein of interest from cell extracts and using high-throughput sequencing to identify the bound RNAs (McHugh et al., 2014). Similarly, most RNA-centric methods for identifying RNA-protein interactions (i.e., asking the question "what proteins bind to my RNA of interest?") involve pulling down an RNA of interest and identifying bound proteins by mass spectrometry. However, because mass spectrometry is not as sensitive as high-throughput sequencing, identifying the proteins that bind to a given RNA of interest can be especially challenging, and is limited to detecting only the most abundant RNA-protein complexes (McHugh et al., 2014).

While the repertoire of techniques available for identifying novel protein-protein interactions is also relatively limited, one technique that has been used widely both to study and to identify protein-protein interactions is the yeast two-hybrid assay (Fields and Song, 1989; Chien et al., 1991). In this assay, a protein of interest is expressed as a fusion to a DNA-binding domain in yeast, tethering the protein upstream of reporter genes that have been engineered into the yeast strain. A second protein of interest is then expressed fused to a transcriptional activation domain, effectively making expression of the reporter genes contingent on an interaction between

the two proteins of interest. Yeast two-hybrid can be used to test for interactions between specific pairs of proteins, or one can fuse a protein of interest to the DNA-binding domain and then screen a library of activation domain-fused proteins for interactions with the protein of interest.

To address the dearth of techniques for identifying proteins that bind to an RNA of interest, I developed CRISPR-assisted RNA/RBP yeast two-hybrid (CARRY two-hybrid), which uses the *Streptococcus pyogenes* CRISPR/Cas9 machinery to adapt the standard yeast two-hybrid system to assay for RNA-protein interactions. *S. pyogenes* Cas9 and its associated single guide RNA (sgRNA) are most often used in genome editing to make directed cuts at specific DNA sequences, which are recognized through base-pairing with the first 20 nucleotides of the sgRNA (Zhang et al., 2014). However, several groups have also used this machinery to target RNAs of interest to specific DNA loci by fusing an RNA of interest to the sgRNA 3′ end and using nuclease-dead Cas9 (dCas9) such that the complex will be targeted without cutting the DNA (Shechner et al., 2015; Zalatan et al., 2015). This same strategy is used in the CARRY two-hybrid system to tether an RNA of interest to the promoters of yeast two-hybrid reporter genes. Identical to traditional yeast two-hybrid, a potential binding protein is fused to a transcriptional activation domain, making reporter-gene expression contingent upon binding between the two hybrid molecules. After setting up this system, I used the well-characterized interaction between the bacteriophage MS2 RNA hairpin and MS2 coat protein to show that CARRY two-hybrid can detect RNA-protein interactions with high specificity and sensitivity.

Next, I used CARRY two-hybrid to investigate the interaction between yeast TERT (Est2) and the telomerase RNA (TLC1) core since the specific recognition elements involved in this interaction have not been fully elucidated. Using CARRY two-hybrid, I found that junction 4 is required for TLC1 to bind Est2, while junction 1 also plays an important role in TERT binding. Additionally, while it has been shown that disrupting pairing in the core-enclosing helix impairs TERT binding (Lin et al., 2004), the importance of this element for the Est2-TLC1 interaction has not been evaluated using a deletion of the core-enclosing helix (CEH) without disrupting the

aforementioned area of required connectivity (ARC). Using a circularly permutated TLC1 core, I showed that deleting the CEH without disrupting the ARC abolishes the interaction between TERT and TLC1, confirming that the CEH is a required part of the Est2 RNA binding site. The results of my experiments with the CARRY two-hybrid system suggest that it will prove to be a valuable tool for identifying proteins that bind to specific RNAs of interest.

Figure 1-1: The telomerase RNP and telomeric chromatin in *S. cerevisiae*.

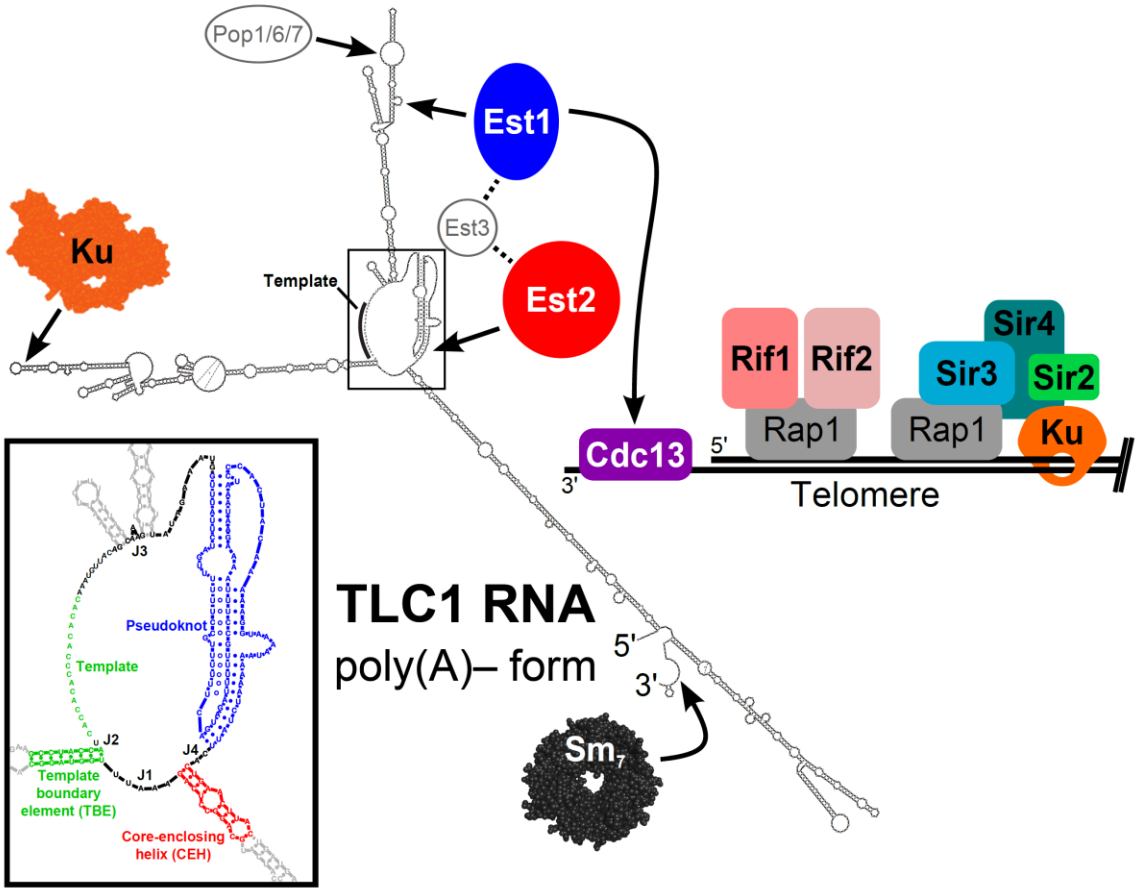

The secondary structure of poly(A)– TLC1 shown here is based on previously published models (Zappulla and Cech, 2004; Niederer and Zappulla, 2015). Ku, Est1, Est2, Sm_7, and Pop1/6/7 bind TLC1, while Est3 associates with Est1 and Est2. The structures shown of Ku and Sm_7 are of the human and yeast complexes, respectively (Walker et al., 2001; Plaschka et al., 2017). An enlarged view of the boxed TLC1 core region is shown at bottom left, highlighting the four conserved secondary structure elements of telomerase RNA cores and the single-stranded junction regions. A diagram summarizing the proteins bound to telomeres is shown at right with Rap1, Ku, Rif1, Rif2, and the Sir2/3/4 complex bound to the double-stranded region of telomeric DNA and Cdc13 bound to the single-stranded 3′ overhang. Cdc13 recruits telomerase to telomeres through its interaction with Est1.

Chapter 2: Ku binds Sir4 to recruit telomerase to telomeres and is inhibited by Rif1 and Rif2

Partially adapted from:

Evan P. Hass and David C. Zappulla. 2015. The Ku subunit of telomerase binds Sir4 to recruit telomerase to lengthen telomeres in S. cerevisiae. *ELife*.

2.1: Introduction

Ku binds telomerase RNA both in yeast (Peterson et al., 2001; Stellwagen et al., 2003; Dalby et al., 2013) and in humans (Ting et al., 2005). In *S. cerevisiae*, Ku binds to the tip of a 74-nt hairpin in the 1157-nt telomerase RNA, TLC1 (Figure 2-1) (Peterson et al., 2001; Stellwagen et al., 2003; Dandjinou et al., 2004; Zappulla and Cech, 2004; Dalby et al., 2013). In cells where the tip of this hairpin is deleted (*tlc1*Δ*48*), telomeres shorten by ~70 base pairs (Peterson et al., 2001; Stellwagen et al., 2003; Zappulla et al., 2011). This defect can be mostly rescued by inserting a Ku-binding hairpin at other locations within the mutant tlc1Δ48 RNA, whereas inserting additional Ku-binding hairpins into wild-type TLC1 causes progressive telomere hyper-elongation (Zappulla et al., 2011). Lack of Ku binding to TLC1 has also been reported to reduce nuclear localization of TLC1 (Gallardo et al., 2008) and recruitment of telomerase to telomeres (Fisher et al., 2004). Telomerase is also recruited to telomeres by the protein Est1, which mediates recruitment through an interaction with the single-stranded telomeric DNA binding protein Cdc13 (Evans and Lundblad, 1999; Qi and Zakian, 2000). In contrast to Est1, the mechanism by which Ku recruits telomerase to telomeres has yet to be elucidated.

An initial working model for Ku-mediated telomerase recruitment to telomeres was that TLC1-bound Ku simply recruits telomerase to telomeres by also binding telomeric DNA (Peterson et al., 2001; Fisher and Zakian, 2005). However, this model has been largely discounted by *in vitro* binding experiments showing that purified Ku cannot bind DNA and RNA concurrently (Pfingsten et al., 2012). It therefore seemed likely that Ku recruits telomerase to telomeres by interacting with a telomere-associated protein. Such a protein must bind Ku and associate with telomeres. Knowing that Ku also plays a role in the formation of telomeric silent chromatin, I chose to investigate its binding partner in this process, the protein Sir4, as a possible candidate. Sir4 associates with telomeres, and an interaction between Sir4 and Ku has been reported previously (Tsukamoto et al., 1997; Roy et al., 2004). Additionally, *sir4*Δ cells have

been shown to have shortened telomeres (Palladino et al., 1993; Askree et al., 2004; Gatbonton et al., 2006), though the cause of this phenotype has remained apparently unexplored.

In this chapter, I provide genetic evidence suggesting that *SIR4* and TLC1-bound Ku promote telomere lengthening through the same pathway and that *SIR4* is required for Ku-mediated telomere lengthening. In contrast, the negative regulators of telomerase, Rif1 and Rif2, which compete with Sir3 and Sir4 for binding to Rap1 (Moretti et al., 1994; Wotton and Shore, 1997), appear to inhibit Ku-mediated telomere lengthening. By measuring telomerase recruitment to telomeres by chromatin immunoprecipitation, I find that a TLC1 RNA containing three Ku-binding sites, TLC1(Ku)$_3$, causes increased telomerase recruitment in wild-type cells. Furthermore, *sir4*Δ cells display a defect in telomerase recruitment indistinguishable from that of *tlc1*Δ*48* cells, even when expressing TLC1(Ku)$_3$. Finally, I show that tethering Sir4 directly to tlcΔ48 RNA restores telomeres to wild-type length, while tethering Sir3 to tlc1Δ48 does not. Together, these results suggest that Ku recruits telomerase to telomeres through its interaction with Sir4 and that this recruitment pathway is counterbalanced by Rif1 and Rif2.

2.2: Results

Ku, *SIR4*, and the *TLC1* Ku-binding site promote telomere lengthening through the same pathway

Although the exact mechanism of Ku-mediated telomerase recruitment remains unclear, a simple model is that Ku recruits telomerase to telomeres by binding a telomere-bound protein. The telomeric silent chromatin protein Sir4 is an attractive candidate for playing this role, since it has been shown to bind Ku and because *sir4*Δ cells have telomeres 50–150 bp shorter than wild type (Palladino et al., 1993; Gatbonton et al., 2006), a phenotype similar to the ~70-bp reduction seen in *tlc1*Δ*48* cells (Peterson et al., 2001; Stellwagen et al., 2003; Zappulla et al., 2011). As a first test of the hypothesis that *SIR4* is involved in Ku's function as a telomerase subunit, I accurately measured the length of telomeres in *sir4*Δ cells and *tlc1*Δ*48* cells, as well as *sir4*Δ

*tlc1*Δ*48* double-mutants. I found that telomeres in *tlc1*Δ*48* cells were 85 ± 23 bp shorter than wild type while those in *sir4*Δ cells were 53 ± 13 bp shorter than wild type (Figure 2-2A, Table 2-1). When these two mutations were combined to make a double-mutant strain, telomeres were 71 ± 26 bp shorter than wild type, a telomere length defect very similar to that of the *tlc1*Δ*48* single-mutant ($p = 0.31$). This genetic epistasis suggests that *SIR4* promotes telomere lengthening in the same pathway as TLC1-bound Ku.

To test if this result is, in fact, indicative of related function in telomere length maintenance between *TLC1*, *Ku*, and *SIR4*, and not simply between *TLC1* and *SIR4*, I performed a similar genetic epistasis experiment with *sir4*Δ and *yku80*Δ mutants. Similar to what has been reported previously, I observed that *yku80*Δ cells supported telomeres 220 ± 14 bp shorter than wild type (Figure 2-2B) (Gravel et al., 1998; Askree et al., 2004; Gatbonton et al., 2006). However, while deleting *SIR4* resulted in a ~70-bp telomere-length defect in a wild-type background, it appeared to have little effect on telomere length in a *yku80*Δ background; telomeres in *sir4*Δ *yku80*Δ cells were 193 ± 19 bp shorter than wild type. None of the strains in these experiments senesced (data not shown), and telomeres have been reported to shorten by as much as ~260 bp in other mutants without causing senescence (Lebo and Zappulla, 2012). Thus, the lack of further telomere shortening in the *sir4*Δ *yku80*Δ double-mutant strain relative to *yku80*Δ is not explained by telomeres already being the shortest-possible length supporting cell growth. These findings suggest that Ku is involved in the same telomere length-maintenance pathway as *SIR4*.

Telomere hyper-lengthening by telomerase RNA with extra Ku-binding sites is *SIR4*-dependent

Inserting an extra Ku-binding hairpin into TLC1 causes progressive telomere hyper-lengthening (Zappulla et al., 2011). Furthermore, my advisor, David Zappulla, has generated a telomerase RNA, TLC1$(Ku)_3$, that contains extra Ku-binding hairpins inserted at positions 446

and 1029.This TLC1(Ku)$_3$ telomerase RNA accumulates to essentially the same level (93 ± 9%) as wild-type TLC1 (discussed below, see Figure 2-6). If *SIR4* is required for Ku's function in maintaining telomere length as a telomerase subunit, deleting *SIR4* should prevent TLC1 alleles with extra Ku-binding hairpins from causing telomere hyper-lengthening. I passaged *TLC1(Ku)$_3$* cells in liquid culture and assessed telomere length over time. TLC1(Ku)$_3$ caused progressive telomere hyper-lengthening over the course of passaging in addition to some telomere shortening (Figure 2-3A), similar to TLC1 RNAs with two Ku-binding sites (Zappulla et al., 2011). I also probed the Southern blot from Figure 2-3A for Y′ telomeric restriction fragments and determined that telomeres in *TLC1(Ku)$_3$* cells range from ~70 bp shorter than wild type to ~1000 bp longer after 220 generations, continuing to progressively elongate at a rate of ~5 bp/generation (Figure 2-4A). This increasingly heterogeneous distribution of telomere lengths in *TLC1(Ku)$_3$* cells could be due to diverse telomere lengths in the population of cells or an abnormality of telomeric DNA structure affecting how it migrates on gels (e.g., extremely long single-stranded tails). To differentiate between these possibilities, I plated the liquid culture-passaged cells for single colonies, and found that telomeres from these clonal isolates were subsets of the heterogeneous liquid-cultured population (Figure 2-5), a behavior of telomeres that has been reported previously (Shampay and Blackburn, 1988; Levy and Blackburn, 2004). These results show that the wide variety in the relative mobility of telomeric restriction fragments in the gel is due to a broad distribution of telomere lengths from the population of cells.

Next, I tested if telomere hyper-lengthening caused by TLC1(Ku)$_3$ is dependent on *SIR4*. Whereas TLC1(Ku)$_3$ caused a combination of telomere hyper-lengthening and shortening in a wild-type *SIR*4 strain, it did not cause any hyper-elongation in *sir4*Δ cells (Figure 2-3B). The average telomeres supported by TLC1(Ku)$_3$ in a *sir4*Δ strain were 148 ± 36 bp shorter than those in wild-type *TLC1 SIR4* cells (Table 2-1). This inability of TLC1(Ku)$_3$ to cause telomere hyper-lengthening without *SIR4* provides further evidence that Sir4 is required for telomerase RNA-bound Ku to promote telomere lengthening in yeast. I also tested whether the other two members

of the Sir2/3/4 complex, Sir2 and Sir3, were required for Ku-mediated telomere lengthening. I observed similar results in *sir2*Δ and *sir3*Δ cells, which, like *sir4*Δ cells, completely lack telomeric silencing, although telomeres supported by TLC1(Ku)$_3$ in these backgrounds were not quite as short as those supported by TLC1(Ku)$_3$ in a *sir4*Δ background (Figure 2-3C, Table 2-1). Of the three members of the Sir2/3/4 complex, only Sir4 has been identified as a binding partner for Ku by screening a two-hybrid library (Tsukamoto et al., 1997; Roy et al., 2004). Deleting *SIR2* or *SIR3* likely affects Ku-mediated telomere lengthening indirectly by substantially, but not completely, removing Sir4 from telomeres (Hoppe et al., 2002).

In addition to promoting telomere lengthening, Ku binding to TLC1 is also known to increase telomerase RNA abundance (Mozdy and Cech, 2006; Zappulla et al., 2011). To test if the telomere-length phenotypes I observed are a function of RNA abundance, I assessed telomerase RNA levels by northern blotting. I found that deleting the 48-nt Ku-binding site in TLC1 (tlc1Δ48) reduced RNA abundance to 61 ± 22% the level of wild type, similar to what has been reported (Figure 2-6) (Zappulla et al., 2011). In contrast to TLC1 RNAs with two Ku-binding sites, which exhibit a ~20% increase in telomerase RNA abundance (Zappulla et al., 2011), TLC1(Ku)$_3$ showed little change relative to wild type (93 ± 9%). Although *sir4*Δ cells display a telomere-length defect very similar to *tlc1*Δ*48* cells, telomerase RNA abundance did not decrease in *sir4*Δ cells relative to wild type; in fact, it increased ~2-fold in *sir4*Δ cells and ~1.5-fold in *sir4*Δ *tlc1*Δ*48* cells, and remained near wild-type levels in *sir4*Δ *TLC1(Ku)$_3$* cells. These results suggest that the telomere-length phenotypes shown in Figure 2-3 are not caused by decreased telomerase RNA abundance.

Ku-mediated telomere lengthening is inhibited by Rif1 and Rif2

In the process of identifying proteins involved in Ku-mediated telomere lengthening, I tested the effects of tlc1Δ48 and TLC1(Ku)$_3$ on telomere length in cells lacking Rif1 or Rif2, negative regulators of telomerase that bind to the same region of Rap1 as Sir3 and Sir4 (Hardy et

al., 1992; Wotton and Shore, 1997; Teng et al., 2000). As shown previously, I found that both *rif1*Δ and *rif2*Δ cells have hyper-elongated telomeres (Figures 2-3 and 2-4). Notably, I found that after ~250 generations of passaging, tlc1Δ48 had caused telomeres to shorten by ~500 bp in *rif1*Δ and *rif2*Δ cells, and after ~650 generations of passaging, this deficit had grown to ~1000 bp (Figure 2-7, compare lanes 10 and 24 to 17 and 31). This is a substantially greater effect than the ~70-bp decrease caused by tlc1Δ48 in a wild-type background, and it suggests that Rif1 and Rif2 inhibit Ku-mediated telomere lengthening. When I introduced TLC1(Ku)$_3$ into *rif1*Δ or *rif2*Δ cells, some telomeres became further hyper-elongated and others became shorter, suggesting that TLC1-bound Ku does not require Rif1 or Rif2 to promote telomere lengthening, in contrast to the requirement I identified for Sir4 as well as Sir2 and Sir3 shown in Figure 2-3.

Ku binds Sir4 *in vitro*

A binding interaction between Ku and Sir4 has been reported previously through yeast two-hybrid forward-genetic screens and by co-immunoprecipitation from yeast cell extracts (Tsukamoto et al., 1997; Roy et al., 2004). Using yeast two-hybrid, the N- and C-termini of Sir4 have been shown to interact with Yku80 and Yku70, respectively, and two different regions of Yku80 have been shown to be important for binding Sir4 (Tsukamoto et al., 1997; Roy et al., 2004; Ribes-Zamora et al., 2007). However, these studies do not rule out the possibility that Ku and Sir4 could be interacting indirectly, bridged by another yeast protein. Using purified yeast Ku heterodimer provided by the Cech lab (Pfingsten et al., 2012; Dalby et al., 2013), I tested for the Ku-Sir4 interaction *in vitro*. [^{35}S]-Sir4 was synthesized by using a rabbit reticulocyte lysate transcription/translation system (RRL) spiked with 35S-methionine. Prior to Sir4 protein synthesis, purified Ku heterodimer (Yku80-Myc•Yku70) was also added to the lysate. After Sir4 protein synthesis, Ku was then immunoprecipitated by anti-myc affinity pull-down. The input, unbound supernatant, and bound fraction were resolved on a gel and subjected to autoradiography. As shown in Figure 2-8, when Ku heterodimer was omitted from this procedure,

a trace amount of radioactive Sir4 was recovered in the bound fraction, indicating a small amount of non-specific Sir4 binding the beads, and when Sir4 template DNA was omitted, no bands were detected. However, when both Ku and Sir4 template DNA were present in the RRL, ~5-fold more radioactive Sir4 was recovered in the bound fraction than in the no-Ku control, providing evidence for a direct interaction between the Ku heterodimer and Sir4. To test if this protein-protein interaction was specific, I repeated this experiment with Ku heterodimer that had been boiled before being added to the RRL. In this condition, only trace amounts of Sir4 were recovered in the bound fraction, similar to what was observed when Ku was omitted altogether. These results indicate that Sir4 participates in a specific protein-protein interaction with the Ku heterodimer, as has been suggested by previous *in vivo* experiments.

SIR4 is required for Ku-mediated telomerase recruitment to telomeres

Having shown that *SIR4* is required for TLC1-bound Ku to promote telomere lengthening, I next tested if *SIR4* is also required for Ku-mediated telomerase recruitment. I assessed the level of telomerase recruitment to telomeres in wild-type and *sir4*Δ cells expressing either TLC1, tlc1Δ48, or TLC1(Ku)$_3$ by performing chromatin immunoprecipitation (ChIP) on myc-tagged telomerase catalytic subunit, TERT (Est2). Quantitative real-time PCR (qPCR) was then used to quantify the enrichment of a telomere-proximal locus relative to a telomere-distal control locus (Sabourin et al., 2007). I assayed for telomerase recruitment at telomeres VI-R and XV-L and observed highly similar results for both of these chromosome ends (Figure 2-9). I observed that TERT enrichment at these telomeres in *tlc1*Δ*48* cells was reduced to 15% of wild type, similar to what has been reported previously (Fisher et al., 2004). In contrast, there was a ~10-fold increase in TERT at telomeres in *TLC1(Ku)$_3$* cells relative to wild type. However, in a *sir4*Δ background, enrichment of TERT at telomeres was decreased relative to wild type, regardless of which *TLC1* allele was expressed. The level of TERT at telomeres in *sir4*Δ *TLC1* and *sir4*Δ *tlc1*Δ*48* cells was reduced to 15% of wild type, and this is indistinguishable from what

was observed in *SIR4 tlc1*Δ*48* cells ($p = 0.80$ and $p = 0.91$, respectively). In *sir4*Δ *TLC1(Ku)*$_3$ cells, telomeric TERT enrichment was decreased to 35% the level of wild type, which is also similar to my observations in *SIR4 tlc1*Δ*48* cells ($p = 0.11$). These telomerase recruitment results suggest strongly that *SIR4* is required for Ku-mediated telomerase recruitment to telomeres.

I also performed ChIP for TERT in *sir3*Δ and *sir2*Δ backgrounds. Compared to wild-type cells, TERT enrichment at telomeres was reduced to 16% in *sir3*Δ *TLC1* cells, to 12% in *sir3*Δ *tlc1*Δ*48* cells, and to 39% in *sir3*Δ *TLC1(Ku)*$_3$ cells (Figure 2-9), similar to my observations in *sir4*Δ cells described above. TERT enrichment at telomeres was also decreased in a *sir2*Δ background relative to wild type but not as extensively as in a *sir3*Δ or *sir4*Δ background. In *sir2*Δ cells expressing TLC1, tlc1Δ48, or TLC1(Ku)$_3$, TERT enrichment at telomeres was reduced to 44%, 21%, or 86% of wild type, respectively. These data suggest that Sir3, and to a lesser degree Sir2, are also important for Ku-mediated telomerase recruitment to telomeres in addition to Sir4.

Sir4 binding to telomeres is promoted by Sir2 and Sir3 and inhibited by Rif1 and Rif2

I have shown that Sir2 and Sir3 are important for Ku-mediated telomere lengthening and telomerase recruitment, but, unlike Sir4, neither Sir2 nor Sir3 has been shown to bind Ku. The simplest explanation is that Sir2 and Sir3 affect Ku-mediated telomerase recruitment indirectly through altering Sir4 association with telomeres, particularly since the amount of telomere-bound Sir4 has been shown to decrease greatly, but not completely, in the absence of Sir2 or Sir3 (Hoppe et al., 2002). I have also shown that the proteins Rif1 and Rif2 function to inhibit Ku-mediated telomere lengthening. Because Rif1 and Rif2 compete with Sir3 and Sir4 for binding to Rap1 (Moretti et al., 1994; Wotton and Shore, 1997), this inhibition of Ku-mediated telomere lengthening could be explained by there being more Sir4 bound to telomeres in the absence of Rif1 or Rif2. To test this hypothesis, I performed ChIP on myc-tagged Sir4 in *rif1*Δ and *rif2*Δ cells as well as in *sir2*Δ and *sir3*Δ cells and used real-time quantitative PCR to measure fold

telomeric enrichment. Similar to what has been shown previously, I observed that Sir4 telomeric enrichment was decreased in *sir2*Δ and *sir3*Δ cells, to 26% and 17% of wild-type levels, respectively (Figure 2-10). In contrast, Sir4 telomeric enrichment was increased ~2.5-fold in *rif1*Δ cells and ~1.5-fold *rif2*Δ cells. These results suggest that Sir2, Sir3, Rif1, and Rif2 affect Ku-mediated telomerase recruitment and telomere lengthening by affecting the amount of Sir4 bound to telomeres.

Tethering Sir4 to tlc1Δ48 RNA restores telomeres to wild-type length, while tethering Sir3 does not

Although disruption of the Est1-Cdc13 telomerase recruitment pathway results in an ever-shortening telomere (EST) phenotype, this can be rescued by tethering Cdc13 to telomerase through a protein fusion with TERT, effectively bypassing the need for Est1 in telomerase recruitment (Evans and Lundblad, 1999). Similarly, if Sir4 is in fact Ku's binding partner in telomerase recruitment, tethering Sir4 directly to telomerase RNA could rescue the short-telomere phenotype of tlc1Δ48 cells. To test this, I tagged the sole chromosomal copy of *SIR4* with sequence encoding two tandem copies of the MS2 coat protein (MS2CP) and expressed either TLC1 or tlc1Δ48 with MS2 RNA hairpins, which have been employed previously to target proteins to telomerase RNA in yeast (Gallardo et al., 2008; Lebo et al., 2015). I passaged these cells for approximately 125 generations and then assessed telomere length. As shown in Figure 2-11, tethering Sir4 to wild-type TLC1 resulted in telomeres ~30-bp longer than the wild-type no-tag control (compare lanes 22 and 23 to 2 and 3), and tethering Sir4 to tlc1Δ48 resulted in approximately wild-type length telomeres (lanes 24 and 25). To test the specificity of telomere length in tlc1Δ48 cells being rescued by tethering Sir4 to the RNA, I also performed the same tethering experiment with Sir3, a telomeric silencing protein which has not been shown to bind Ku. When Sir3 was tethered to tlc1Δ48 (lanes 16 and 17), telomeres remained 107-bp shorter than the wild-type no-tag control. The MS2CP tags on Sir3 caused a small amount of telomere

shortening (lanes 10 and 11), and tethering Sir3 to wild-type TLC1 (lanes 14 and 15) restored telomeres to approximately wild-type length, but, again, this was dependent on the 48-nt TLC1 binding site for Ku (lanes 16 and 17). In summary, the finding that specifically tethering Sir4 to Ku-binding-defective tlc1Δ48 RNA restores wild-type length telomeres provides direct support for Sir4 being the telomere-associated factor required for Ku-mediated telomerase recruitment.

In my experiments in artificially tethering telomeric proteins to TLC1, I also tested whether Sir2 or Sir3 were required for TLC1-thethered Sir4 to promote telomere lengthening. In contrast to their effects on Ku-mediated telomere lengthening, Sir2 and Sir3 were completely dispensable for the telomere lengthening caused by Sir4-TLC1 tethering (Figure 2-12). This suggests that while the small amount of Sir4 that remains telomere-bound in *sir2*Δ and *sir3*Δ cells is limiting for the endogenous Ku-mediated telomerase recruitment pathway, it is not limiting for the artificial recruitment pathway constructed here using MS2 and MS2CP. This is likely because an array of 10 MS2 hairpins was inserted in TLC1 here, meaning that it has a higher capacity for binding to Sir4 at telomeres than the natural telomerase RNP.

I also tested the effects of tethering Yku80 to TLC1 via MS2. Similar to Sir4, Yku80 caused telomere lengthening when artificially tethered to TLC1 via MS2 (Figure 2-13), but Yku80 had a larger effect on telomere length than Sir4 in this context. As would be expected given that 10 MS2 hairpins were inserted in TLC1, tethering Yku80 to TLC1 in this manner caused both telomere shortening and telomere hyper-lengthening, a telomere-length phenotype similar to that caused by TLC1$(Ku)_3$ and other TLC1 RNAs with multiple Ku-binding sites (see Figure 2-3) (Zappulla et al., 2011).

Disrupting the Ku-Sir4 interaction shortens telomeres and reduces telomerase recruitment

During my thesis work, my advisor and I were invited to collaborate with Ming Lei and his colleagues, who had performed biochemical studies on the Ku-Sir4 interaction. In their experiments, Lei and colleagues found that binding was disrupted by the Sir4 mutations L107A

and L111R (Lei et al., unpublished data). To directly test whether the Ku-Sir4 interaction is important for telomere lengthening, I performed telomeric Southern blots on cells harboring each of these *SIR4* mutations. Similar to *sir4*Δ cells, *sir4(L107A)* and *sir4(L111R)* cells both showed modestly shortened telomeres relative to wild type, consistent with observations made by Lei and colleagues (Figure 2-14A). The average telomere-length defects in *sir4(L107A)* and *sir4(L111R)* cells were 58 and 41 base pairs shorter than wild-type on average, respectively, while telomeres in *sir4*Δ cells were 71 base pairs shorter than wild type on average. To test if these phenotypes were caused by reduced telomerase recruitment to telomeres, I performed ChIP on Est2 in cells harboring these *SIR4* point mutations and then performed quantitative real-time PCR to measure enrichment at telomeres. Closely mirroring their telomere-length defects, *sir4(L107A)* and *sir4(L111R)* cells both showed an ~80% decrease in Est2 telomeric enrichment relative to wild type, very similar to the phenotype observed in *sir4*Δ cells (Figure 2-14B). These data show that the Ku-Sir4 interaction is important for telomere lengthening and telomerase recruitment and strongly support the hypothesis that Ku recruits telomerase to telomeres through its interaction with Sir4.

2.3: Discussion

Telomerase faces formidable challenges in binding and extending telomeres in the nucleus. Obstacles include the enzyme's extremely low concentration (Mozdy and Cech, 2006), the short period of time when telomerase has to act at the end of S phase (Diede and Gottschling, 1999), and the fact that chromosome ends are likely difficult to access due to telomeric heterochromatin (Guertin and Lis, 2013).Considering these impediments, it becomes clearer why telomerase would have multiple recruitment pathways assisting in providing enzyme access to telomeres. Furthermore, carefully regulating telomerase activity is critical — it is upregulated in 90% of cancers (Shay and Bacchetti, 1997) and reduced in telomere syndromes (Armanios and Blackburn, 2012) — and multiple pathways provide opportunities for layers of regulatory control.

In *S. cerevisiae*, the primary telomerase recruitment pathway is essential and requires the Est1 telomerase subunit binding to the telomere-specific DNA-binding protein Cdc13 (Evans and Lundblad, 1999). In humans, it has been shown that telomere-bound Pot1•Tpp1 recruits telomerase through the Tpp1 "TEL patch" binding TERT (Zhong et al., 2012; Nandakumar and Cech, 2013; Schmidt et al., 2014). A second recruitment pathway in yeast has been identified that requires the Ku telomerase subunit and its binding to TLC1 (Peterson et al., 2001; Stellwagen et al., 2003; Fisher et al., 2004). In this chapter, I provide evidence that Ku recruits telomerase to telomeres in yeast through its binding to the telomeric transcriptional silencing protein Sir4.

There is substantial evidence for the existence of the Ku-mediated telomerase recruitment pathway in *S. cerevisiae*. Ku binding to TLC1 promotes telomere lengthening (Peterson et al., 2001; Stellwagen et al., 2003; Zappulla et al., 2011) and recruitment of the telomerase catalytic protein subunit to telomeres as assessed by chromatin immunoprecipitation (Fisher et al., 2004). My findings support this Ku-mediated recruitment pathway and provide the first evidence that it is achieved by binding the telomeric silencing protein Sir4. First, I showed genetic epistasis between *SIR4* and the Ku-binding site in *TLC1* with respect to telomere-length maintenance. Second, I showed that telomere hyper-elongation caused by a TLC1 RNA containing three Ku-binding sites, TLC1(Ku)$_3$, is dependent on *SIR4*. Third, using chromatin immunoprecipitation, I showed that deleting *SIR4* causes low levels of telomerase catalytic subunit at telomeres and that this low degree of recruitment is indistinguishable from what is observed in *tlc1*Δ*48* cells. Furthermore, TLC1 with two extra Ku-binding sites causes a 10-fold increase in TERT enrichment at telomeres, and this increase in telomerase recruitment requires *SIR4*. I also demonstrated that tethering Sir4 directly to a TLC1 RNA lacking its Ku-binding site restores telomeres to wild-type length, whereas tethering Sir3 to Ku-binding-defective TLC1 RNA does not. Lastly, I showed that point mutations in Sir4 that disrupt binding to Ku cause defects in telomerase recruitment to telomeres similar to *sir4*Δ cells, suggesting strongly that Ku recruits telomerase to telomeres through its interaction with Sir4.

Based on these results, I propose that Ku mediates telomerase recruitment to telomeres by binding to Sir4 (Figure 2-15). Since Ku-mediated telomerase recruitment occurs via Sir4 associating with telomeric DNA-bound Rap1, regulation of Sir4 association with Rap1, in turn, can control the ability of the Ku-Sir4 recruitment pathway to assist in telomere lengthening. As shown in Figure 2-10, Sir4 association with telomeres is increased in the absence of Rif1 or Rif2, suggesting that Rif1 and Rif2 inhibit Sir4 binding to telomeres. The Rif1 and Rif2 proteins have been proposed to represent a "counting mechanism" for telomere-length homeostasis, in which decreased binding of the Rif proteins — negative regulators of telomerase — leads to increased telomerase recruitment at short telomeres (Marcand et al., 1997; Levy and Blackburn, 2004; Teixeira et al., 2004; Bianchi and Shore, 2007). My model provides a parsimonious explanation for one way in which Rif1 and Rif2 regulate telomere length; i.e., as competitive inhibitors of Sir4 binding to Rap1 and, therefore, the Sir4-Ku telomerase recruitment pathway. The model that the Ku-Sir4 recruitment pathway is subject to Rif protein-mediated negative regulation is supported by my findings and reports in the literature. First, I showed that TLC1(Ku)$_3$, a telomerase RNA with three Ku-binding sites, causes many telomeres to become hyper-elongated, which is similar to telomere hyper-elongation exhibited by *rif1*Δ and *rif2*Δ mutants. Second, deleting the Ku-binding site in TLC1 greatly reduces the telomere hyper-lengthening observed in *rif1*Δ and *rif2*Δ cells (see Figures 2-3 and 2-7). Similarly, it has been shown that the hyper-lengthening of telomeres in *rif2*Δ as well as *rif1*Δ *rif2*Δ mutants is greatly reduced when combined with a *yku*70Δ mutation (Mishra and Shore, 1999). Regulation of the Ku-Sir4 pathway by Rif1 and Rif2 likely modulates, in turn, the essential Est1-Cdc13 telomerase-recruitment pathway. Ku-mediated telomerase recruitment has been proposed to promote function of the Est1-Cdc13 pathway by increasing Est1 association with telomeres (Fisher et al., 2004; Williams et al., 2014), a mechanism that is complementary to my model for Ku-mediated telomerase recruitment.

Sir4-mediated telomerase recruitment via Ku suggests that there is a relationship between (semi-stable) telomeric silencing and telomerase recruitment. Such a relationship has already been suggested by the fact that Rif1 and Rif2 proteins compete for silencing proteins Sir3 and Sir4 association with telomere-bound Rap1 and inhibit telomerase acting at longer telomeres. Accordingly, I propose that the Ku-Sir4 recruitment pathway tends to occur at shorter telomeres and is part of the negative feedback loop regulating telomere length homeostasis. This is supported by telomerase preferentially acting at shortened telomeres (Teixeira et al., 2004), which tend to have weaker silencing than longer telomeres and have fewer Rif proteins (Kyrion et al., 1993; Park and Lustig, 2000). My results and previous studies show that when telomeric transcriptional silencing is absent due to *sir2*Δ or *sir3*Δ mutation, a reduced but detectable amount of Sir4 is found at telomeres by ChIP (Hoppe et al., 2002). Thus, in wild-type cells, it may be that Sir4 binds to Rap1 to recruit telomerase via its Ku subunit without having established telomeric silent chromatin at the end. In summary, it seems most likely that short, non-silenced chromosome ends are the ones targeted for extension by the Sir4-Ku telomerase recruitment pathway and that this is an important part of the negative-feedback loop that maintains telomere length homeostasis.

Although the Ku-Sir4 recruitment mechanism I propose is inhibited by the important negative regulators of telomerase Rif1 and Rif2, it is clear that the Ku-Sir4 pathway normally has a more modest role in telomere length maintenance than the Est1-Cdc13 pathway. Disrupting the Ku-Sir4 pathway results in short but stable telomeres, whereas, in contrast, loss of Est1-Cdc13 recruitment causes complete loss of telomeres and cellular senescence. The typically smaller magnitude of the effects of the Ku-Sir4 pathway makes its disruption more likely to have been missed in prior studies. Furthermore, it has been difficult to separate the roles of Sir proteins in telomerase recruitment from competing negative roles of Rif1 and Rif2. The C-terminal domain of the Rap1 protein that binds telomeric dsDNA repeats is bound by Rif1 and Rif2 and recruits Sir3 and Sir4 to telomeres. Deleting the C-terminal domain of Rap1 therefore not only disrupts

Sir-dependent silencing at telomeres, but also abolishes Rif-protein inhibition of telomerase and, consequently, the net result is that telomeres become extremely long in a mutant lacking the Rap1 C-terminus (Kyrion et al., 1992). However, my model cannot fully explain the long-telomere phenotype of this mutant. In the absence of Rif1 and Rif2 binding at telomeres in *rap1*Δ*c* cells, telomeres will only become hyper-elongated if a process that the Rif proteins inhibit persists. Because mutants lacking the Rap1 C-terminus have long telomeres despite having lost Sir4 binding at telomeres (at least via Rap1), the Ku-Sir4-mediated recruitment pathway I propose is not the only one inhibited by Rif1 and Rif2.

There are, however, a few noteworthy results in the literature suggesting that telomeric silent chromatin factors, particularly Rap1, contribute to telomere length maintenance. First, deleting *SIR3* or *SIR4* causes telomere-length maintenance defects (Palladino et al., 1993; Askree et al., 2004; Gatbonton et al., 2006). Second, the Rap1 M763A mutation, which abolishes the Rap1-Sir3 interaction and slightly impairs telomeric silencing, has been shown to cause shortened telomeres (Feeser and Wolberger, 2008). Lastly, Rap1 binding near a telomeric seed sequence has been shown to promote telomerase-dependent *de novo* telomere formation, although this activity was reportedly *SIR4*-independent (Ray and Runge, 1998).

In summary, I have shown that telomerase RNA-bound Ku recruits telomerase to telomeres by binding the telomeric silent chromatin protein Sir4. The Ku-Sir4 pathway is inhibited by the telomerase regulators Rif1 and Rif2 and likely promotes telomerase recruitment through the essential Est1-Cdc13 recruitment pathway. Thus, this pathway represents an important mechanism by which telomerase is regulated to maintain telomere length in *S. cerevisiae* and it may be generally conserved in many other species. For instance, both telomeric silent chromatin and the Ku-telomerase RNA interaction are present in humans (Baur et al., 2001; Ting et al., 2005). Although humans lack an obvious Sir4 homolog, the protein HP1α has been implicated in human telomeric silencing (Koering et al., 2002; Arnoult et al., 2012) and has been

shown to bind Ku70 (Song et al., 2001), so it will be interesting to learn if these interactions also comprise a telomerase recruitment pathway.

2.4: Materials and methods

Experiments in yeast

Experiments described in Figures 2-2A, 2-3, 2-4, 2-5, 2-6, 2-7, 2-9, 2-11, 2-12, and 2-13 are all based on *tlc1*Δ complementation assays reported previously (Lebo et al., 2015). Plasmid pRS414-based constructs containing *TLC1* alleles were transformed into a *tlc1*Δ strain harboring a *pTLC1-LYS2-CEN* or *pTLC1-URA3-CEN* "cover" plasmid. The *TLC1*-containing cover plasmid was then shuffled out by plating transformants on medium containing α-aminoadipate to select for LYS– cells that lost the *pTLC1-LYS2-CEN* cover plasmid or medium with 5-fluoroorotic acid to select for URA– cells that lost the *pTLC1-URA3-CEN* cover plasmid. In Figure 2-9, cells were streaked once to solid minimal medium lacking tryptophan before being grown for chromatin immunoprecipitation. In all other cases, cells were passaged by one of two methods after cover plasmid loss. In Figures 2-2A, 2-3C, 2-4B, 2-7, 2-11, 2-12, and 2-13, cells were passaged by serially re-streaking single colonies on solid minimal medium lacking tryptophan. When using this passaging technique, generation time was estimated as 25 generations per re-streak (including the streak used to shuffle out the cover plasmid). For Figures 2-3A, 2-3B, 2-4A, 2-5, and 2-6, cells were passaged differently. First, after the streak used to shuffle-out the cover plasmid, cells were re-streaked once to solid minimal medium lacking tryptophan. Colonies from this minus-tryptophan (–TRP) plate were then used to inoculate 20-mL –TRP liquid cultures and culturing was performed at 30˚C for ~24 hours. Cells were then back-diluted by a factor of 210 into 20-mL cultures of fresh medium, which were grown for another ~24 hours before being passaged again. Cultures reached the same approximate density each day as measured spectrophotometrically (600-nm light). In these experiments, generation time was approximated as 50 generations (25 generations for the colony forming after streaking to solid medium when shuffling out the cover

plasmid plus 25 more for the –TRP medium growth) plus 10 generations for each day of passaging in liquid cultures.

In Figure 2-14A, a *tlc1*Δ *sir4*Δ strain bearing a *pTLC1-TRP1-CEN* cover plasmid was transformed with pRS316-based plasmids containing different alleles of *SIR4* (or in the case of the "*sir4*Δ" condition, containing no insert at all). These transformants were serially re-streaked five times to minimal media lacking tryptophan and uracil. In Figure 2-14B, a *sir4*Δ strain was transformed with the same pRS316-based plasmids as in Figure 2-14A, but cells were not passaged before performing chromatin immunoprecipitation.

In Figure 2-2B, a *SIR4*/*sir4*Δ *YKU80*/*yku80*Δ diploid was sporulated, and tetrads were dissected to isolate tetratype spores. The spores from this ascus were then re-streaked three successive times on rich YPD medium before telomere length was assessed.

Southern blotting

Southern blotting was performed as described previously (Zappulla et al., 2005; Zappulla et al., 2011; Lebo et al., 2015). Briefly, cells were pelleted either directly from liquid cultures used for passaging or from cultures grown from serial re-streaking plates. Genomic DNA was isolated from these cells (Gentra Puregene system), and roughly equal amounts of genomic DNA were digested with XhoI. Digested genomic DNA samples were resolved on a 1.1% agarose gel. The DNA was then transferred to Hybond-N+ Nylon membrane (GE) which was probed for telomeric sequence and for a 1627-bp, non-telomeric XhoI restriction fragment from within chromosome IV and then imaged using phosphor screens and a Typhoon 9410 Variable Mode Imager (Friedman and Cech, 1999). Average Y′ telomere length was calculated using the weighted average mobility (WAM) method as previously described (Zappulla et al., 2011). In Figure 2-4, Southern blots were probed for Y′ sequence. Y′ probe was made by first performing PCR with the following primers using genomic DNA as template DNA: 5′-TGTTGTCTCTTACCCGGATGTTCAACC-3′, 5′-AAAGTTGGAGTTTTTCAGCGTTTGCG-

3′. The DNA amplified in this reaction was in turn used as template for making the radiolabeled Y′ probe.

Northern blotting

Northern blotting was performed as previously described (Zappulla et al., 2005; Lebo et al., 2015). Briefly, cells were harvested in the same manner as those used for Southern blots, and total RNA was isolated using the hot-phenol method (Kohrer and Domdey, 1991). 10–15 μg of RNA from each sample was boiled and then resolved by urea-PAGE. The RNA was transferred to Hybond-N+ Nylon membrane (GE), which was then UV-crosslinked and probed for TLC1 and U1 sequences. Due to the low abundance of TLC1 RNA relative to U1, blots were probed with 100-fold fewer counts of U1 probe than TLC1 probe. Blots were then imaged using phosphor screens and a Typhoon 9410 Variable Mode Imager (GE).

Chromatin immunoprecipitation and quantitative PCR

Chromatin immunoprecipitation (ChIP) was performed similarly to that described (Fisher et al., 2004). Briefly, cells were grown to saturation in 10-mL cultures of liquid minimal medium, back-diluted into 60 mL cultures, and then grown to an OD600 of 0.5–0.8. 50 mL of cells were crosslinked with formaldehyde, pelleted, rinsed in lysis buffer, and then re-suspended in lysis buffer. Cells were flash-frozen, thawed, and then lysed using sterile glass beads. Lysates were then sonicated to shear crosslinked chromatin. Anti-myc immunoprecipitation was carried out using mouse anti-myc monoclonal antibodies (Clontech) and Protein G Dynabeads (Life Technologies). After immunoprecipitation, formaldehyde crosslinks were reversed, and DNA was purified using reagents from the Qiagen PCR Purification Kit.

Fold telomeric enrichment in ChIP DNA samples was quantified by quantitative real-time PCR (qPCR) using iQTM SYBR® Green Supermix and a CFX96TM Real-Time Cycler

(Bio-Rad). The primer sets used at telomere VI-R, telomere XV-L, and the ARO1 locus were the same as those described previously (Sabourin et al., 2007; McGee et al., 2010). For a given sample of DNA obtained from ChIP, qPCR reactions for each primer set were performed in technical duplicate or triplicate, and the C_T values were averaged together. Using these averages, fold telomeric enrichment was then calculated as $2^{[(C_{T(ARO\ IP)}-C_{T(ARO\ Input)})-(C_{T(TEL\ IP)}-CT(TEL\ Input))]}$. Additionally, each time qPCR was performed, the efficiency of amplification for was calculated for each primer set being used. From a sample of ChIP input DNA, a series of 10-fold dilutions were made and used as template DNA for qPCR reactions. For these reactions, –log(dilution factor) was plotted against C_T value, and a line of best fit was found for the graph. Using the slope of this line, percent amplification efficiency was calculated as $100*[10^{(-1/slope)}-1]$. If amplification efficiency was between 70% and 95%, average C_T values were corrected using the slope and Y-intercept values from the line of best fit: Relative amount = $10^{[(AvgC_T-intercept)/slope]}$. Then, fold telomeric enrichment was instead calculated as $(RelAmt_{TEL\ IP}/RelAmt_{TEL\ Input})/(RelAmt_{ARO\ IP}/RelAmt_{ARO\ Input})$. All fold telomeric enrichment values are expressed relative to wild type.

In vitro protein-protein binding experiments

First, ~16 pmol of purified, myc-tagged yeast Ku heterodimer (Pfingsten et al., 2012; Dalby et al., 2013) was added to the rabbit reticulocyte lysate (RRL) transcription and translation system (TNT Quick Coupled, Promega). In the "boiled" condition in Figure 2-8, the Ku heterodimer was heated at 95°C for 5 minutes before being added to the RRL. Sir4 synthesis was then initiated by adding 1 µg of *SIR4* template DNA and ^{35}S-L-methionine to the RRL, and the reaction was incubated at 30°C for approximately 90 minutes. 5 µL of mouse anti-myc monoclonal antibodies (Clontech, used at a 1:400 dilution in TBST) were added to the reaction, which was then incubated at 4°C for 1 hour. 40 µL of Protein G Dynabeads (Life Technologies) were prepared for each RRL reaction by first pipetting off the storage buffer, rinsing once in 1

mL of “standard” Ku-Sir4 buffer (25 mM HEPES pH 7.5, 100 mM NaCl, 1 mM DTT, 10% glycerol, 1 mM EDTA, 0.1% IGEPAL), and then re-suspended in 40 µL of “standard” Ku-Sir4 buffer per RRL reaction. Before adding beads to the RRL reactions, a 2 µL aliquot was taken from the RRL and set aside to be used as the input sample for the protein gel. 40 µL of prepared beads were added to each RRL reaction, and the reactions were left to rotate at 4°C overnight. The next morning, the beads were pulled down with a magnet, and a 2 µL aliquot of the supernatant was set aside to be used as the unbound sample for the protein gel. The remaining supernatant was discarded, and the beads were washed twice with 500 µL of “stringent” Ku-Sir4 buffer (same as “standard” Ku-Sir4 buffer but with 200 mM NaCl and 0.2% IGEPAL). Beads were then re-suspended in 120 µL TE +1% SDS and heated at 95°C for 5 minutes. The beads were pulled down with a magnet, and the entire supernatant was saved as the bound fraction. 2 µL of 2X protein sample buffer was added to the input and unbound aliquots which were then heated at 95°C for 5 minutes. These samples along with a bound sample (10 µL of the bound fraction plus 10 µL of 2X protein sample buffer) were resolved by SDS-PAGE on a 7.5% polyacrylamide gel. The resulting gel was imaged using phosphor screens and a Typhoon 9410 Variable Mode Imager. It should be noted that the “standard” and “stringent” Ku-Sir4 buffers were designed based off of the buffers used in co-immunuprecipitation experiments described previously (Roy et al., 2004).

Table 2-1: Average Y′ telomere length in *sir*Δ cells containing TLC1, tlc1Δ48, or TLC1(Ku)$_3$

SIR Genotype	*TLC1* Genotype		
	TLC1	*tlc1Δ48*	*TLC1(Ku)$_3$*
SIR	0	–86 ± 23[b]	Dysregulated[a]
*sir4*Δ	–53 ± 13[b]	–71 ± 26[b]	–148 ± 36[c]
*sir2*Δ[d]	–41 ± 16	–50 ± 74	–71 ± 26
*sir3*Δ[d]	–51 ± 20	–84 ± 14	–123 ± 2

The weighted-average mobility of the Y′ telomeric restriction fragments was calculated as described in the Materials and Methods. The numbers shown are averages of multiple biological-replicate samples ± standard deviation.

[a] Y′ telomere length was not quantified in this condition because signal from Y′ telomere restriction fragments overlapped with that from the non-telomeric control fragment.

[b] n = 6

[c] n = 4

[d] n = 2

Figure 2-1: Ku binds to TLC1 RNA.

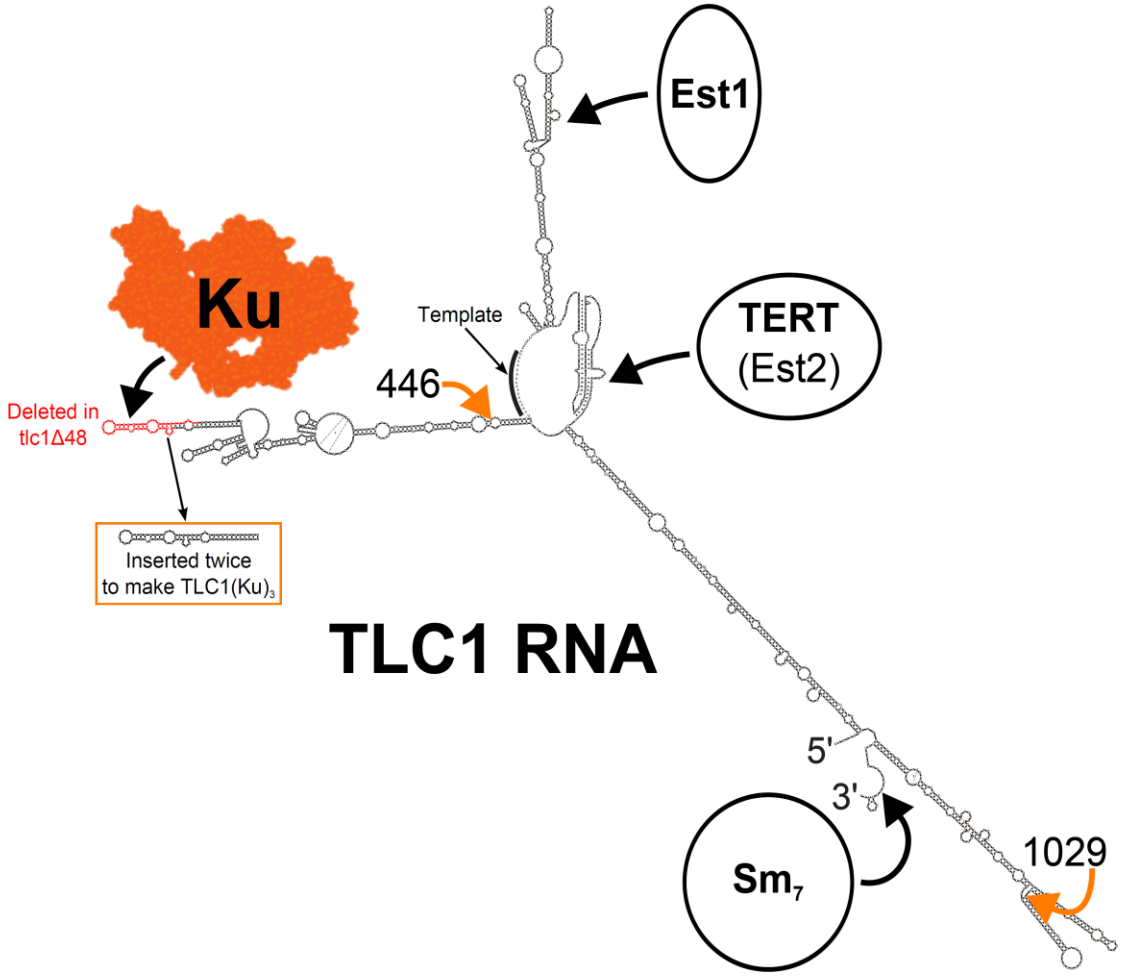

The 48 nucleotides deleted in tlc1Δ48 are highlighted in red. The 74-nucleotide hairpin shown in the orange box was inserted at positions 446 and 1029 (indicated by the orange arrows) to create TLC1(Ku)$_3$. The structures of TLC1 and Ku are the same as those shown in Figure 1-1.

Figure 2-2: *SIR4*, Ku, and the Ku-binding site in TLC1 are in the same telomere-lengthening pathway.

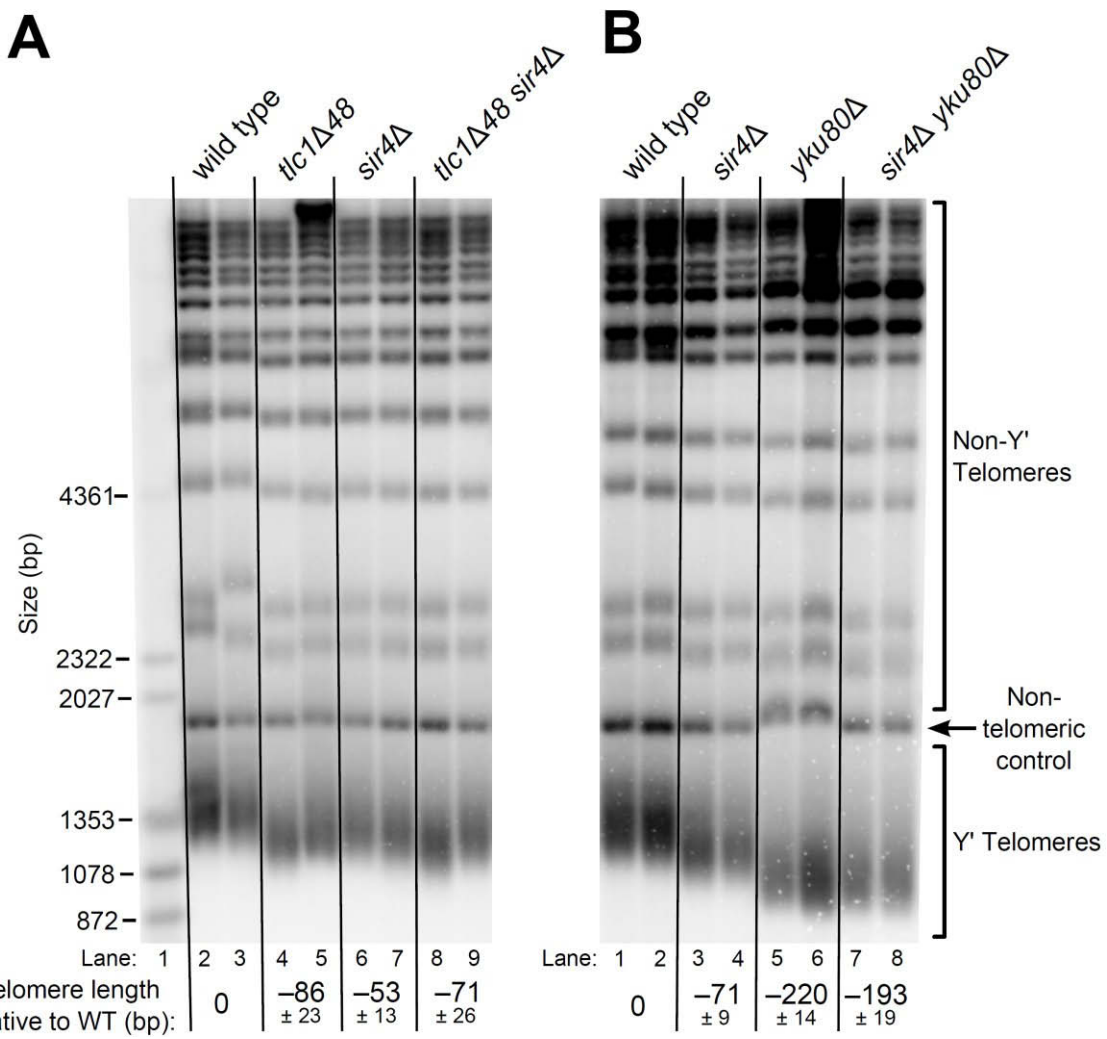

(**A**) Deleting *SIR4* in *tlc1Δ48* cells does not cause further telomere shortening. A *tlc1*Δ *pTLC1-URA3* strain and an isogenic *sir4*Δ strain were transformed with centromeric plasmids expressing either TLC1 or tlc1Δ48, and then the *pTLC1-URA3* cover plasmid was shuffled out. The cells were serially re-streaked five times and genomic DNA was isolated and analyzed by Southern blotting. The Southern blot was probed for telomeric sequence and for a 1621-bp non-telomeric XhoI restriction fragment from chromosome IV ("Non-telomeric control") used as a relative-mobility control. Pairs of lanes represent independent transformants. Changes in telomere length were quantitated using the Y′ telomere bands as described in Materials and Methods. Telomere

lengths calculated from the two sets of replicates shown were averaged with telomere lengths from four other sets of replicate samples from similar experiments to give the numbers shown, ± standard deviation. The numbers shown here are the same as those in Table 2-1. (**B**) Deleting *SIR4* in *yku8*0Δ cells does not cause further telomere shortening. A *SIR4*/*sir4*Δ *YKU80*/*yku80*Δ diploid strain was sporulated, and tetrads were dissected. The haploid spores of a tetratype tetrad were serially re-streaked four times on plates to equilibrate telomere length before Southern blot analysis. The pairs of lanes on the blot shown are different colonies from streak-outs of the haploid spores. Telomere lengths calculated from the two sets of replicates shown were averaged with telomere lengths from a third set of replicate samples to give the numbers shown, ± the standard deviation.

Figure 2-3: TLC1-bound Ku requires *SIR4* to promote telomere lengthening.

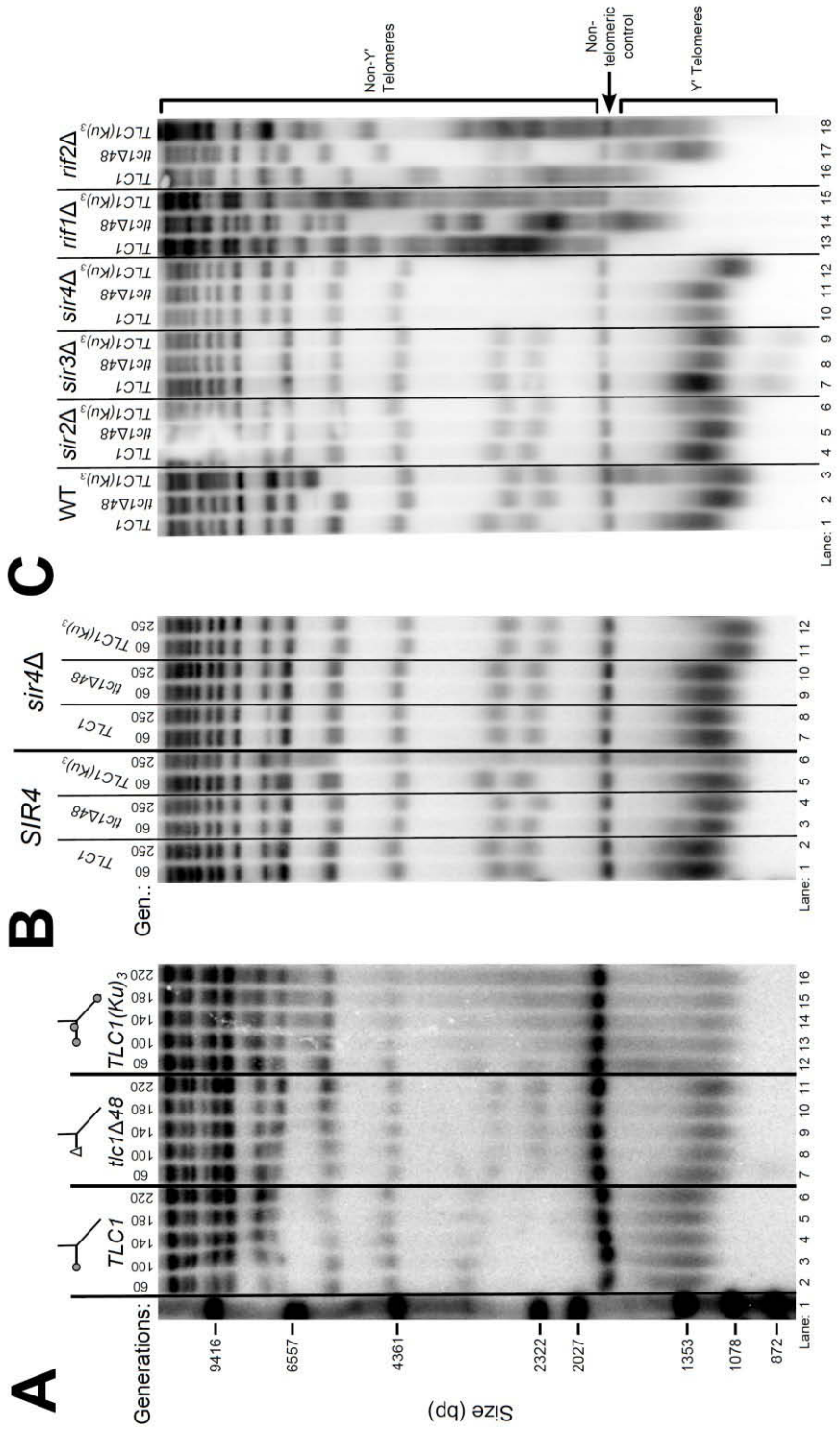

(**A**) TLC1(Ku)$_3$, a TLC1 RNA containing two extra Ku-binding sites, causes both telomere hyper-lengthening and shortening. This experiment was performed as described in Figure 2-2A, except a *tlc1*Δ *pTLC1-LYS2 rad52*Δ strain was used. Additionally, instead of passaging cells on plates, single colonies were inoculated to liquid cultures which were then serially passaged and harvested at various points throughout the passaging process. (**B**) TLC1(Ku)$_3$ does not cause telomere hyper-lengthening in *sir4*Δ cells. This experiment was performed as described in Figure 2-2A, but the liquid culture passaging method described in Figure 2-3A was used instead of re-streaking single colonies on plates. (**C**) TLC1(Ku)$_3$ does not cause telomere hyper-lengthening in *sir2*Δ or *sir3*Δ cells, and tlc1Δ48 causes greater telomere shortening in *rif1*Δ and *rif2*Δ cells than in wild-type cells. This experiment was performed as described in Figure 2-3B except that cells were passaged to ~250 generations by re-streaking on plates rather than passaging in liquid cultures.

Figure 2-4: TLC1(Ku)$_3$ causes Y′ telomere shortening and hyper-lengthening, while deletion of *RIF1* or *RIF2* causes Y′ telomere hyper-lengthening.

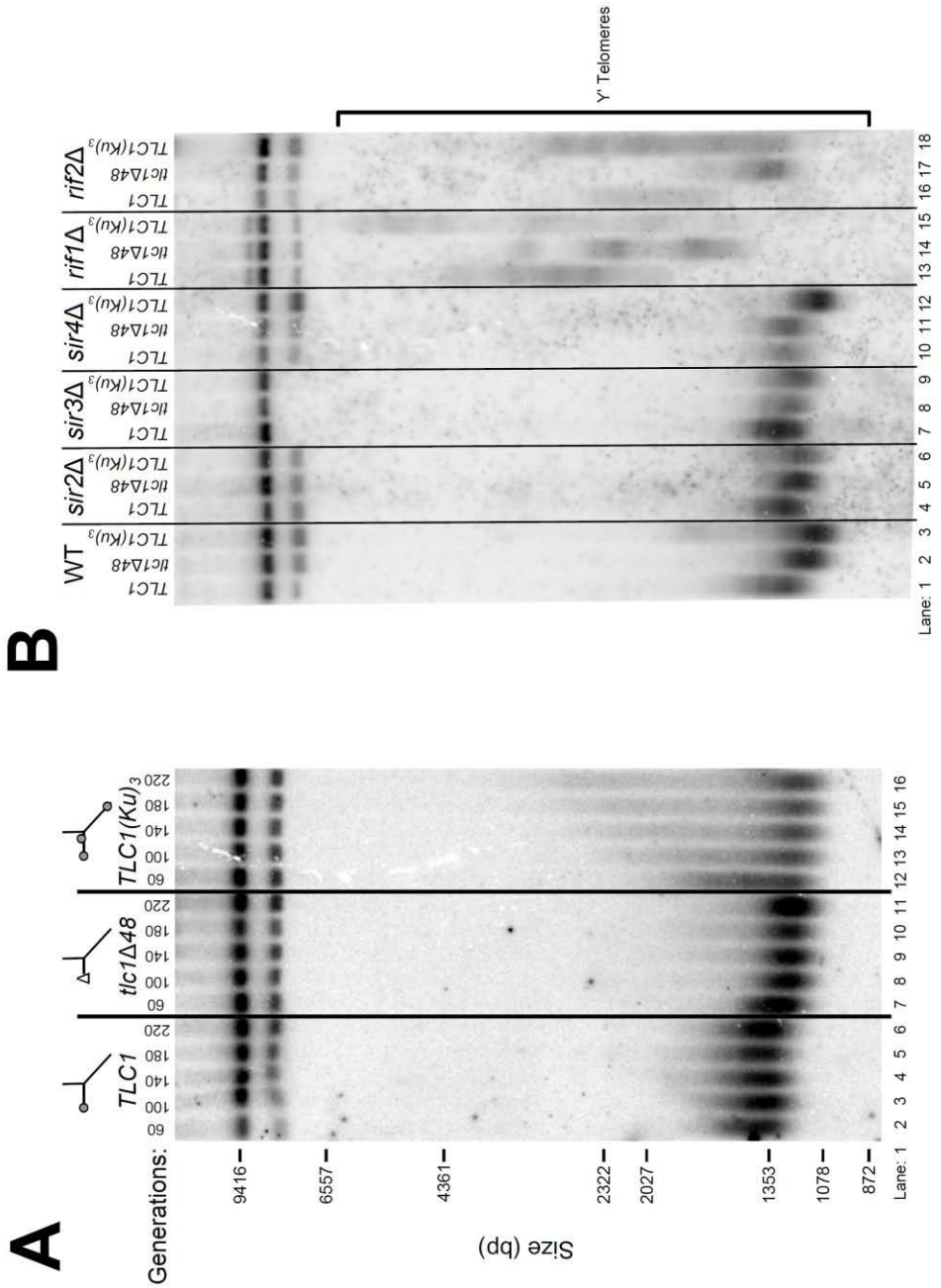

The blot from Figures 2-3A (**A**) and 2-3C (**B**) were re-probed with Y′ probe and re-imaged.

Figure 2-5: Three Ku-binding sites in yeast telomerase RNA increases telomere-length heterogeneity.

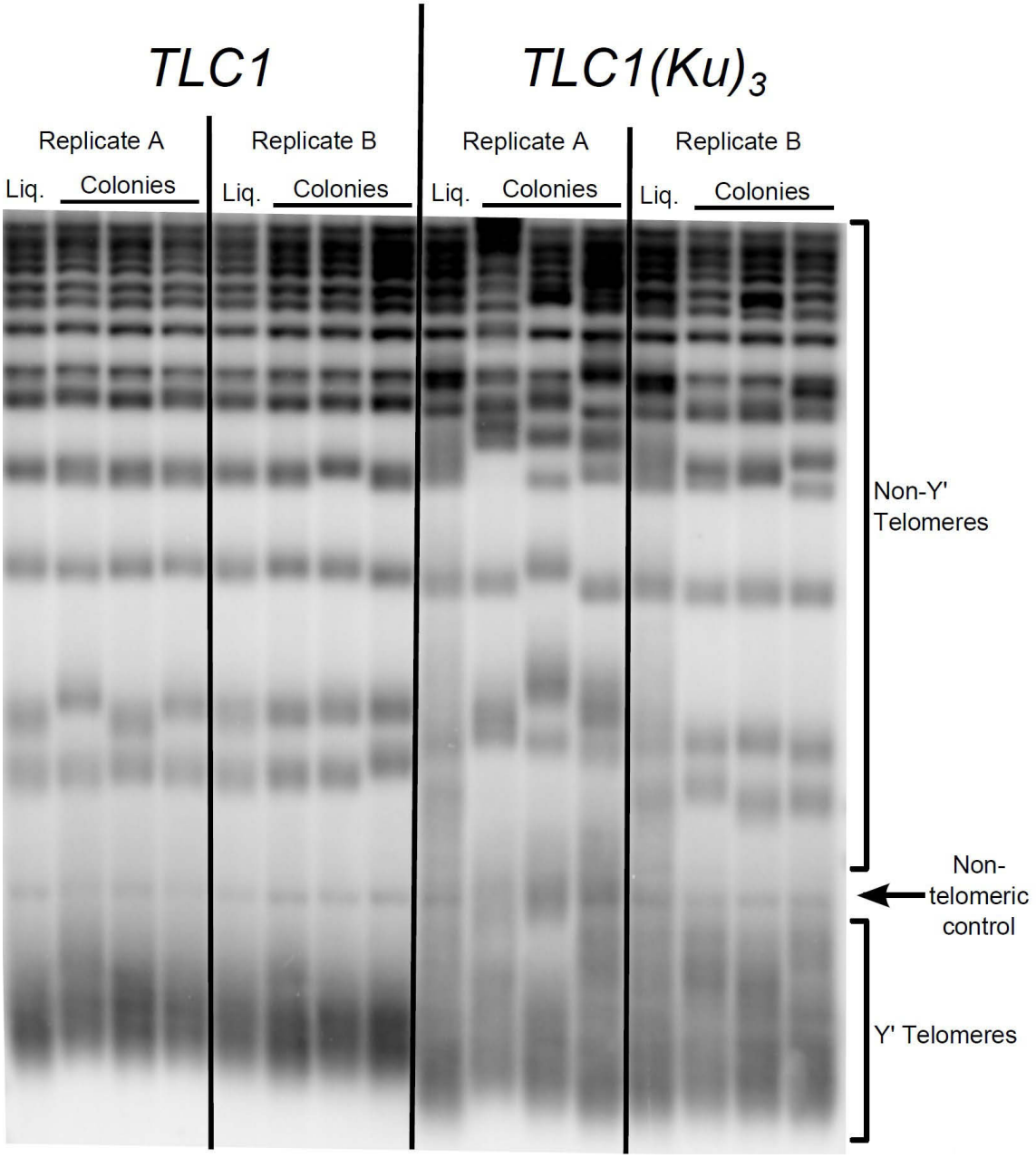

Cells were initially serially passaged in liquid culture as described in Figure 2-3A and then ~25 generations before the end of passaging, liquid cultures were plated for single colonies. Genomic DNA was isolated from both the liquid-passaged cultures ("Liq.") and from cells cultured from the (clonal) colonies from solid medium ("Colonies").

Figure 2-6: TLC1 RNA abundance is largely unaffected in *TLC1(Ku)$_3$* cells and is not decreased in *sir4*Δ cells.

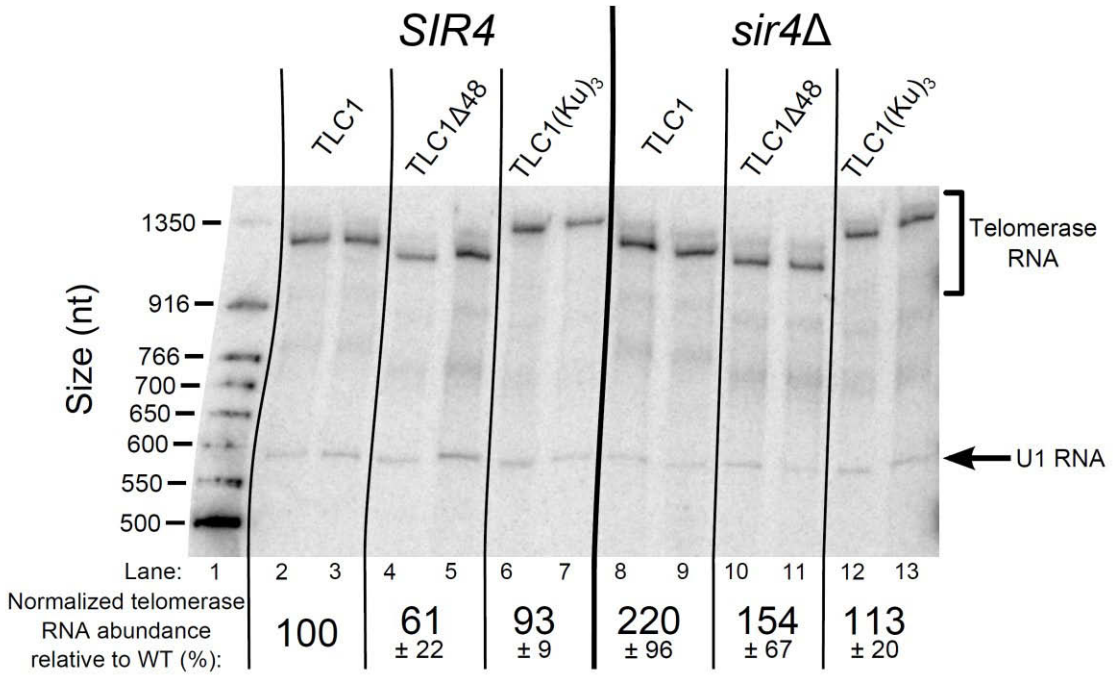

Total RNA was isolated from the cells used in the experiment described in Figure 2-3B and subjected to Northern blot analysis. The pairs of lanes on the Northern blot represent two independent sets of biological replicates. The blot was probed for TLC1 and for the U1 snRNA. Telomerase RNA abundance was normalized to U1 and is expressed relative to the *SIR4 TLC1* condition. The values shown are averages of these two replicates and another set biological replicates from a separate Northern blot, ± the standard deviation.

Figure 2-7: Deleting the Ku-binding site in TLC1 reverses a large amount of telomere hyper-lengthening in *rif1*Δ and *rif2*Δ cells.

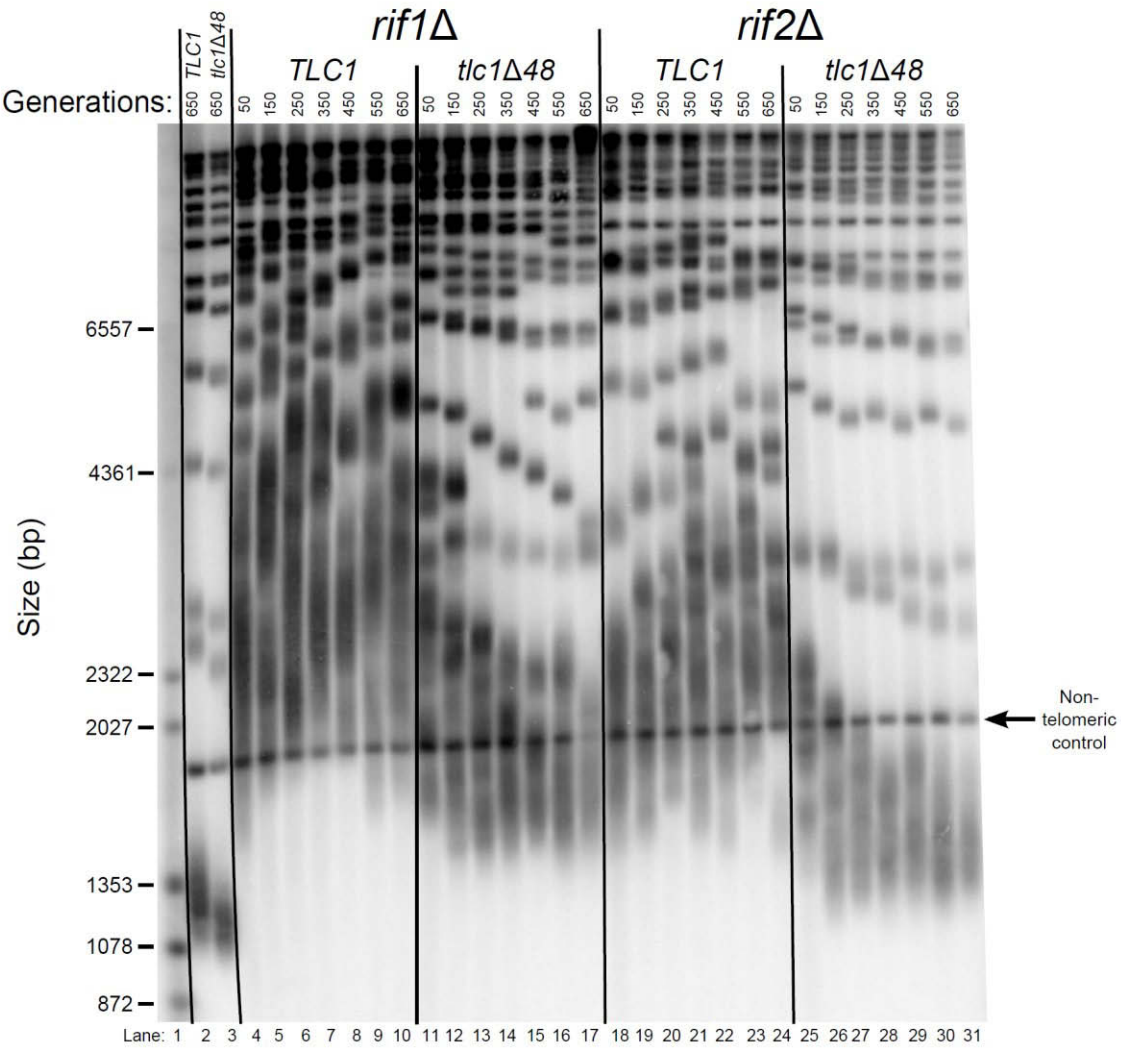

This experiment was performed as in Figure 2-2A, but cells were passaged for 650 generations.

Figure 2-8: Purified Ku binds Sir4 *in vitro*.

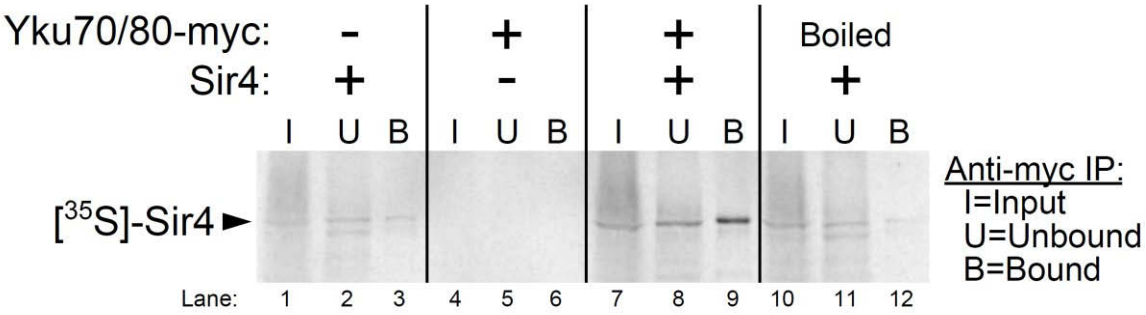

^{35}S-methionine-labeled Sir4 was synthesized *in vitro* in a rabbit reticulocyte lysate transcription/translation system (RRL) to which purified Ku heterodimer – bearing a 2myc epitope on the C-terminus of Yku80 – was added. After Sir4 synthesis, the RRL was subjected to anti-myc immunoprecipitation. The input, unbound, and bound fractions were run on an SDS polyacrylamide gel which was imaged by autoradiography.

Figure 2-9: Ku-mediated telomerase recruitment to telomeres requires *SIR4*.

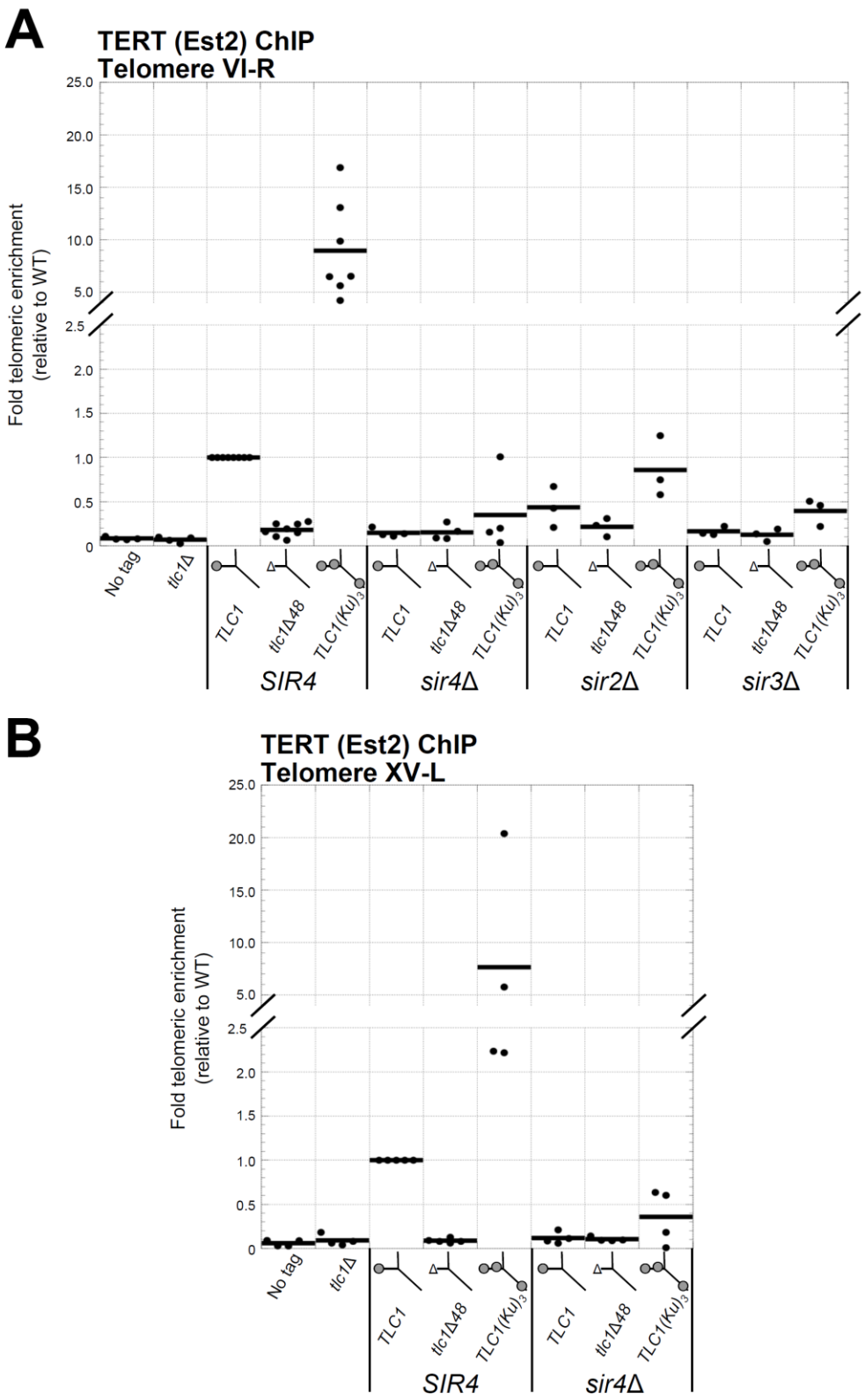

(**A**,**B**) In strains similar to those used in Figure 2-3B, TERT (Est2) was expressed from its endogenous locus bearing a C-terminal 13myc tag, separated by an 8-glycine linker. TLC1, tlc1Δ48, and TLC1(Ku)$_3$ were expressed as in Figure 2-3B, but cells were not passaged after loss of the *pTLC1-URA3* cover plasmid. Cells were crosslinked and subjected to chromatin immunoprecipitation using the myc epitopes on TERT, as described (Fisher et al., 2004). Telomeric enrichment was measured using qPCR amplicons close to telomere VI-R (**A**) and telomere XV-L (**B**). An amplicon at the *ARO1* locus was used as a non-telomeric control locus. The thick horizontal lines on the graphs represent averages of three to five independent biological replicates which themselves are indicated by black dots.

Figure 2-10: Sir4 binding to telomeres is decreased in *sir2*Δ and *sir3*Δ cells and increased in *rif1*Δ and *rif2*Δ cells.

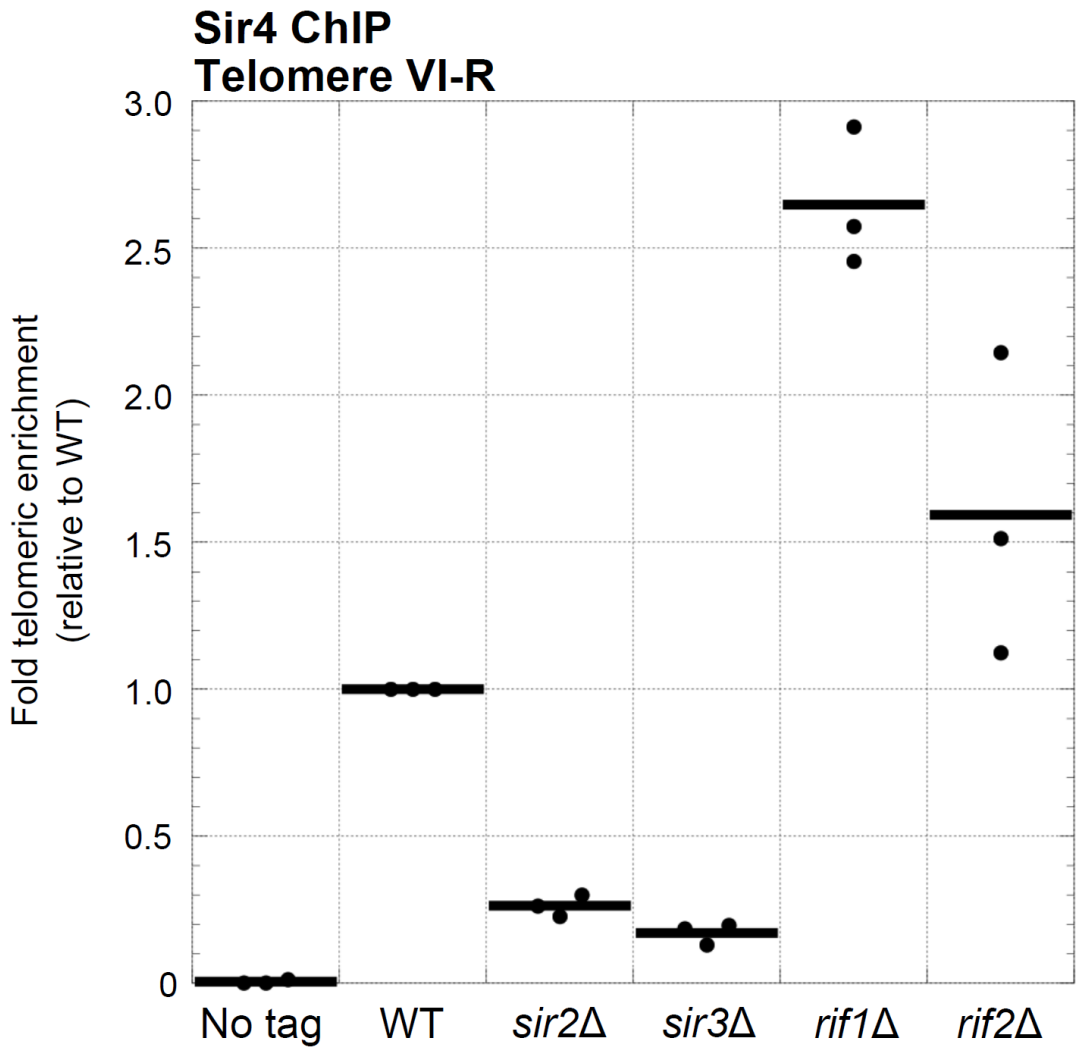

Sir4 bearing a C-terminal 13myc tag on an 8-glycine linker was expressed from its endogenous chromosomal gene locus. Cells were crosslinked and subjected to chromatin immunoprecipitation using the myc epitopes. Telomere VI-R enrichment was measured using real-time quantitative PCR as in Figure 2-9A. The thick horizontal lines on the graph represent averages of three independent biological replicates indicated by black dots.

Figure 2-11: Tethering Sir4 to the tlc1Δ48 RNA restores telomeres to wild-type length.

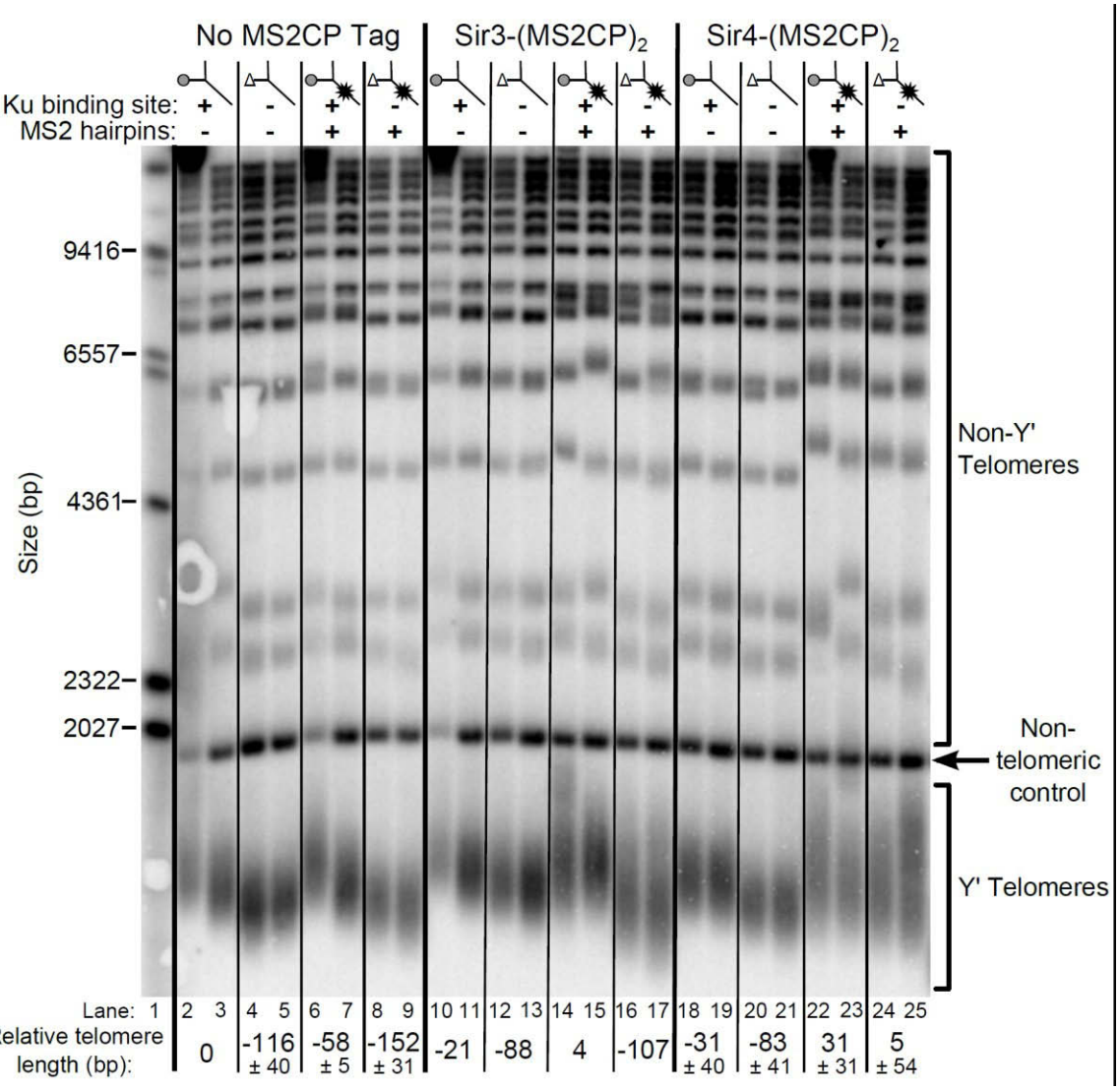

Using the same *tlc1Δ pTLC1-URA3* strain background from Figure 2-2A, Sir3 and Sir4 were expressed from their endogenous loci bearing C-terminal $(MS2CP)_2$ tags, separated by an 8-glycine linker. These strains were transformed with centromeric plasmids containing either *TLC1*, *tlc1Δ48*, *TLC1(MS2)*$_{10}$, or *tlc1Δ48(MS2)*$_{10}$. Cells were then cured of the *pTLC1-URA3* cover plasmid and passaged as in Figure 2-2A. Each pair of lanes represents two independent biological replicates, and the relative telomere length values are averages of the two replicates. In the No MS2CP Tag and Sir4-$(MS2CP)_2$ conditions, values from a third set of replicates were included in the average, allowing for standard deviation to be calculated.

Figure 2-12: Tethering Sir4 to tlc1Δ48 RNA restores telomeres to wild-type length in the absence of Sir2 or Sir3.

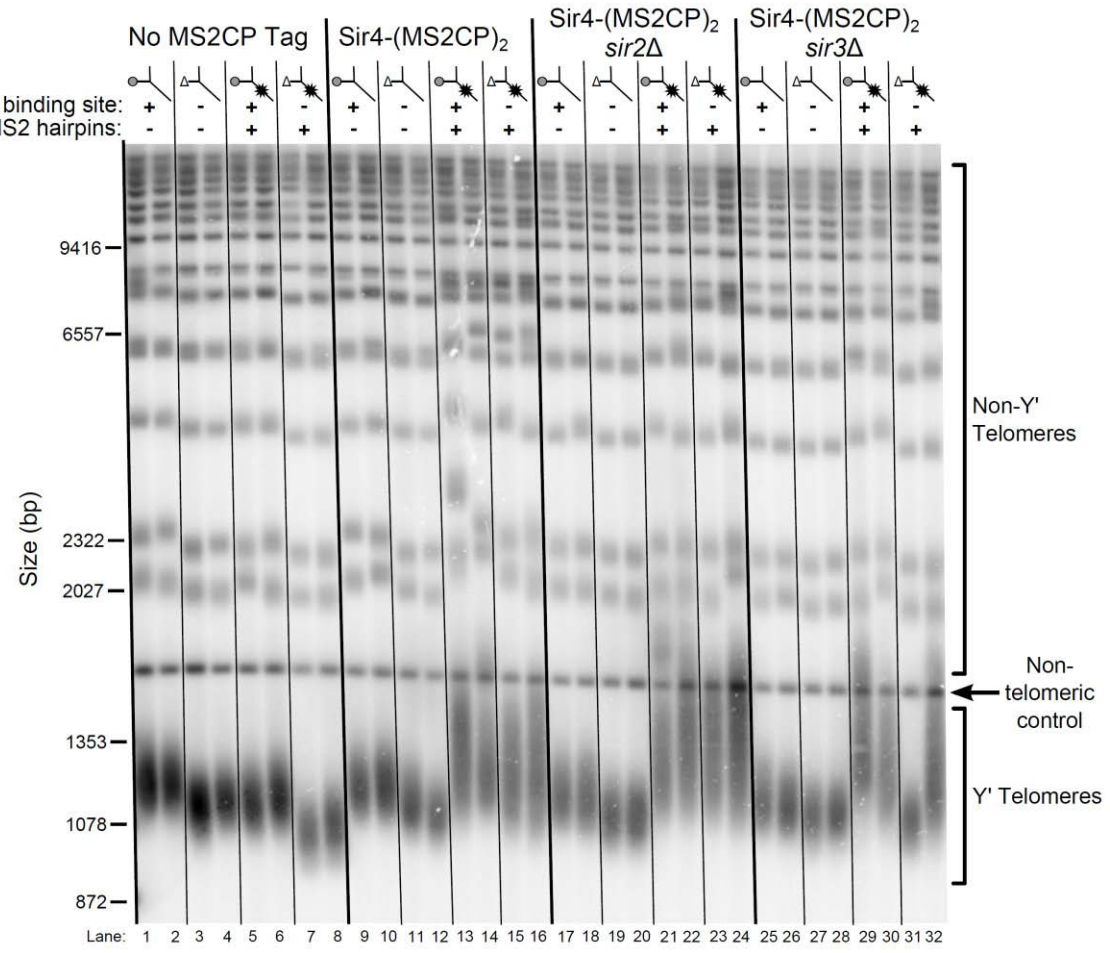

Yeast were transformed and passaged as in Figure 2-11. Pairs of lanes represent independent biological replicates.

Figure 2-13: Tethering Yku80 to TLC1 RNA causes more telomere hyper-lengthening than tethering Sir4 to TLC1.

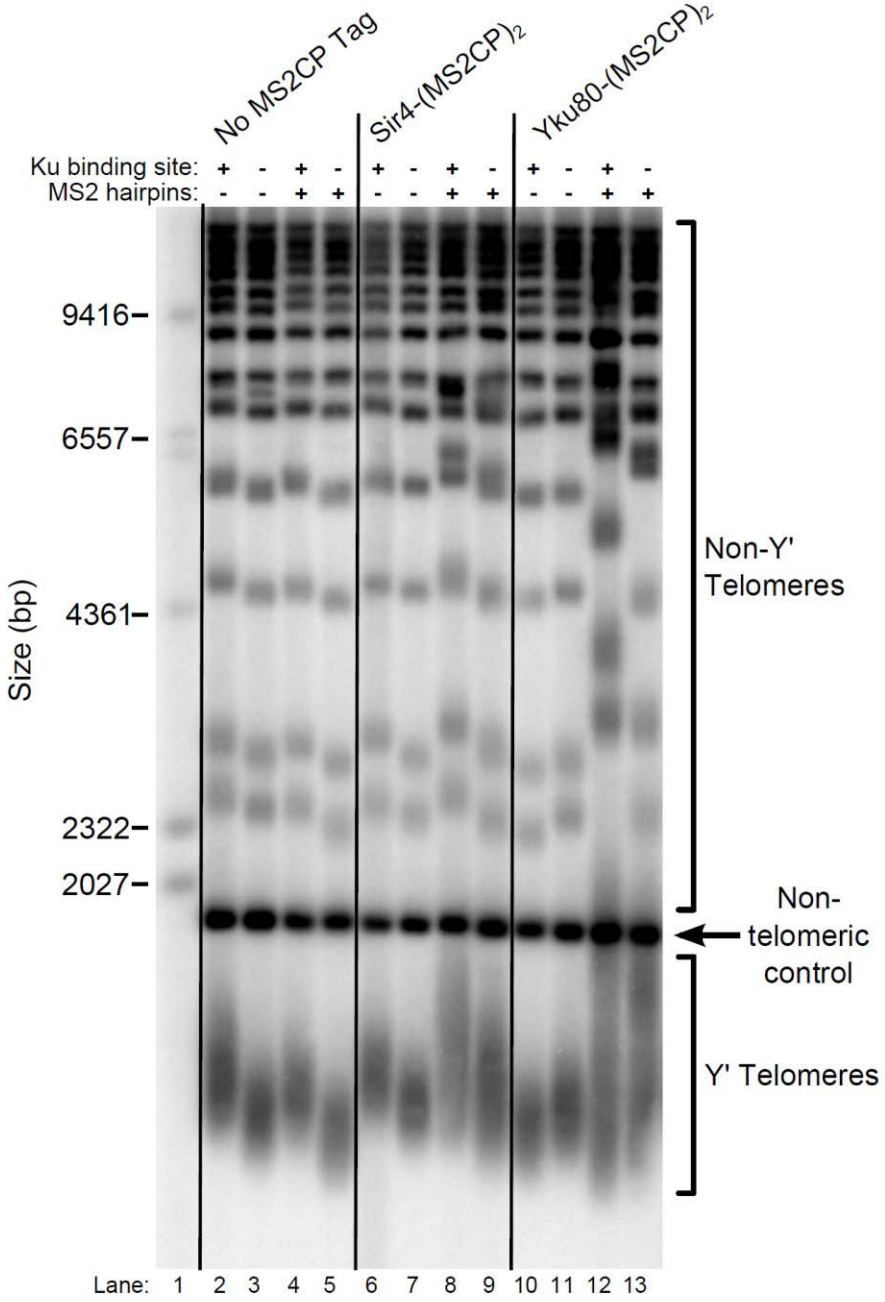

Similar to Sir3 and Sir4 in Figure 2-11, Yku80 was expressed from its endogenous locus bearing a C-terminal $(MS2CP)_2$ tag, separated by an 8-glycine linker. Yeast were transformed and passaged as in Figure 2-11.

Figure 2-14: Disrupting the Ku-Sir4 interaction shortens telomeres and impairs telomerase recruitment.

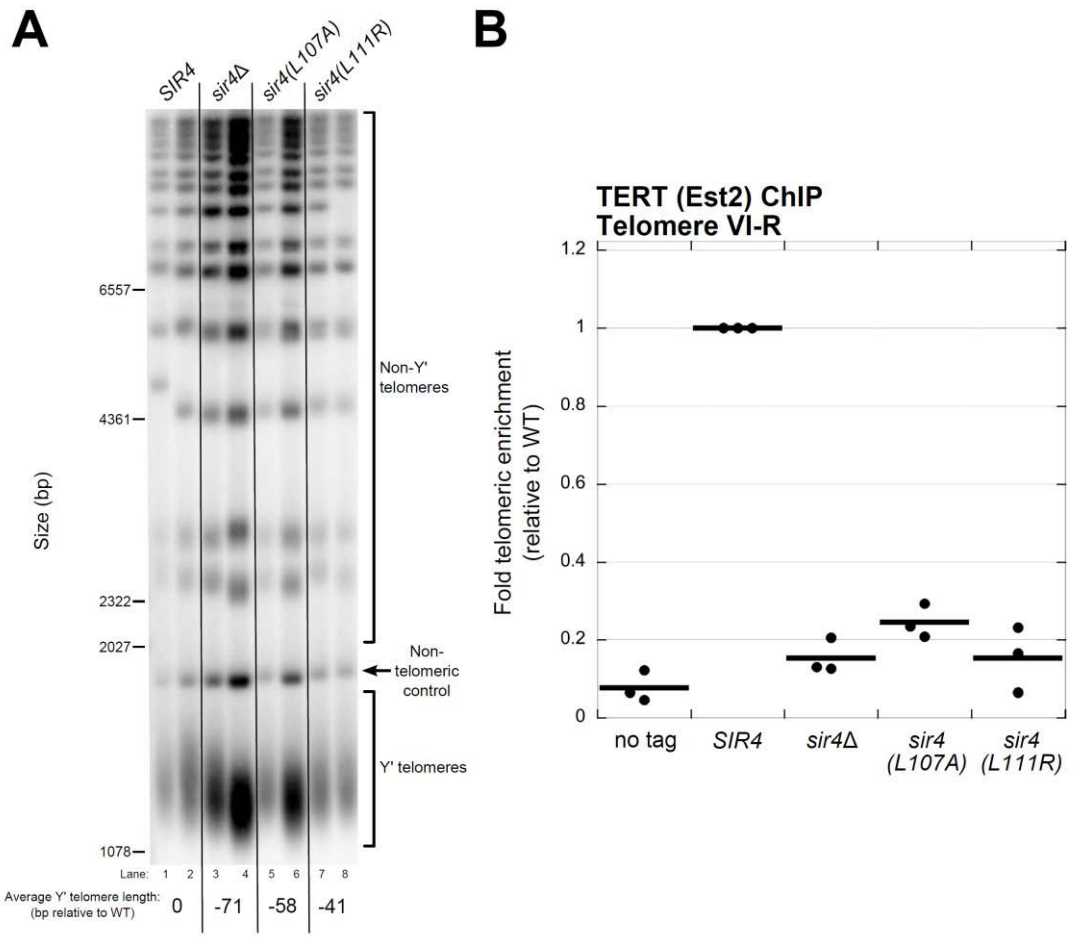

(**A**) Sir4 mutations that disrupt the Ku-Sir4 interaction cause telomere shortening. A *sir4*Δ *tlc1*Δ *pTLC1-CEN* strain was transformed with centromeric plasmids containing different alleles of *SIR4*, and transformants were serially passaged for ~150 generations. Pairs of lanes represent independent biological replicates, and the telomere length values shown are averages of these pairs of samples. (**B**) Sir4 mutations that disrupt the Ku-Sir4 interaction cause telomerase recruitment deficits similar to that caused by *SIR4* deletion. Est2 was expressed in a *sir4*Δ strain from its endogenous locus bearing a C-terminal 7myc tag, separated by an 8-glycine linker. The strain was transformed with the same centromeric *SIR4* plasmids as used in Figure 2-14A. ChIP

and qPCR were performed as in Figure 2-9. Black dots indicate data from individual biological replicates, while the average enrichment values are indicated by thick black lines.

Figure 2-15: Model for Ku-Sir4 telomerase recruitment to telomeres and its role in telomere-length regulation in *Saccharomyces cerevisiae*.

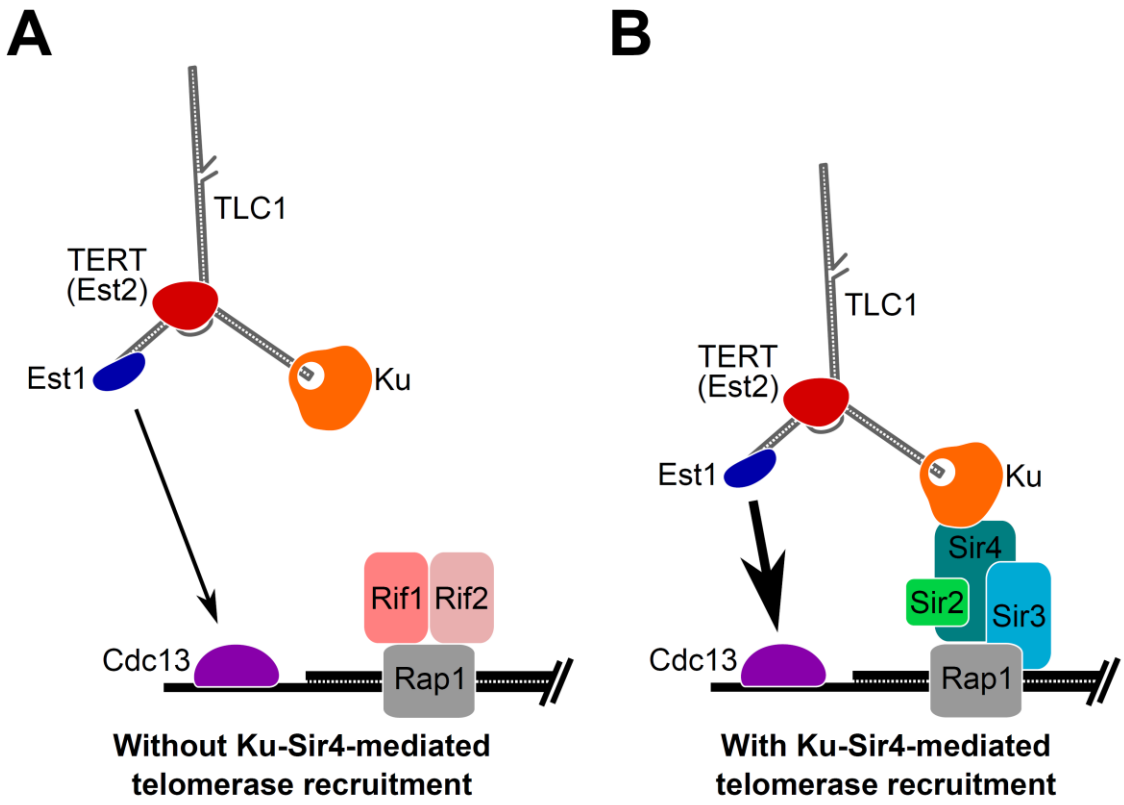

Telomerase has previously been shown to extend an individual telomere infrequently, and shorter telomeres are preferentially extended. I propose here that Ku recruits telomerase to telomeres by binding Sir4. Since it has been shown that Rif1 and Rif2 compete with Sir4 and Sir3 for binding telomere-bound Rap1, the Ku-Sir4 telomerase recruitment pathway is inhibited by Rif1 and 2, providing a simple mechanistic explanation for one way in which Rif proteins function to inhibit telomerase action at telomeres. (**A**) Ku recruitment of telomerase via Sir4 is inhibited by Rif1/2 competition for Rap1 binding with Sir4. In situations where Ku-Sir4-mediated telomerase recruitment does not occur, Est1-Cdc13-mediated telomerase recruitment can still happen, although with low efficiency. (**B**) When telomerase is recruited to a telomere through the Ku-Sir4 pathway, subsequent Est1-Cdc13-mediated recruitment to the end of the telomere becomes more efficient, resulting in increased telomerase extension of telomeres. The counterbalancing of Ku-

Sir4 telomerase recruitment and Rif1/Rif2 occlusion of Sir4 binding to Rap1 may represent a system for maintaining telomere-length homeostasis in yeast.

Chapter 3: Repositioning the Sm-binding site in TLC1 reveals organizational flexibility and Sm-directed 3′-end formation

Partially adapted from:

Evan P. Hass and David C. Zappulla. Repositioning the Sm-binding site in TLC1 reveals organizational flexibility and Sm-directed 3′-end formation. *bioRxiv*.

3.1: Introduction

In addition to Est1, Ku, and TERT (Est2), TLC1 is bound by the Sm_7 complex (Seto et al., 1999). Sm_7 is a heteroheptameric protein complex involved in biogenesis and stabilization of most spliceosomal snRNAs (Jones and Guthrie, 1990; Will and Luhrmann, 2001). The complex binds to the consensus sequence $AU_{5-6}GR$ (Branlant et al., 1982; Liautard et al., 1982; Mattaj and De Robertis, 1985; Hamm et al., 1987), which is present in TLC1 at nucleotides 1143–1150 (Figure 3-1A) (Seto et al., 1999). This site is located just 7 nucleotides 5′ of position 1157, which is the 3′ end of poly(A)– TLC1 (Bosoy et al., 2003), the aforementioned most-abundant ("major") isoform of TLC1. A less-abundant ("minor") isoform, poly(A)+ TLC1, contains an extra ~100 nucleotides of TLC1 sequence on its 3′ end, as well as a poly(A) tail (Chapon et al., 1997). In addition, there are very low-abundance TLC1 transcripts terminated by the Nrd1-Nab3-Sen1 (NNS) complex that only have ~50 extra nucleotides beyond the poly(A)– TLC1 3′ end at position 1157 (Jamonnak et al., 2011; Noel et al., 2012), but these transcripts are presumably not stable and are not detectable by northern blot.

In wild-type cells, the major poly(A)– TLC1 isoform is present at ~29 molecules per cell, while poly(A)+ TLC1 is present at only ~1 molecule per cell (Mozdy and Cech, 2006). However, when the Sm consensus in TLC1 is mutated, only the minor poly(A)+ TLC1 isoform is detectable, likely because poly(A)– TLC1 is not stable without Sm_7 bound (Seto et al., 1999). Due to this critically low abundance of telomerase RNA, these mutant cells (*tlc1-Sm*$^-$ cells) display senescence-related growth defects (e.g., small or mixed colony sizes), but do not display a fully senescent phenotype (Seto et al., 1999). This "near-senescent" growth phenotype seems to be in agreement with the fact that poly(A)+ TLC1 is present at only ~1 molecule per cell on average. Because 1 molecule of TLC1 per cell is the average over a population of cells, some cells in the population will probably have fewer molecules than average (i.e., none) and will eventually senesce, while others cells in the same population will have more than one molecule of TLC1 and will be able to lengthen their telomeres enough to continue dividing.

Although it was shown 18 years ago that Sm_7 binds to TLC1 (Seto et al., 1999), several questions about Sm function in the telomerase RNP remain unanswered. First, while it has been shown that Sm_7 can retain function when repositioned within Mini-T along with repositioning of the 5′ and 3′ ends of the RNA (also called "circular permutation") (Mefford et al., 2013), the flexible scaffold model has not been tested for Sm_7 in full-length TLC1 as it has been for Est1 and Ku. Additionally, there are several open questions regarding Sm_7 function in TLC1 biogenesis. It was proposed that TLC1 is initially transcribed as poly(A)+ TLC1 and that this RNA is then processed into poly(A)– TLC1 (Chapon et al., 1997). It has also been proposed that the nuclear exosome exonucleolytically trims poly(A)+ TLC1 from 3′ to 5′ and is then sterically blocked at nucleotide 1157 by Sm_7, thus generating poly(A)– TLC1 (Coy et al., 2013). Although it has been shown that nuclear exosome mutants accumulate more poly(A)+ TLC1 than wild type (Coy et al., 2013), the hypothesis that Sm_7 defines the mature 3′ end of poly(A)– TLC1 via this mechanism has remained untested. It also remains unclear whether poly(A)+ TLC1 is in fact the precursor of poly(A)– TLC1 or if NNS-terminated TLC1 transcripts are processed into the poly(A)– isoform.

Here, I show that Sm_7 retains its function in telomerase when repositioned via circular permutation in full-length TLC1, demonstrating that the Sm complex and the RNA ends are an organizationally flexible module on the telomerase RNP's RNA scaffold. Having shown that the Sm-binding site can function at diverse positions within circularly permuted TLC1, I next used Sm-site repositioning in the context of the unpermuted RNA to test the hypothesis that the Sm binding position defines the mature 3′ end of poly(A)– TLC1. When I repositioned the Sm site further 5′ in telomerase RNA, the stabilized poly(A)– TLC1 RNAs were correspondingly shorter than wild-type poly(A)– TLC1. This shows that Sm_7, in addition to providing stability, dictates formation of the mature end of this RNA just 3′ of its binding site. I also tested whether poly(A)+ TLC1 or the unstable NNS-terminated TLC1 transcripts are the unprocessed precursors of poly(A)– TLC1. When I repositioned the Sm-binding site further 3′ such that it would only be

present in poly(A)+ TLC1, not in the NNS-terminated TLC1 transcripts, the repositioned Sm site was unable to stabilize poly(A)– TLC1. While this result is consistent with a model in which only NNS-terminated TLC1 transcripts, not poly(A)+ TLC1, are processed to form poly(A)– TLC1, I cannot rule out other confounding possibilities for why this repositioned site did not stabilize poly(A)– TLC1 (e.g., misfolding of the Sm site at its new position).

3.2: Results

Sm_7 retains function when its binding site is repositioned by circular permutation in TLC1

To test if the Sm_7 protein complex retains its functions in the telomerase RNP when its binding site is repositioned in TLC1, I chose to reposition the Sm-binding site and the 3′ end together by circular permutation. Thus, Sm repositioning by circular permutation ("SmCP") alleles allow assessment of Sm functions at new locations in the RNP while retaining the Sm binding site location relative to the 3′ end of the RNA. I designed these *TLC1-SmCP* alleles using the TLC1 RNA secondary structure as a guide. As shown in Figure 3-2A, position 1134 was fused to position 1, thus excising the endogenous Sm site from its native location along with the downstream transcriptional termination sequences (Figure 3-1A). Then, newly encoded ends were introduced at 4 different positions in the *TLC1* sequence, while the Sm-binding region and transcriptional termination sequences (nucleotide 1130 to the end of the *TLC1* locus) were appended to the new 3′ end of the gene. Additionally, to maintain endogenous expression of TLC1, the *TLC1* promoter and first 10 nucleotides from the wild-type 5′ end were retained at the 5′ end of the new gene. SmCP alleles were created in this manner at positions 211, 451, and 1024 (Figures 3-1, 3-2A) — the same three positions used to reposition the Est1-binding region previously (Zappulla and Cech, 2004). Furthermore, in order to test the positional flexibility of Sm function in all three arms of TLC1, I also created an SmCP allele in the Est1 arm of TLC1, at position 546.

First, to test if these SmCP alleles maintain telomerase function and prevent senescence like wild-type TLC1, these RNAs were expressed from the *TLC1* promoter on a centromeric plasmid in a *tlc1*Δ background, and growth was monitored for ~250 generations. Notably, *TLC1-SmCP@211*, *@546*, and *@1024* all supported wild-type growth throughout the ~250 cell divisions (Figure 3-2B). This shows that the Sm_7 complex is functioning when its binding site is moved to these three different locations in TLC1. In contrast to these three alleles, one Sm site-repositioning circular permutant, *TLC1-SmCP@451*, led to a near-senescent phenotype very similar to *tlc1-Sm*$^-$ cells, causing mixed or small colony sizes after ~125 generations. However, when compared with the growth phenotype observed when the Sm site was mutated in this allele, this result suggests that Sm_7 in fact retains partial function in the SmCP@451 telomerase RNP. To control for whether the SmCP alleles affected growth for reasons other than Sm function, I also created "Sm$^-$CP" alleles, in which the repositioned Sm-binding consensus was mutated so that it is rendered binding-incompetent (Raker et al., 1999; Seto et al., 1999). Unlike the near-senescent cells expressing the conventional *tlc1-Sm*$^-$ allele, and in contrast to the sustained viability of cells expressing the SmCP alleles, cells expressing any of the 4 Sm$^-$CP alleles completely senesced by ~150 generations. The long-term viability of all SmCP strains compared to the senescence of all Sm$^-$CP strains shows that the Sm_7 protein complex retains its functions when bound at each of the four different positions in the circularly permuted TLC1 RNAs. Furthermore, these are the first circular permutants of full-length TLC1 RNA to be tested, and it is noteworthy that the telomerase RNA ends themselves can be repositioned to any of these four locations while permitting telomerase functionality *in vivo*. However, because unpermuted TLC1 with a mutated Sm site (tlc1-Sm$^-$) does not quite cause a senescent phenotype, the contrasting senescent phenotype of all of the Sm$^-$CP alleles suggests that circular permutation of the RNA interferes at least slightly with TLC1 function and/or accumulation.

Next, I assessed how TLC1 RNA processing and abundance was affected in the SmCP alleles. For all four SmCP alleles, the poly(A)– TLC1 isoform — predicted to be just 15 nt longer

than wild type (see Materials and methods) — was readily detectable by northern blotting, although at a lower abundance than wild type (Figure 3-2C). This shows that Sm_7 can perform its function in TLC1 3′-end processing and (to a lesser extent) RNA accumulation when its binding site is repositioned. The particularly low abundance of the SmCP@451 poly(A)– RNA probably contributes to why these cells exhibit a near-senescent phenotype. When I assessed TLC1 RNA abundance in the four Sm^{-}CP alleles, I observed that poly(A)+ TLC1 was essentially undetectable, unlike in cells containing the un-permuted *tlc1-Sm*$^{-}$ allele (Figure 3-2C; compare lanes 9–12 with lane 4). This shows that while cells expressing *tlc1-Sm*$^{-}$ accumulate just enough functional TLC1 RNA (poly(A)+) to prevent complete senescence, circularly permuting TLC1 without also including a functional Sm-binding site at the new 3′ end reduces RNA abundance to negligible levels, resulting in senescence.

I next assessed the effect of the Sm site repositioning and circular permutation on telomere length. I isolated genomic DNA from *TLC1-SmCP* cells at the end of passaging (i.e., ~250 and ~75 generations for the non-senescent and senescent conditions, respectively) and subjected the DNA to Southern blotting with a telomeric probe. The results show that cells expressing *SmCP@211* and *@546* alleles had the longest telomeres, although all four SmCP constructs supported lengths substantially shorter than wild type (Figure 3-2D, lanes 8–15). Overall, the telomere-length phenotypes were consistent with the cell-growth results, and they confirmed that telomeres were stably maintained through 250 generations, unlike in Sm^{-}CP cells. Telomeres were longer in *TLC1-SmCP@211* and *@546* cells than in the near-senescent *tlc1-Sm*$^{-}$ cells, providing additional evidence that Sm_7 is functioning when repositioned. As expected, the near-senescent *TLC1-SmCP@451* cells had the shortest telomeres of any of the SmCP alleles, averaging 212 bp shorter than wild type (lanes 10 and 11). Considering that the *SmCP@451* allele supported the shortest telomeres and the lowest RNA abundance, while the *SmCP@211* and *@546* cells had the longest telomeres and the highest RNA levels, these data suggest that relocated Sm_7 functioned best at positions 211 and 546 and that SmCP telomerase RNAs do not

support full-length telomeres primarily, or potentially entirely, because of their low levels of accumulation.

Sm binding defines the mature 3′ end of poly(A)- TLC1 RNA

It has been hypothesized that Sm_7 binding to TLC1 at nucleotides 1143–1150 defines the mature 3’ end of poly(A)– TLC1 at nucleotide 1157 by blocking exonucleolytic trimming of the 3′ end of an initially longer transcript (Seto et al., 1999; Coy et al., 2013). Although genetic data suggest that the nuclear exosome is involved in the maturation of poly(A)– TLC1 (Coy et al., 2013), the model that Sm-binding defines the mature 3′ end of poly(A)– TLC1 has not been rigorously tested. Having observed that Sm_7 functions when its binding site is repositioned in the telomerase RNA, I next tested the hypothesis that Sm_7 controls 3′-end formation in poly(A)– TLC1 by repositioning the Sm-binding site further 5′ in TLC1 without circular permutation. If the Sm binding site position defines the 3′ end of poly(A)– TLC1, repositioning the Sm-binding site to a position further 5′ in the RNA should correspondingly result in a truncated poly(A)– form. In the published secondary structure model of poly(A)+ TLC1 (nts 1–1251), the Sm-binding consensus is on the 5′ portion of an internal loop on the side of a hairpin, while nucleotide 1157 (the poly(A)– 3′ end) is predicted to be on the other side of this loop, directly across from the Sm-binding consensus (Figure 3-1B, inset) (Zappulla and Cech, 2004). Additionally, the nucleotides in and around this putative internal loop show higher sequence conservation (Zappulla and Cech, 2004; Mefford et al., 2013), suggesting that this predicted structure as a whole, not just the 8-nucleotide Sm-binding consensus, is required for Sm_7 to perform its function. Thus, based on this conservation and predicted local secondary structure, I chose nucleotides 1138 to 1165 as an RNA module that would be most likely to be functional when repositioned within TLC1. I then inserted this Sm-binding site in tlc1-Sm^- at positions 1089, 1003, and 926 (Figure 3-1B, inset). All three of these positions are predicted to be within bulged loops located on the distal half of the terminal arm, a region that is dispensable for telomerase function (Zappulla et al., 2005).

Cells expressing TLC1 RNAs with these relocated Sm sites were passaged for 250 generations to assay for senescence. Strains expressing tlc1-Sm⁻+Sm@1089 and @926 displayed wild-type growth, whereas *tlc1-Sm⁻+Sm@1003* cells exhibited a near-senescent growth phenotype, similar to *tlc1-Sm⁻* cells (Figure 3-3A). Northern blotting analysis revealed that, in agreement with the observed growth phenotypes, the Sm-binding sites inserted in tlc1-Sm⁻ at positions 1089 and 926 were functional in stabilizing poly(A)– TLC1 (at 1% and 7% of wild-type poly(A)– TLC1 abundance, respectively), while the Sm site inserted at position 1003 was not (Figure 3-3B). Additionally, the poly(A)– RNAs that were stabilized by the inserted Sm sites at positions 1089 and 926 were shorter than wild-type poly(A)– TLC1 RNA (red arrowheads, lanes 8, 9, 12, and 13), and their lengths were measured based on the northern blot to be within 0.1% and 1.9%, respectively, of their expected sizes given the positions of the inserted Sm sites (red arrowheads, lanes 8, 9, 12, and 13). This provides strong evidence that the position of Sm binding on TLC1 RNA defines the mature 3′ end of poly(A)– TLC1.

The Sm binding site does not function when repositioned further 3′ in the RNA, past the NNS site at position 1217

While it has been widely hypothesized that poly(A)– TLC1 is formed via processing of a longer RNA transcript (Chapon et al., 1997; Seto et al., 1999; Coy et al., 2013), it has not been shown definitively what this longer precursor is. Some have proposed that poly(A)+ TLC1 is an unprocessed precursor transcript of poly(A)– TLC1 (Chapon et al., 1997; Seto et al., 1999), but poly(A)+ TLC1 is not the only possible precursor to poly(A)– TLC1. TLC1 transcription can be terminated through one of two mechanisms. Poly(A)+ TLC1 is generated via termination by the polyadenylation machinery, resulting in polyadenylated transcripts ending between nucleotides 1239 and 1252 (Chapon et al., 1997). Alternatively, transcription can be terminated by the Nrd1-Nab3-Sen1 complex, resulting in oligoadenylated transcripts ending between nucleotide 1189 and 1221 (Jamonnak et al., 2011; Noel et al., 2012). To test which of these two transcripts are

processed into poly(A)– TLC1, I inserted an Sm-binding site at position 1217 (Figure 3-1), such that this repositioned Sm-binding site will only be present in transcripts terminated by the polyadenylation machinery, not those terminated by the NNS complex (since it is mostly 3′ of this site). The Sm site was inserted in both TLC1 and tlc1-Sm$^-$, and the inserted site was cloned with both a wild-type and mutated Sm consensus, resulting in four different alleles.

Upon expressing the four alleles with Sm sites at position 1217 in a *tlc1*Δ background and passaging the cells for ~250 generations, *TLC1+Sm@1217* and *+Sm$^-$@1217* cells displayed wild-type growth, whereas *tlc1-Sm$^-$+Sm@1217* and *tlc1-Sm$^-$+Sm$^-$@1217* cells both displayed a near-senescent phenotype (Figure 3-4A). This suggests that an Sm site inserted at position 1217 cannot compensate for loss of function at the native Sm site. In agreement with this result, northern blot analysis showed that inserting a wild-type Sm site at position 1217 did not have any observable effect on poly(A)– TLC1 biogenesis (Figure 3-4B). *TLC1+Sm@1217* cells did not have a longer poly(A)– TLC1 RNA as would be expected when repositioning the Sm site further 3′, and *tlc1-Sm$^-$+Sm@1217* cells did not have any stabilized poly(A)– TLC1.

The fact that an Sm site inserted at position 1217 does not function in stabilizing poly(A)– TLC1 could be explained in one of two ways. The first explanation is that poly(A)+ TLC1 is not the unprocessed precursor of poly(A)– TLC1, and only transcripts terminated by the NNS complex (short of the Sm site inserted at position 1217) are processed into poly(A)– TLC1. Alternatively, an Sm site inserted at position 1217, similar to an Sm site at position 1003, may be non-functional for reasons indirectly related to TLC1 biogenesis (e.g., improper folding of the Sm site at the new position, thus preventing Sm binding). In an attempt to distinguish between these possibilities, I tested whether a tract of 18 guanosines could stabilize poly(A)– TLC1. Poly(G) tracts have been shown previously to stabilize otherwise unstable RNAs by acting as a block to exonucleolytic degradation, and, unlike the Sm site, a poly(G) tract is hypothesized to form a G-quartet structure and therefore would not depend on protein binding in order to form this block (Muhlrad et al., 1995). I inserted a G_{18} tract at position 1217 in both TLC1 and tlc1-Sm$^-$ and at

positions 1136 (just 5′ of the native Sm site) and 1089 as controls. The G_{18} tract was largely unable to stabilize poly(A)– TLC1, regardless of where it was inserted in the RNA (Figure 3-5). *tlc1-Sm⁻+G₁₈@1136* and *@1217* cells both showed near-senescent growth phenotypes (although these cells did appear to grow incrementally more healthily than *tlc1-Sm⁻* cells), and *tlc1-Sm⁻ +G₁₈@1089* cells displayed a fully senescent phenotype (Figure 3-5A). Northern blot analysis showed a very small amount of poly(A)– TLC1 RNA stabilized in *tlc1-Sm⁻+G₁₈@1136* cells (lanes 10 and 11, red arrowhead), but none in either *tlc1-Sm⁻+G₁₈@1089* or *@1217* cells (Figure 3-5B).

3.3: Discussion

The telomerase RNA differs in many ways from other large, well-studied, non-coding RNAs such as ribosomal and spliceosomal RNAs. Although its existence is highly conserved among eukaryotes, its sequence and length vary greatly between species (Chen and Greider, 2004). Considering the rapid evolution of telomerase RNA along with experimental results has led to the model that telomerase RNA functions as a flexible scaffold for protein subunits in the telomerase RNP (Zappulla and Cech, 2004; Zappulla and Cech, 2006; Lebo and Zappulla, 2012; Mefford et al., 2013). Thus, unlike other large RNP enzymes that require a precise structural organization of components in the complex for function (e.g., the ribosome), the *S. cerevisiae* telomerase RNP has organization that has been shown to be strikingly flexible and this has provided a paradigm for many long noncoding RNAs (Zappulla and Cech, 2004; Zappulla et al., 2011; Mefford et al., 2013).

Here, I have shown that organizational flexibility of the yeast telomerase RNP extends to include the Sm_7 subunit, which binds just before the 3′ end of its RNA subunit's most abundant isoform and stabilizes it. Despite repositioning of the Sm site within TLC1 via circular permutation to four dramatically different locations across all three RNA arms, Sm_7 was still able to promote processing and stabilization of the major (poly(A)–) TLC1 isoform. Although

poly(A)– TLC1 RNA abundance was reduced in these SmCP alleles, Sm_7 still retained at least partial function at all positions tested. This demonstrates that Sm_7 and its binding site in TLC1 function as an organizationally flexible module, along with the RNA ends in the telomerase RNP. Between the results presented here and previous repositioning studies for the binding sites of Est1 and Ku subunits (Zappulla and Cech, 2004; Zappulla et al., 2011), it is now evident that TLC1 is an organizationally flexible scaffold for these three well-established RNA-bound holoenzyme subunits of telomerase. While organizational flexibility has not yet been tested for the Pop1/Pop6/Pop7 complex that was recently reported to bind to an essential sequence in TLC1 near the Est1-binding site (Lemieux et al., 2016), the entire Est1-Pop1/6/7-binding region of TLC1 has been shown to function when it is expressed in trans as a separate RNA while Est1 is artificially tethered to TLC1 (Lebo et al., 2015), suggesting that the flexible scaffold model applies to the Pop1/6/7 proteins as well.

After determining that Sm_7 can function at several different non-native positions within the telomerase RNP in the context of circular permutation, I next used Sm-site repositioning to test hypotheses regarding Sm functions in TLC1 RNA biogenesis. I first tested whether the position of Sm binding defines the mature 3′ end of poly(A)– TLC1 by repositioning the Sm-binding site further 5′ in the RNA. At 5′-shifted positions where the Sm site was functional, this resulted in stabilization of correspondingly shorter poly(A)– TLC1 RNAs, showing that Sm_7 does indeed direct 3′-end formation of poly(A)– TLC1. I also tested whether an Sm site inserted at position 1217 could stabilize poly(A)– TLC1. Because an Sm site inserted at position 1217 will not be included in NNS-terminated TLC1 transcripts, this experiment tested the hypothesis that poly(A)+ TLC1 is a precursor of poly(A)– TLC1. I found that when a wild-type Sm site was inserted at position 1217 in tlc1-Sm^-, poly(A)– TLC1 was not stabilized. This result is consistent with a model in which poly(A)+ TLC1 is not a precursor of poly(A)– TLC1 as previously hypothesized and only NNS-terminated TLC1 transcripts are processed into poly(A)– TLC1.

However, I cannot rule out the possibility that the Sm-binding site inserted at position 1217 itself was non-functional, so I cannot make any definitive conclusions from this experiment.

In an attempt to clarify the ambiguous results of the Sm@1217 experiments, I tested whether a tract of 18 guanines, previously shown to stabilize otherwise unstable RNAs (Muhlrad et al., 1995), could stabilize poly(A)– TLC1 in lieu of Sm_7 binding, but the G_{18} tract was unable to perform this function nearly as well as Sm_7 if at all. When the tract was inserted at position 1136 or 1217 in tlc1-Sm^-, there was a noticeable improvement in the near-senescent growth phenotype, but wild-type growth was not fully restored. This small yet detectable improvement in growth would seem to imply that small amounts of poly(A)– TLC1 was stabilized in *tlc1-*Sm^- *+*G_{18}*@1217* cells, which would in turn imply that poly(A)+ is indeed the unprocessed precursor of poly(A)– TLC1. However, no poly(A)– TLC1 was detected in *tlc1-*Sm^-*+*G_{18}*@1217* cells. While poly(A)– TLC1 was detected in *tlc1-*Sm^-*+*G_{18}*@1136* cells, the RNA was only 0.3% of wild-type RNA abundance, barely distinguishable from the background noise of the northern blot. Thus, though these experiments do not definitively indicate that NNS-terminated TLC1 transcripts are precursors of poly(A)– TLC1, neither do these experiments provide evidence for the previously proposed model that poly(A)+ TLC1 is the precursor of poly(A)– TLC1.

If NNS-terminated TLC1 transcripts, which are 20–50 nucleotides shorter than poly(A)+ TLC1 (Jamonnak et al. 2011), are bound by Sm_7 and undergo processing, the Sm-binding site in these RNAs likely adopts a conformation different from that in the published secondary structure model of the 1251-nt poly(A)+ TLC1 (Zappulla and Cech 2004). The most common site of NNS-mediated transcription termination in TLC1 is nucleotide 1195 (Jamonnak et al. 2011), and I observe that in an *Mfold* secondary-structure prediction of TLC1 RNA terminated at 1195, the Sm-binding consensus indeed does not form the same hairpin and internal-loop structure as that shown in the published secondary-structure model for poly(A)+ TLC1 (Figure 3-6). In this secondary-structure prediction for the 1195-nt form of TLC1, the Sm-binding consensus is largely single-stranded (except for a two-base pair hairpin that seems unlikely to be stable enough

to actually form), with the remaining sequence 3′ of the consensus forming a hairpin. Unlike the published secondary-structure model for poly(A)+ TLC1, this structural prediction of the 1195-nt form of TLC1 fits with the observation that many Sm-binding sites are single-stranded and are followed and/or preceded by hairpin structures (Branlant et al., 1982; Liautard et al., 1982). Given the similarities between this structural prediction and other more well-characterized Sm-binding sites, it is possible that the Sm-binding site in TLC1 adopts this conformation in at least some, if not all, unprocessed forms of TLC1.

In summary, repositioning the Sm-binding site and the ends of yeast telomerase RNA has yielded insights about the organizationally flexible nature of the RNA and the mechanistic role of Sm_7 in its biogenesis. Sm_7 can functionally tolerate repositioning of its binding site within TLC1 along with the RNA ends. Furthermore, the telomerase enzyme's fundamental functions can also endure the substantial reorganization of the RNA induced by circular permutations. Sm-site repositioning also has revealed that the mature 3′ end of poly(A)– TLC1 appears to be controlled by the location of Sm_7 binding to the RNA. The experimental approach of repositioning the Sm binding site in order to move the mature 3′ end of poly(A)– TLC1 may ultimately prove useful in identifying the precursor of poly(A)– TLC1 and fully characterizing the pathway for telomerase RNA biogenesis in budding yeasts.

3.4: Materials and methods

Construction of *TLC1-SmCP* alleles

The *TLC1-SmCP* alleles were constructed using a plasmid containing two tandem copies of *TLC1*. In this construct, the two copies of *TLC1* are fused into a single gene such that nucleotide 1134 of the first *TLC1* copy is followed directly by nucleotide 1 (see Figure 3-2A) of the second *TLC1* copy, meaning that the Sm site and transcriptional termination sequences are absent in the first *TLC1* sequence. Circular permutation was performed by PCR-amplifying specific segments of this template DNA beginning at the site of repositioning in the first *TLC1*

copy and ending at the same site in the second copy (e.g., for *SmCP@211*, this resulted in a PCR product containing base pairs 211–1134 followed by 1–210). These circularly permuted DNAs were inserted into a separate plasmid containing the natural ends of the *TLC1* gene such that sequences from nucleotide 10 upstream and from nucleotide 1130 downstream (which includes the Sm site) are retained at the ends of the new gene. As an example, the sequence of *TLC1-SmCP@211* is laid out from promoter to terminator as follows: the *TLC1* promoter through nucleotide 10, 211–1134, 1–210, and 1130 through the transcriptional terminator and natural end of the TLC1 gene (see Figure 3-2A). As a result of this construction scheme, nucleotides 1–10 and 1130–1134 are contained twice in all *TLC1-SmCP* alleles, making the RNAs 15 nucleotides longer than wild-type *TLC1*.

Experiments in yeast

All experiments were performed in the strain TCy43 (*MATa ura3-53 lys2-801 ade2-101 trp1-1 his3-Δ200 leu2-Δ1 VR::ADE2-TEL adh4::URA3-TEL tlc1::LEU2 rad52::HIS3 pTLC1-LYS2-CEN*) (Seto et al., 1999). All *TLC1* alleles were expressed from centromeric plasmids derived from pSD107 (*pTLC1-TRP1-CEN*) (Diede and Gottschling, 1999). TCy43 was transformed with *TLC1*-containing plasmids, and colonies were streaked to minimal –TRP–LYS medium. Loss of the *pTLC1-LYS2-CEN* cover plasmid was selected for by re-streaking cells to minimal –TRP medium containing α-aminoadipate. These cells were then serially re-streaked nine times to minimal –TRP medium and photographed after each round of growth. When estimating the number of generations at different points throughout passaging, each round of growth after loss of the cover plasmid (including the round of growth in the presence of α-aminoadipate) is approximated as 25 generations.

Northern blotting

Northern blotting was performed as described previously (Zappulla et al., 2005; Zappulla et al., 2011; Hass and Zappulla, 2015; Lebo et al., 2015). Briefly, cells from the serial passaging plates were grown in liquid cultures to an OD600 of ~1.0 and harvested, and total RNA was isolated using the hot-phenol method (Kohrer and Domdey, 1991). 15-30 µg of total RNA from each sample was boiled, separated by urea-PAGE, and then transferred to Hybond-N^+ Nylon membrane (GE). The membrane was UV-crosslinked and probed for both TLC1 and U1 sequence. The membrane was probed with ~100-fold fewer counts of U1 probe than TLC1 probe to account for the large difference in abundance between the two RNAs. TLC1 RNA abundance was calculated by normalizing to U1 abundance, and numbers in the text and figures are expressed relative to the wild-type TLC1 condition. Lengths of poly(A)– TLC1 RNAs in Figure 3-3B were calculated using the molecular weight standard shown.

Southern blotting

Southern blotting was performed as described previously (Zappulla et al., 2005; Zappulla et al., 2011; Hass and Zappulla, 2015; Lebo et al., 2015). Briefly, cells were grown and harvested in the same manner as those used for northern blots, and genomic DNA was isolated from these pellets (Gentra Puregene system). Roughly equal amounts of genomic DNA were digested with XhoI and then separated on a 1.1% agarose gel. DNA was transferred to Hybond-N^+ Nylon membrane (GE) to which it was UV-crosslinked, and the membrane was probed for yeast telomeric sequence and a 1621-bp non-telomeric XhoI fragment that served as a non-telomeric control band (Friedman and Cech, 1999). Average Y′ telomere length was calculated using the weighted average mobility method described previously (Zappulla et al., 2011).

Figure 3-1: TLC1 sequence schematic and secondary-structure models.

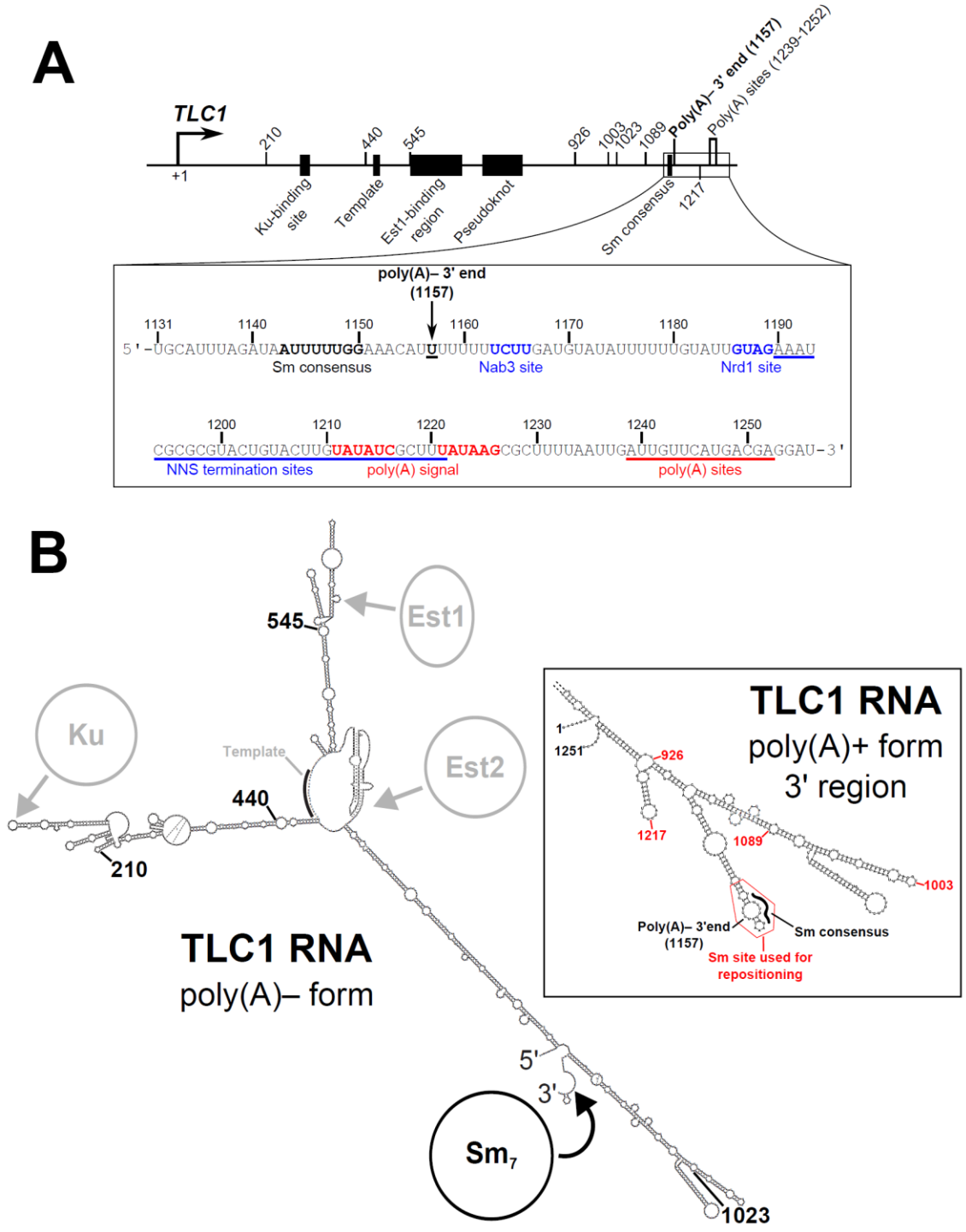

(**A**) Schematic of the *TLC1* gene sequence. The *TLC1* regions encoding the Ku-binding site, template, Est1-binding region, pseudoknot, and Sm consensus in the RNA are denoted as black rectangles. Locations of all Sm-repositioning sites are noted by tick marks, as are the poly(A)– 3′

end and the polyadenylation sites. The inset shows the RNA sequence of the TLC1 3′ region. The Sm consensus and poly(A)– 3′ end are noted in bold. The Nab3 and Nrd1 binding sites are bolded in blue, and the region containing NNS termination sites is underlined in blue (Jamonnak et al., 2011; Noel et al., 2012). Similarly, the polyadenylation signal is red boldface, and the region containing polyadenylation are underscored by a red line (Chapon et al., 1997). (**B**) Secondary structure models of 1157- and 1251-nt forms of TLC1. The pictured secondary structure of poly(A)– TLC1 is the same as that shown in Figure 1-1. The location of Sm binding is indicated in black as are the four locations to which the Sm binding site and the 5′ and 3′ ends are repositioned in the SmCP alleles used in Figure 3-2. The binding regions for Ku, Est1, and Est2 and the template region are indicated in gray. The inset shows the secondary structure model of the 3′ region of poly(A)+ TLC1 based on a previously published model (Zappulla and Cech, 2004). The portion of the RNA used when repositioning the Sm-binding site (nucleotides 1138 to 1165) is outlined in red. The locations of the Sm consensus and poly(A)– 3’ end are noted in black, and the four positions to which this Sm-binding site was repositioned in Figures 3-3 and 3-4 are indicated in red.

Figure 3-2: Sm_7 retains function in telomerase RNA when its binding site is repositioned via circular permutation.

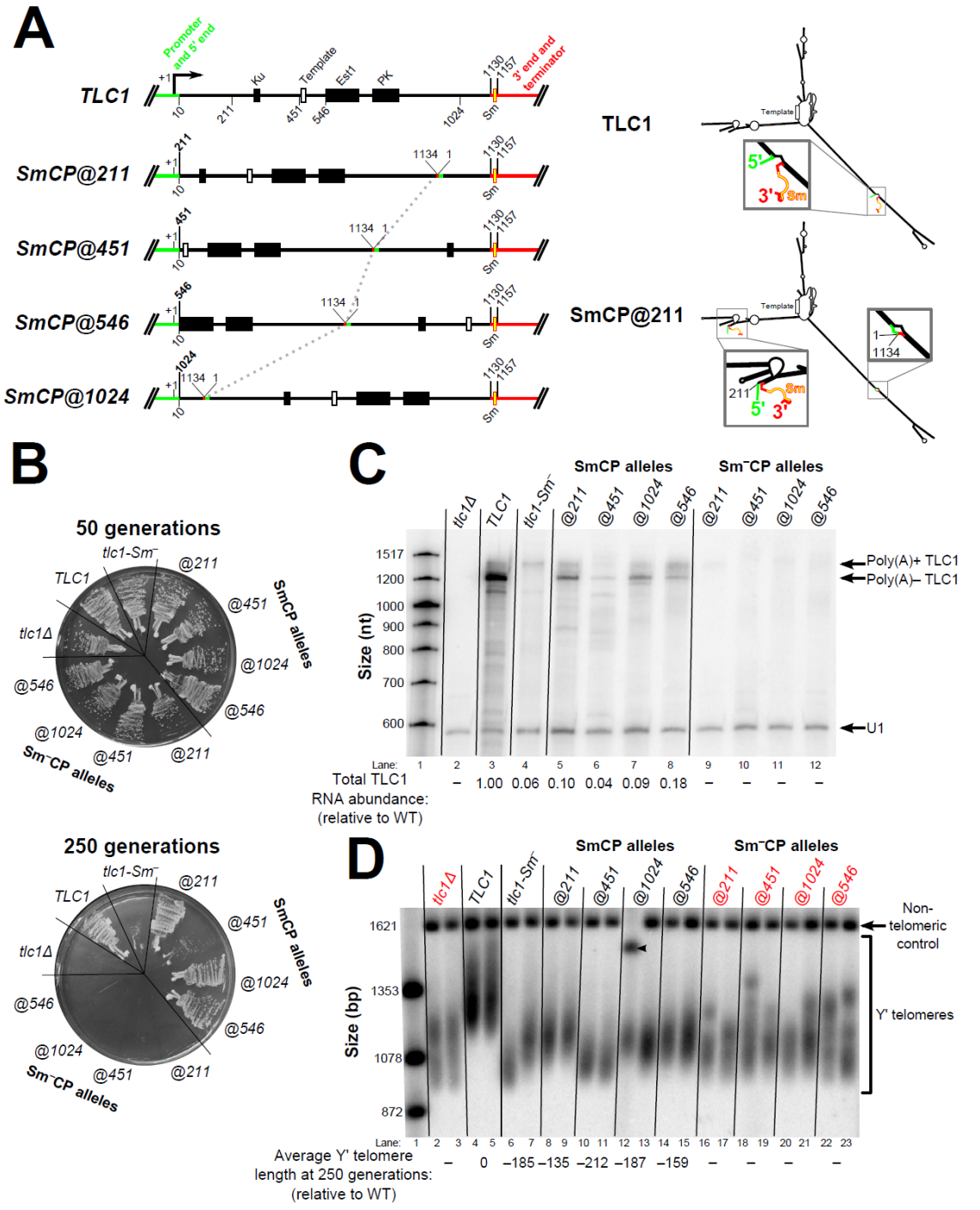

(**A**) Schematics of *SmCP* gene construction and expected RNA structure. The native ends of the *TLC1* gene were effectively sealed off by connecting nucleotide 1134 with nucleotide 1, thus

removing the Sm site from its native position in the RNA. A dashed line connects the location of this 1134-to-1 fusion between the 4 circularly permuted alleles. The wild-type *TLC1* promoter through nucleotide 10 (green) as well as the sequence from nucleotide 1130 on (red) flank the circularly permutated central 1–1130 region, thereby repositioning the Sm-binding site (yellow) along with the 5′ and 3′ ends in the encoded transcript. Black rectangles indicate the Ku-binding site, Est1-binding region, and pseudoknot (PK). A white rectangle indicates the template. The secondary-structure models of wild-type TLC1 and an example of an SmCP (TLC1-SmCP@211) are schematized to the right, using the same coloring scheme as in the gene diagrams to the left. Details of the secondary structure of these large RNAs are omitted in these low-resolution schematics for the sake of simplicity, but, in fact, these regions of TLC1 have wild-type sequence and predicted secondary structure very similar to wild type as well. (**B**) *TLC1-SmCP* alleles with a wild-type Sm-binding site support sustained growth and do not cause cells to senesce. All *TLC1* alleles were expressed from centromeric plasmids in a *tlc1*Δ *rad52*Δ background, and cells were serially passaged on solid media for ~250 generations (10 re-streaks). (**C**) Sm_7 confers poly(A)–telomerase RNA stabilization and appropriate 3′-end formation when repositioned via circular permutation. Total RNA was isolated from cells used in the passaging experiment shown in Figure 3-2B and analyzed by northern blotting with TLC1 and U1 snRNA probes. Total TLC1 RNA abundance was normalized to U1 abundance to control for sample loading in each lane and then set relative to the wild-type condition. The numbers displayed below the blot are averages of two independent biological replicates. (**D**) SmCP alleles support stable, short telomeres. Genomic DNA was isolated from cells in the passaging experiment in Figure 3-2B at ~250 generations for non-senescent conditions (labeled in black) and ~75 generations for senescent conditions (labeled in red). Telomere length was then analyzed by Southern blotting. The blot was probed for telomeric sequence and for a 1621-bp non-telomeric restriction fragment (non-telomeric control). The pairs of lanes in the blot shown are independent biological-replicate samples, and the telomere length numbers are averages of the two replicates except in the *TLC1-SmCP@1024*

condition. In this condition, the telomere length could not be quantified in the first replicate due to anomalous migration of the non-telomeric control (black arrowhead), so the displayed telomere length number in this condition is a quantitation of only the second replicate sample.

Figure 3-3: Repositioning the Sm binding site at two of three positions further 5′ in TLC1 results in stabilization of shorter poly(A)– TLC1 RNAs.

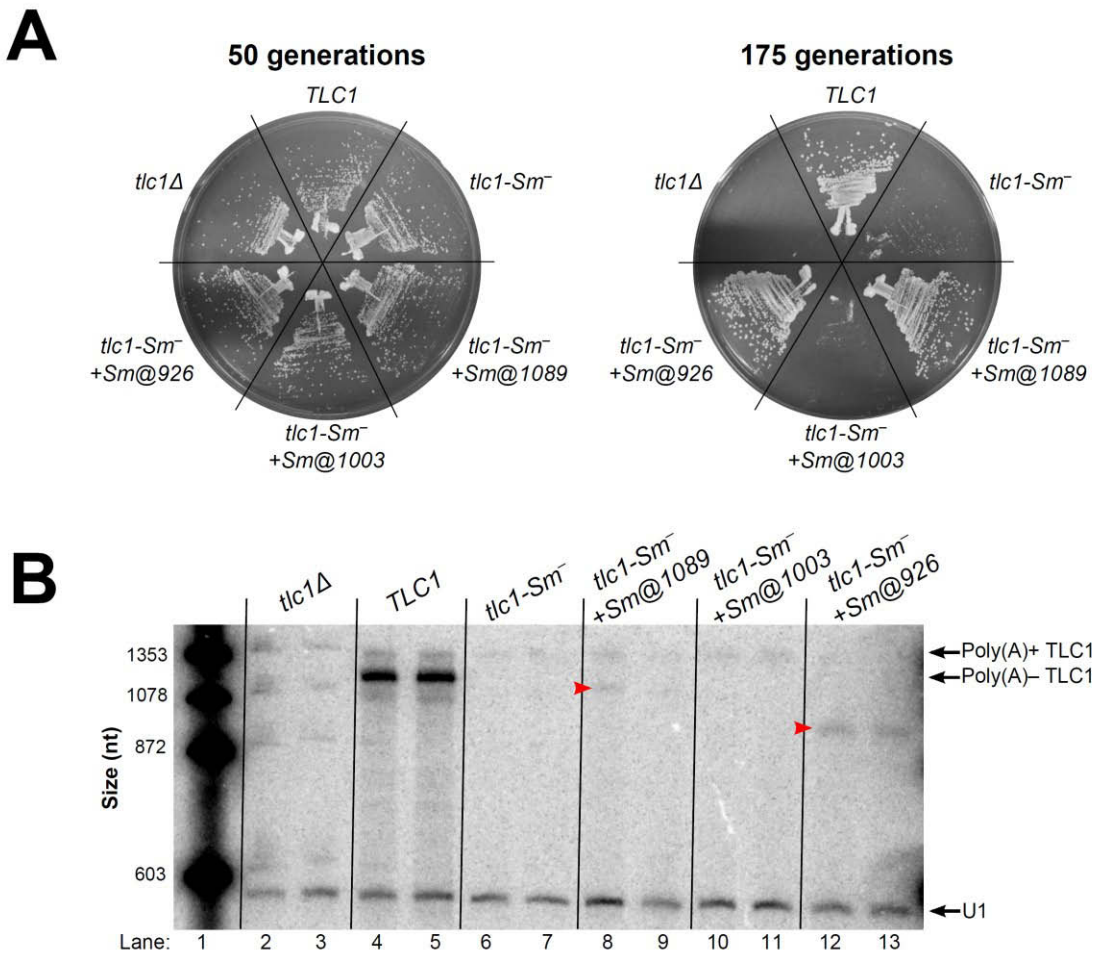

(**A**) Sm sites inserted in tlc1-Sm⁻ restored robust growth at positions 1089 and 926, but not at 1003. *TLC1* alleles were expressed and cells were passaged as in Figure 3-2. (**B**) Functional Sm sites inserted 5′ of the native position in tlc1-Sm⁻ stabilized shorter poly(A)– TLC1 RNAs. Total RNA was isolated from cells used in the passaging experiment in Figure 3-3A and analyzed by northern blotting as in Figure 3-2C. Red arrowheads indicate the shorter poly(A)– TLC1 RNAs stabilized in *tlc1-Sm⁻+Sm@1089* and *tlc1-Sm⁻+Sm@926* cells. The pairs of lanes represent independent biological-replicate samples.

Figure 3-4: An Sm site inserted at position 1217 cannot stabilize poly(A)– TLC1.

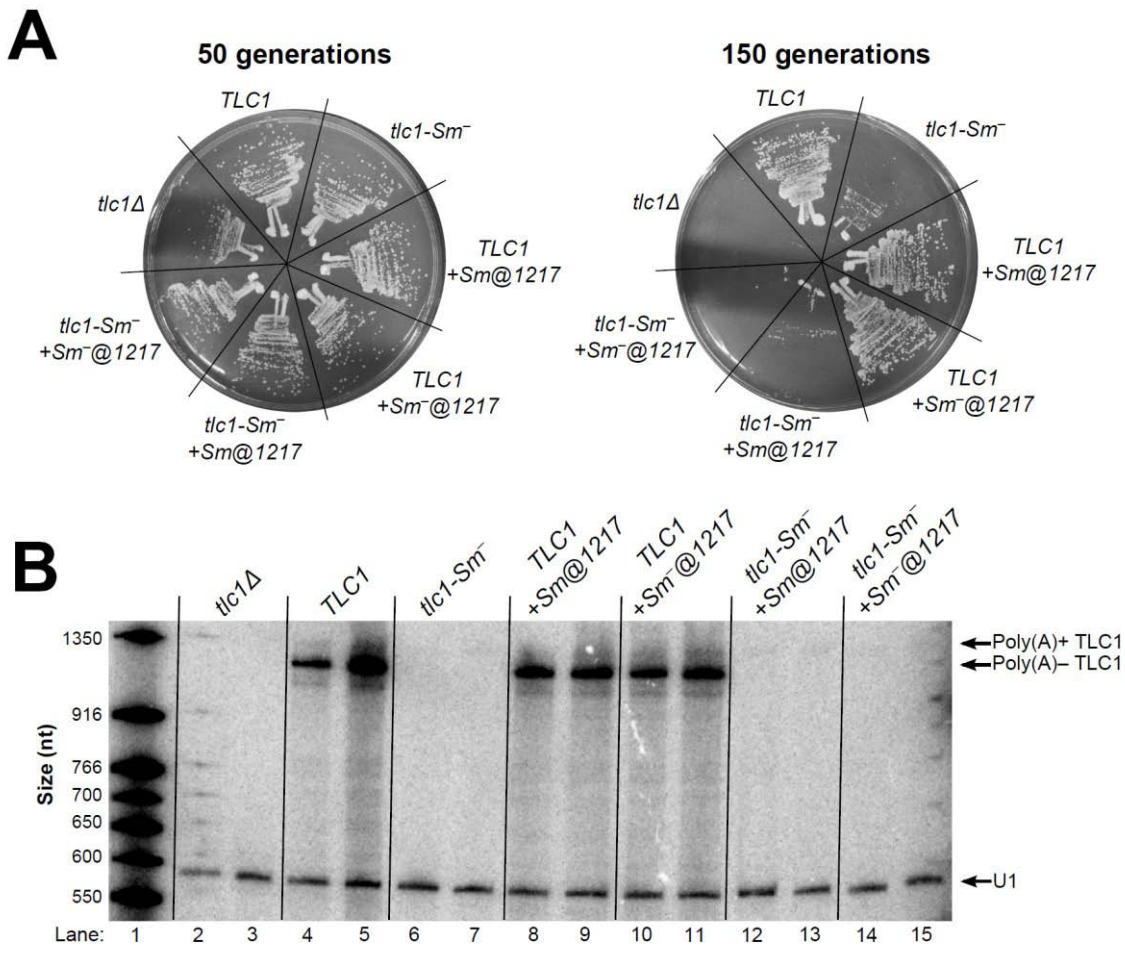

(**A**) Inserting an Sm site at position 1217 in tlc1-Sm⁻ does not prevent a near-senescent phenotype. TLC1 alleles were expressed and cells were passaged as in Figure 3-2. (**B**) An Sm site inserted at position 1217 does not function in stabilization or 3′-end definition of poly(A)– TLC1. Total RNA was isolated from cells used in the passaging experiment in Figure 3-4A and was subsequently analyzed by northern blotting as in Figure 3-2C. The pairs of lanes represent independent biological replicate samples.

Figure 3-5: Inserting a G_{18} tract in TLC1 cannot compensate for loss of Sm function.

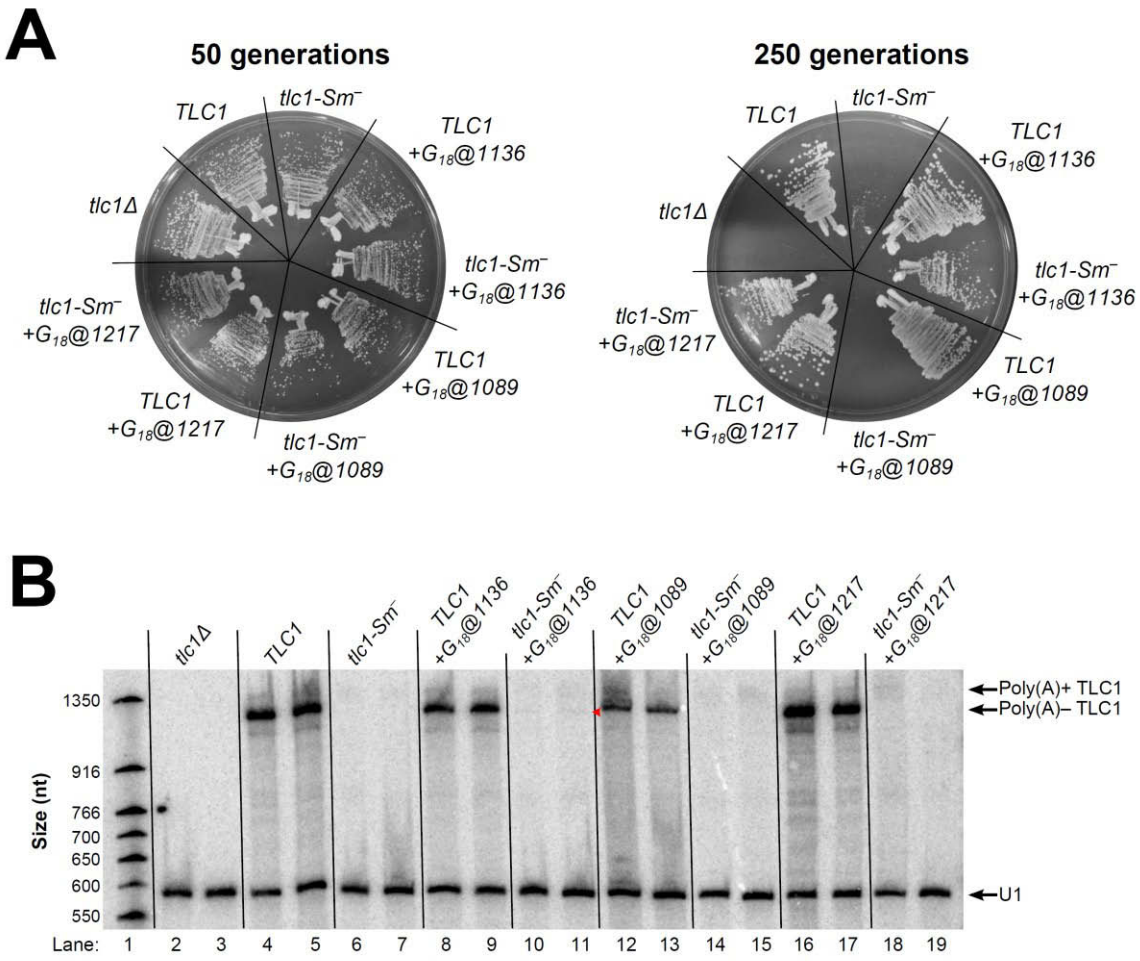

(**A**) Inserting G_{18} tracts in tlc1-Sm⁻ slightly improves near-senescent growth at positions 1136 and 1217, but causes senescence when inserted at position 1089. TLC1 alleles were expressed and cells were passaged as in Figure 2. (**B**) G_{18} tracts inserted in tlc1-Sm⁻ stabilize very little to no poly(A)– TLC1 RNA. Total RNA was isolated from cells used in the passaging experiment in Figure 3-5A and was subsequently analyzed by northern blotting as in Figure 3-2C. The red arrowhead indicates the very small amount of poly(A)– TLC1 RNA that appears to be stabilized in *tlc1-Sm⁻+G₁₈@1136* cells. The pairs of lanes represent independent biological replicate samples.

Figure 3-6: *Mfold* software prediction for the secondary structure of NNS-terminated TLC1 (nucleotides 1–1195).

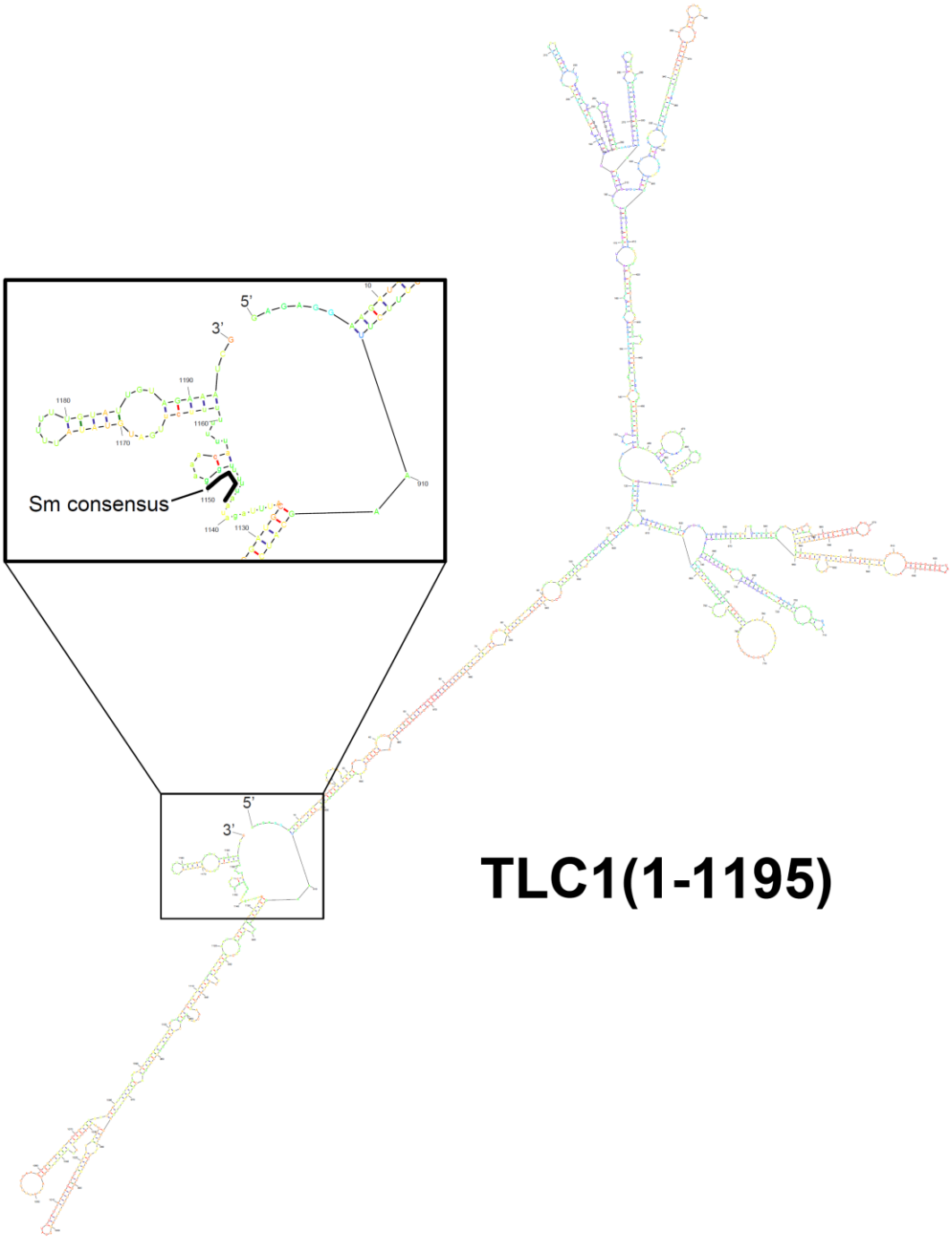

The structure is colored using the pnum preset on the *Mfold* RNA web server to reflect the determinedness based on free-energy calculations (Zuker and Jacobson, 1998). The 3′ end of the RNA structure is enlarged in the inset, and the Sm-binding consensus is outlined in black.

Chapter 4: CARRY two-hybrid: A CRISPR-based yeast two-hybrid system for studying RNA-protein interactions

Partially adapted from:

Evan P. Hass and David C. Zappulla. 2017. A CRISPR-based yeast-two hybrid system for investigating RNA-protein interactions. *bioRxiv*.

4.1: Introduction

RNA-binding proteins are integral to the function of RNAs. Many RNA functions are mediated by associated proteins (e.g., chromatin modification by lncRNA-bound enzymes, recruitment of telomerase RNA to telomeres by protein subunits of telomerase). As for functional RNAs that ultimately act protein-independently (e.g., peptide-bond formation by ribosomal RNA, mRNA splicing by spliceosomal RNA), these transcripts still require associated proteins for their proper folding, processing, modification, stabilization, and localization. Because so many cellular RNA-protein interactions remain unknown, it is advantageous to pursue their discovery using high-throughput approaches. The advent and continual improvement of high-throughput DNA sequencing technology has led to the development of many powerful techniques, such as RIP-seq and CLIP-seq, which can be used to identify the full repertoire of RNAs bound by a protein of interest. However, relatively fewer protocols exist for identifying proteins that bind to a particular RNA. Most available techniques involve RNA pull-down followed by protein identification via mass spectrometry, which requires large amounts of starting material, meaning that low-abundance RNA-protein complexes are difficult to study with this approach (McHugh et al., 2014).

In an effort to address the relative dearth of techniques for identifying binding partners for a given RNA, I have developed a novel technique: CRISPR-assisted RNA/RBP yeast (CARRY) two-hybrid (Figure 4-1A). Like the original yeast two-hybrid assay (Fields and Song, 1989; Chien et al., 1991), CARRY two-hybrid interrogates binding between two biological macromolecules by tethering one to the promoter of a reporter gene and fusing the second to a transcriptional activation domain. Expression of the reporter gene occurs when there is binding between the two macromolecules. Unlike the original yeast two-hybrid system, instead of tethering a protein of interest to the promoter by fusing it to a DNA-binding domain, CARRY two-hybrid tethers an RNA of interest. RNA tethering is achieved using the *Streptococcus pyogenes* CRISPR machinery. While the CRISPR/Cas9 system has commonly been co-opted for

the purpose of making targeted cuts in DNA, nuclease-deactivated Cas9 (dCas9) can target an RNA or protein of interest to a specific genomic locus by fusing it to the CRISPR single-guide RNA (sgRNA) or to Cas9, respectively (Shechner et al., 2015; Zalatan et al., 2015). CARRY two-hybrid uses the former of these two strategies to target an RNA of interest to a shared sequence at the promoters of the yeast two-hybrid reporter genes, *HIS3* and *LacZ*. These reporter genes are then activated if a protein that has been fused to the Gal4 transcriptional activation domain (GAD) binds to the promoter-tethered RNA (Figure 4-1A).

In this chapter, I show that CARRY two-hybrid works. The yeast two-hybrid reporter genes are activated contingent on binding between an sgRNA-fused RNA and GAD-fused protein. Furthermore, CARRY two-hybrid is specific, and my experiments using the MS2 hairpin and MS2 coat protein from the MS2 phage show that this method is sufficiently sensitive to detect RNA-protein interactions with near-micromolar dissociation constants. CARRY two-hybrid can also detect the interaction between the minimal TLC1 RNA core and Est2. Using this assay to test mutants of TLC1 for TERT binding, I find that the core-enclosing helix, a conserved secondary structure element in telomerase RNA cores, and a neighboring single-stranded junction region are required for TERT binding. Based on my experiments with CARRY two-hybrid, I expect that the system will prove to be a very useful new tool for the identification and characterization of RNA-protein interactions.

4.2: Results

Design and construction of a yeast two-hybrid system to study RNA-protein binding

I constructed the yeast strain used for CARRY two-hybrid, "CARRYeast (1.0)," by integrating a dCas9 expression cassette (Zalatan et al., 2015) in the genome of a previously published yeast two-hybrid strain, L40, which contains the reporter genes *HIS3* and *LacZ* with 4 and 8 LexA-binding sites inserted in their promoters, respectively (Hollenberg et al., 1995). While several adaptations of the CRISPR/Cas9 system used in *S. cerevisiae* express the sgRNA

from an RNA polymerase III promoter (DiCarlo et al., 2013; Laughery et al., 2015), I chose to express the hybrid sgRNA for CARRY two-hybrid using an RNA polymerase II promoter, since RNA polymerase III transcription can be terminated by even a relatively short poly(U) tract (Allison and Hall, 1985), whereas RNA polymerase II termination signals are more complex and therefore should be rarer (Tian and Graber, 2012; Porrua and Libri, 2015). Thus, because premature termination of transcription in the middle of the hybrid sgRNA would make the CARRY two-hybrid system unusable, RNA polymerase II ultimately imposes fewer restrictions than RNA polymerase III on the RNA sequences that can be tested in this system.

In order to express the hybrid sgRNA, I modified a previously published RNA polymerase II sgRNA expression construct (Zalatan et al., 2015) (Figure 4-1B). Because the mRNA promoter and terminator introduce extraneous sequence at the 5′ and 3′ ends of the expressed RNA (e.g., the poly(A) tail), I chose to use a construct that employs a ribozyme-guide RNA-ribozyme (RGR) cassette for sgRNA processing (Gao and Zhao, 2014). In an RGR cassette, an sgRNA is flanked by the hammerhead and HDV ribozymes that self-cleave, thus excising the sgRNA from the longer initial transcript *in vivo*. I cloned this RNA polymerase II RGR sgRNA expression cassette into a centromeric yeast vector and changed the guide sequence at the 5′ end of the sgRNA to target the RNA to the LexA-binding sites upstream of both the *HIS3* and *LacZ* reporter genes. Finally, in order to facilitate the cloning of diverse RNA domains into this hybrid sgRNA expression vector, I inserted a multiple-cloning site (MCS) containing five unique, commonly used restriction-enzyme cleavage sites near the 3′ end of the sgRNA, four nucleotides 5′ of the HDV ribozyme cleavage site. Because at least some of the MCS will ultimately be part of the transcribed hybrid sgRNA (depending on the restriction sites used for subcloning), it was designed to form a hairpin when transcribed, making it less likely to pair with and disrupt folding of the inserted RNA of interest. In an *Mfold* computational prediction of the sgRNA-MCS secondary structure, in which the guide sequence was forced to be single-stranded, most of the MCS sequence is indeed predicted to form a hairpin, as designed (Figure 4-1C). Although the

first four nucleotides of the MCS sequence are predicted to pair with part of the sgRNA rather than with the last four nucleotides of the MCS sequence, these few predicted base pairs (one of which is a G•U pair) apparently did not prevent the expected tethering of the sgRNA to its target sites by dCas9 based on reporter-gene activation results (see below).

CARRY two-hybrid can specifically detect the MS2-MCP interaction

I first sought to test the CARRY two-hybrid system with a well-understood RNA-protein interaction, such as the MS2 bacteriophage's RNA hairpin binding to the phage's coat protein. I cloned the MS2 RNA hairpin mutant, U-5C — which binds the MS2 coat protein more tightly than the wild-type hairpin (Romaniuk et al., 1987) — into the sgRNA expression vector, and I also cloned a tandem dimer of the MS2 coat protein (MCP_2) into a standard vector for expression of Gal4-activating domain (GAD) fusion proteins in the yeast two-hybrid system, pGAD424 (Chien et al., 1991; Bartel et al., 1993). These plasmids were then transformed into CARRYeast (1.0), and expression of *HIS3* and *LacZ* were assessed by growth of cells on medium lacking histidine and by a colorimetric assay, respectively. When both the sgRNA-U-5C MS2 hybrid RNA and the GAD-MCP_2 hybrid protein were expressed, expression of both *HIS3* and *LacZ* was strongly induced (Figure 4-2A, third row; Figure 4-2B, bottom right). Importantly, activation was dependent on the MS2 hairpin being fused to the sgRNA (Figure 4-2A, rows 1 and 2; Figure 4-2B, top panels), and MCP_2 being fused to GAD (Figure 4-2A, rows 2 and 4; Figure 4-2B, left panels). This indicates that the CARRY two-hybrid system is able to detect RNA-protein interactions, and that it does so specifically. Furthermore, while I observed some low-level background expression of the *LacZ* reporter gene in some negative controls, as is often observed in the standard yeast two-hybrid system using the CARRYeast (1.0)'s parent strain L40 (Andrulis et al., 2002; Zappulla et al., 2006), the *HIS3* reporter gene (which is the reporter gene to be used for forward-genetic selection of GAD fusion-protein libraries), consistently showed no background signal with negative controls.

CARRY two-hybrid can detect RNA-protein interactions with near-micromolar dissociation constants

Next, to test the sensitivity of the CARRY two-hybrid system, I replaced the U-5C MS2 hairpin with the wild-type MS2 hairpin and several biochemically characterized mutants of the MS2 hairpin with a range of weaker binding affinities for the MS2 coat protein (Romaniuk et al., 1987). In my tests of these MS2 hairpin mutants, *HIS3* and *LacZ* were activated by interactions several orders of magnitude weaker than the U-5C MS2 interaction with MCP ($K_d \approx 20$ pM) (Figure 4-3). For the wild-type MS2 hairpin ($K_d \approx 3$ nM) and the C-14A/U-12A/A1U/G3U MS2 hairpin ($K_d \approx 45$ nM, hereafter referred to as the AU-helix MS2 hairpin), activation of the *HIS3* and *LacZ* reporters appeared just as strong as that for the U-5C hairpin. For the A-7C hairpin ($K_d \approx 300$ nM), activation of the *HIS3* reporter was detectable when undiluted culture was spotted on medium lacking histidine (Figure 4-3B, row 5), whereas no activation of the *LacZ* reporter was observed (Figure 3C, lower left panel). Finally, the A-7U hairpin, which binds to MCP with a dissociation constant ≥10 μM, did not activate either *HIS3* or *LacZ*.

Next, to test if I could increase the sensitivity of the CARRY two-hybrid system, I subcloned the sgRNA expression cassette from a ~single-copy centromeric plasmid to a high-copy 2μ (2-micron) plasmid and re-tested activation for several of the MS2 hairpin mutants. Although expression of the hybrid sgRNA from the high-copy plasmid could not increase the already-maximal *HIS3* activation for the U-5C or AU-helix mutant MS2 hairpins (Figure 4-4A, compare row 2 with 6 and 3 with 7), in contrast, the activation of the *HIS3* reporter was increased ~10,000-fold for the A-7C MS2 RNA hairpin (Figure 4-4A, compare rows 4 and 8) compared to when the sgRNA was expressed from a low-copy plasmid. Importantly, the negative controls — either expressing the sgRNA alone or GAD alone when using the high-copy plasmid — did not result in any detectable *HIS3* activation (Figure 4-4B) or *LacZ* activation (data not shown). In contrast to results with the *HIS3* reporter gene, activation of the *LacZ* reporter was not visibly

increased by expressing the hybrid sgRNA from a high-copy plasmid (Figure 4-4C). Thus, in summary, although the *LacZ* reporter in the CARRY two-hybrid system is not very responsive, the *HIS3* reporter is sensitive, with low background and substantial dynamic range, making it highly useful as an in vivo indicator of RNA-protein binding.

Using CARRY two-hybrid to detect and investigate the TLC1-Est2 binding interaction

Having demonstrated the capabilities of the CARRY two-hybrid system using the MS2-MCP interaction, I sought to use the assay to answer a biological question about the yeast telomerase RNP, the focus of my thesis research. Of the many subunits in the telomerase RNPs from yeast and other organisms, the only two universally conserved subunits are TERT and the telomerase RNA. In TLC1, as in all other telomerase RNAs, the conserved core region contains the major binding site for TERT (Livengood et al., 2002; Chappell and Lundblad, 2004; Lin et al., 2004). The TLC1 core contains four secondary structure elements that are highly conserved in telomerase RNAs and are always present in the same 5′-to-3′ order (Lin et al., 2004): the core-enclosing helix (CEH), the template-boundary element (TBE), the single-stranded template, and the pseudoknot, which then connects back to the 3′ half of the core-enclosing helix (Figure 4-5A). These elements are separated by four single-stranded regions named junctions 1, 2, 3, and 4. Previous studies have implicated the core-enclosing helix and the second stem of the pseudoknot in binding Est2 (Chappell and Lundblad, 2004; Lin et al., 2004), but the full details of what features are required for TERT binding remain unclear. This is especially true of the single-stranded junction regions. Deleting junction 1 impairs telomerase activity, while deleting junction 4, only two nucleotides long, completely abolishes telomerase activity (Mefford et al., 2013). It remains unclear whether junctions 1 and 4 play roles in assembly of the core enzyme (i.e., TERT binding) or in function of the assembled telomerase enzyme.

To investigate in greater detail what parts of the TLC1 core are bound by Est2, I cloned the minimal 170-nucleotide TLC1 core (Qiao and Cech, 2008) and Est2 into the CARRY two-

hybrid system and assayed for this RNA-protein interaction. When both the sgRNA-TLC1 core and GAD-Est2 fusions were expressed in CARRYeast(1.0), I observed moderate activation of the *HIS3* reporter gene (Figure 4-5B) but no activation of the *LacZ* reporter (data not shown). Next, I sought to evaluate the role of the junction regions in this interaction. Similar to their effects on telomerase activity, I found that deleting junction 1 in the minimal TLC1 core reduced *HIS3* activation, while deleting junction 4 completely abolished activation. As a control, I also tested whether deleting junction 3, which has no effect on telomerase activity (Mefford et al., 2013), impaired TERT binding as assayed by CARRY two-hybrid. Surprisingly, deleting junction 3 completely abolished *HIS3* activation, similar to the effects of deleting junction 4. However, considering that the TLC1 core lacking junction 3 is still active and therefore must be competent for binding TERT, this disruption of *HIS3* activation is likely an artefact of the CARRY two-hybrid system. While junctions 1 and 4 are only 5 and 2 nucleotides long, respectively, junction 3 is 15 nucleotides long, so deleting junction 3 may have disrupted folding of the TLC1 core in ways that deleting junctions 1 or 4 wouldn't.

It has been shown previously that disrupting pairing in the core-enclosing helix disrupts Est2 binding to TLC1 (Lin et al., 2004). However, when this pairing is disrupted, it is possible that the nucleotides of the core-enclosing helix then participate in other, non-native pairings, disrupting the folding of other structures in the TLC1 core. Instead of simply disrupting pairing in the CEH, it is possible to delete this element while maintaining connectivity between the pseudoknot and template-boundary element, the so-called area of required connectivity (ARC) (Mefford et al., 2013). This is achieved by performing a circular permutation to move the 5′ and 3′ ends to the end of the template-boundary element helix ("cpTBE"). Performing this circular permutation does not affect telomerase activity, but deleting the CEH in this context ("cpTBEΔCEH") completely abolishes activity even though connectivity in the ARC is maintained.

To test if a clean deletion of the core-enclosing helix causes a loss of TERT binding, I cloned both the cpTBE and cpTBEΔCEH TLC1 cores into the CARRY two-hybrid system. Very similar to their effects on telomerase activity, I found that cpTBE did not affect *HIS3* activation by the TLC1-Est2 interaction, while *HIS3* activation was completely abolished when the core-enclosing helix was deleted in this context (Figure 4-5B). Together, my CARRY two-hybrid experiments with the TLC1 core show that the core-enclosing helix and junction 4 are required for TERT binding, while junction 1 also plays an important role in this interaction.

4.3: Discussion

I have developed a new assay for investigating RNA-protein interactions, "CARRY two-hybrid," that combines CRISPR/dCas9 RNP-mediated targeting of RNA to a specific DNA sequence with the highly effective yeast two-hybrid protein-protein interaction assay. As evidenced by tests I performed using CARRY two-hybrid to analyze bacteriophage MS2 hairpin binding to MS2 coat protein, this new assay can detect RNA-protein interactions *in vivo* with high specificity (i.e., virtually no background signal for the *HIS3* reporter gene) and can detect interactions with near-micromolar dissociation constants. I also used this assay to investigate the interaction between Est2 and the TLC1 RNA core and found that junction 4 and the core-enclosing helix are required for this interaction, while junction 1 is also important.

Given the simplicity of the CARRY two-hybrid system and the ease with which it has functioned in my hands thus far, I expect that it will prove to be a highly effective method for dissecting known RNA-protein interfaces, as well as for the discovery of new RNA-protein interactions. I have constructed a vector with a multiple-cloning site to facilitate fusing an RNA of interest to the sgRNA (see Figure 4-1C). The RNA polymerase II promoter allows CARRY two-hybrid to be used to study a large variety of RNA-encoding DNA sequences, and the self-cleaving ribozymes in the initial transcript RNA "bait" in the two-hybrid system trim extraneous sequences from the 5′ and 3′ ends (Gao and Zhao, 2014; Zalatan et al., 2015) (Figure 4-1B).

Additionally, because the CARRY two-hybrid assay is built upon the well-established protein-protein yeast two-hybrid system (Vidal and Fields, 2014), the existing GAD fusion libraries constructed by labs and companies can now also be used for studying proteins binding to RNA.

CARRY two-hybrid is similar to the yeast "three-hybrid" system in the sense that the three-hybrid method also assays for RNA-protein interactions by building upon the basic principles underlying the original yeast two-hybrid assay. The three-hybrid system, published over 15 years ago, employs the well-characterized, high-affinity MS2-MCP RNA-protein interaction (or RRE-RevM10 from HIV (Putz et al., 1996)) to tether RNAs of interest to reporter-gene promoters by way of fusing them to the MS2 hairpin, while also appending MCP to a specific DNA-binding protein domain; thus, there is a total of three hybrid molecules (SenGupta et al., 1996). However, there has been limited success using the three-hybrid system, as evidenced by the relative paucity of publications referencing use of three-hybrid. Although I have yet to directly compare the capabilities of CARRY two-hybrid with those of yeast three-hybrid, I anticipate that CARRY two-hybrid is likely to prove to be even more useful. The recruitment of the Gal4 activating domain to the reporter genes in yeast three-hybrid necessitates three different binding interactions (e.g., DNA LexA sites • LexADBD–MCP • MS2 RNA–X • Y–GAD). In contrast, the CARRY two-hybrid system uses CRISPR/dCas9 to directly target RNA to DNA. By reducing the number of stable binding events required for activating reporter genes to two, as well as other features that promote efficiency and robustness described above, CARRY two-hybrid is likely to be more effective at detecting RNA-protein interactions. Future studies will show if this bears out.

In my experiments using CARRY two-hybrid to study the Est2-TLC1 interaction, I found that junction 4 and the core-enclosing helix are required for this interaction, while junction 1 is also important. My finding that the core-enclosing helix is required for TERT binding confirms previous results, and my findings with respect to junctions 1 and 4 represent new understanding regarding the TERT-TLC1 interaction. Given that junction 4 is only two nucleotides long, it is

quite striking that its deletion causes a complete loss of telomerase function and TERT binding to TLC1 (Mefford et al., 2013). However, in contrast to deletion of junction 4, lengthening junction 4 only impairs telomerase function, and mutation of junction 4 does not affect telomerase activity at all (Mefford et al., 2013), suggesting that TERT may not in fact bind junction 4 directly. Though it is possible that TERT binds junction 4 through sequence non-specific contacts, junction 4 may not in fact be directly contacted by TERT. Given that junction 4 is positioned directly between the second stem of the pseudoknot and the core-enclosing helix, the two paired elements implicated in TERT-binding (Chappell and Lundblad, 2004; Lin et al., 2004), junction 4 instead may be required to maintain proper spacing of these two elements. This could explain why deleting junction 4 abolishes telomerase function while lengthening junction 4 only partially impairs telomerase function (Mefford et al., 2013). Given that the core-enclosing helix and pseudoknot likely need a minimum distance between them in order to reach their proper contact points on TERT, deleting junction 4 would restrict them from reaching these sites, while lengthening junction 4 would simply cause the extra nucleotides to bulge out from the normal position of junction 4 in the TERT-TLC1 complex. It is possible that junction 1 plays a similar spacing role, despite the fact that deleting junction 1 does not cause as drastic an effect as deleting junction 4. Similar to junction 4, lengthening junction 1 impairs telomerase activity but changing its sequence has no effect (Mefford et al., 2013), suggesting that the length of junction 1 is its most important property for proper telomerase function. If junction 1 is indeed required for proper spacing of the TLC1 core, this in turn would suggest that the template boundary-element contains a part of the TERT binding site that must be properly spaced with the core-enclosing helix for maximal function of telomerase. However, further experiments are required to test this hypothesis.

4.4: Materials and methods

Construction of yeast strains and plasmids for CARRY two-hybrid

CARRYeast (1.0) was generated by modifying the yeast two-hybrid strain L40 (*MATa his3Δ200 trp1-901 leu2-3,112 ade2 LYS2::(4LexAop-HIS3) URA3::(8LexAop-LacZ)*) (Hollenberg et al., 1995). First, yeast cells were transformed with linearized pJZC518 (Zalatan et al., 2015) containing a cassette for expression of the *S. pyogenes* dCas9 in *S. cerevisiae*, *C. glabrata LEU2* selectable marker, and homology arms for integration at the *S. cerevisiae LEU2* locus. In the resulting yeast strain, the *C. glabrata LEU2* selectable marker was subsequently deleted using a cassette generated using pFA6a-KanMX6 (Longtine et al., 1998).

The sgRNA expression vectors, pCARRY1 and pCARRY2, were based on pJZC625 (Zalatan et al., 2015). This plasmid contains a ribozyme-guide RNA-ribozyme (RGR) cassette (Gao and Zhao, 2014). The sgRNA in pJZC625 contained a guide sequence targeted to the TET operator and a U-5C MS2 hairpin inserted 4 nucleotides before the HDV ribozyme cut site. The RGR cassette is flanked by the *S. cerevisiae ADH1* promoter and the *C. albicans ADH1 terminator*. To generate pCARRY1, pJZC625 was digested with ApaI and BglII, and the full expression cassette was cloned into pRS414 (Sikorski and Hieter, 1989) that had been digested with ApaI and BamHI. Second, the guide sequence of the sgRNA was changed to target the LexA operator sequence ACTGCTGTATATAAAACCAG, which is followed by a protospacer adjacent motif (PAM) with sequence TGG in the LexA operators present in CARRYeast (1.0). Additionally, in order to maintain base-pairing in the H1 stem of the hammerhead ribozyme of the RGR cassette (the 3′ half of which consists of the first 6 nucleotides of the sgRNA guide sequence), the sequence of the 5′ half of the H1 stem was changed to AGCAGT. Third, the MS2 hairpin was replaced with GGATCCCATGGGTCGACCCCGGGAATTC, an earlier-designed version of the hairpin-forming multiple-cloning site sequence (MCSv0.5). This sequence was later replaced with the MCS sequence shown in Figure 4-1C (GGATCCGTCCATGGAGTCGACTCCCGGGCGAATTC), generating pCARRY1. This modified version of the original RGR expression construct was then subcloned into pRS424 (Christianson et al., 1992) using KpnI and SpeI to generate pCARRY2. The original U-5C MS2

hairpin sequence present in pJZC625 (GCGCACATGAGGATCACCCATGTGC), the minimal 170-nucleotide TLC1core (Qiao and Cech, 2008), and mutants thereof were cloned into pCARRY1 and pCARRY2 using BamHI and EcoRI.

The vectors used to express the GAD-MCP_2 and GAD-Est2 fusion proteins were cloned using pGAD424 (Bartel et al., 1993). For MCP_2, DNA encoding a tandem MCP dimer and an N-terminal linker (i.e., ultimately between GAD and MCP_2 in the final plasmid) with amino-acid sequence GGGR was PCR amplified from the plasmid pDZ349 (Lebo et al., 2015) and cloned into pGAD424 using XmaI and PstI. Both MCP monomers contain the N55K mutation, reported to strengthen binding to the MS2 hairpin ~10-fold (Lim et al., 1994), while the first monomer also contains the incidental mutations K57R and I104V. For Est2, an insert containing the *EST2* ORF and an N-terminal 8-glycine linker was PCR amplified from yeast genomic DNA and cloned into pGAD424 using XmaI and PstI.

HIS3 reporter gene spot assay

Expression of the *HIS3* reporter gene in CARRYeast (1.0) was assayed by first growing yeast in liquid culture (using minimal medium lacking tryptophan and leucine) to saturation overnight. 100-µL aliquots were taken from these cultures and used to make six 10-fold serial dilutions of the culture. 5 µL of the undiluted aliquot and each serial dilution were pipetted onto both solid –Trp –Leu and –Trp –Leu –His minimal media. These spotted cells were then incubated for two days at 30°C and photographed.

LacZ reporter gene assay

Colorimetric *LacZ* reporter gene expression assays were performed as described previously (Bartel et al., 1993). Briefly, expression of the *LacZ* reporter gene in CARRYeast (1.0) was assayed by first streaking the cells as patches on –Trp –Leu medium and incubating for ~15–24 hours at 30°C. Yeast were then removed from the agar plate by applying and removing a

circular nitrocellulose membrane. Yeast attached to the nitrocellulose were lysed by brief submergence in liquid nitrogen. Then, in a petri dish, a piece of Whatman filter paper was wetted with 1.8 mL of 100 mM sodium phosphate buffer pH 7.0 with 10 mM KCl, 1 mM $MgSO_4$, and 333 μg/mL X-gal. The nitrocellulose filter was soaked in the X-gal solution by laying it, face up, on top of the Whatman paper, and the petri dish was incubated at 30°C. The color of the lysed yeast cells was monitored and photographed at time intervals over ~24 hours, or until the dish had dried out and the reaction had stopped.

Figure 4-1: The CARRY two-hybrid assay for interrogating RNA-protein interactions.

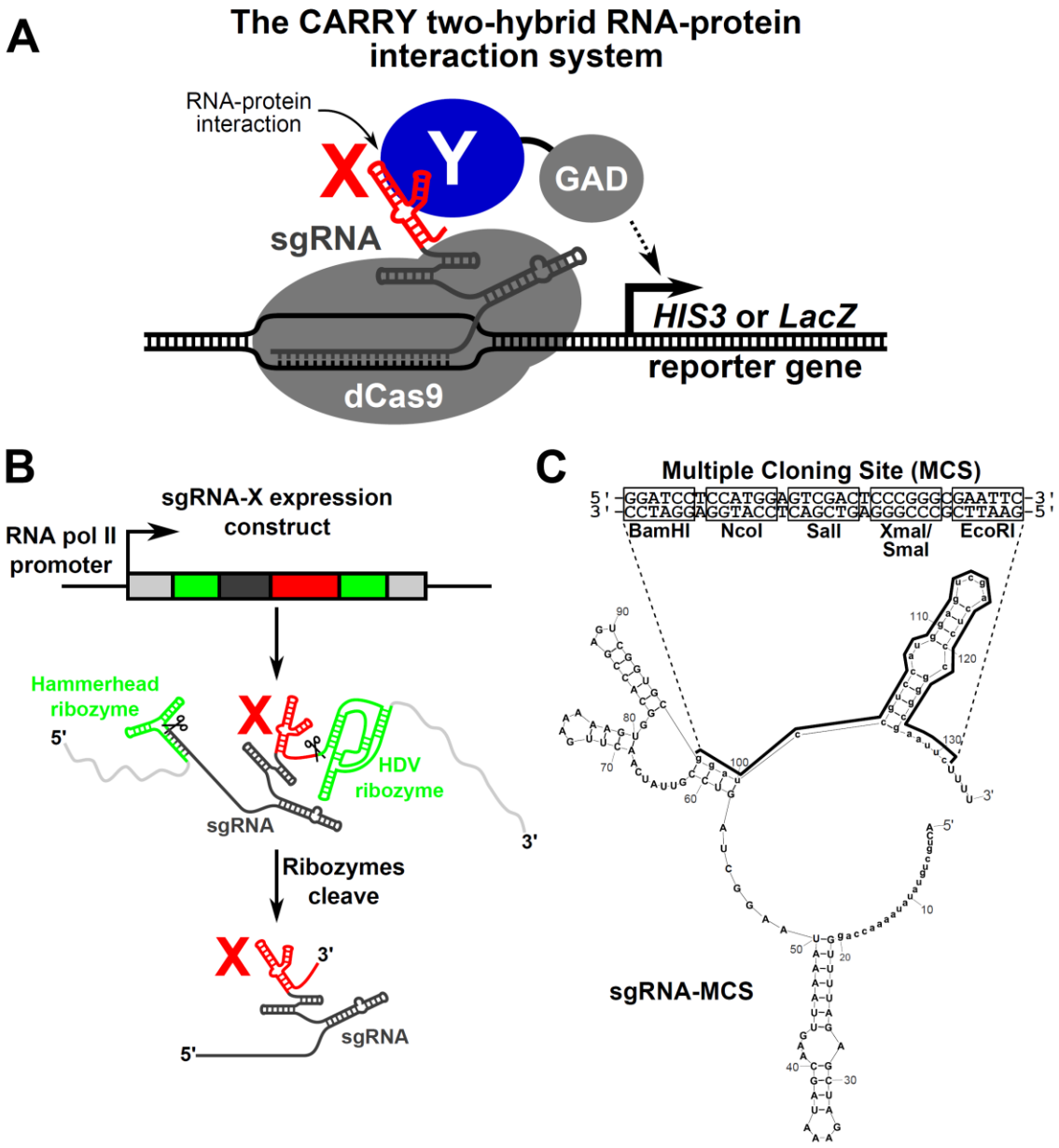

(**A**) Schematic of the CARRY two-hybrid system. An RNA of interest ("X", red) is fused to a CRISPR single guide RNA (sgRNA), which is targeted to the promoters of the reporter genes *HIS3* and *LacZ* with assistance from the nuclease-deactivated *Streptococcus pyogenes* Cas9 protein (dCas9). If the RNA of interest fused to the sgRNA binds to the protein ("Y", blue) fused to the Gal4 activation domain (GAD), the transcription of the reporter gene is activated. (**B**) A schematic of the "RGR" sgRNA expression cassette (Gao and Zhao, 2014; Zalatan et al., 2015).

The hybrid sgRNA is expressed from an RNA polymerase II promoter, flanked by the hammerhead and HDV ribozymes (green). Once transcribed, the ribozymes catalyze self-cleavage of the RNA, processing the mature hybrid sgRNA out of the longer transcript. (**C**) The hybrid sgRNA plasmid used in CARRY two-hybrid contains a multiple-cloning site (MCS) that forms a hairpin when transcribed into RNA. Shown is an *Mfold* prediction of the secondary structure of the sgRNA-MCS, in which the guide of the sgRNA was forced to be single-stranded. The MCS RNA sequence is bracketed, and its DNA sequence is shown underneath, with its five unique restriction sites annotated.

Figure 4-2: The MS2-MCP interaction strongly activates the *HIS3* and *LacZ* reporter genes of the CARRY two-hybrid system.

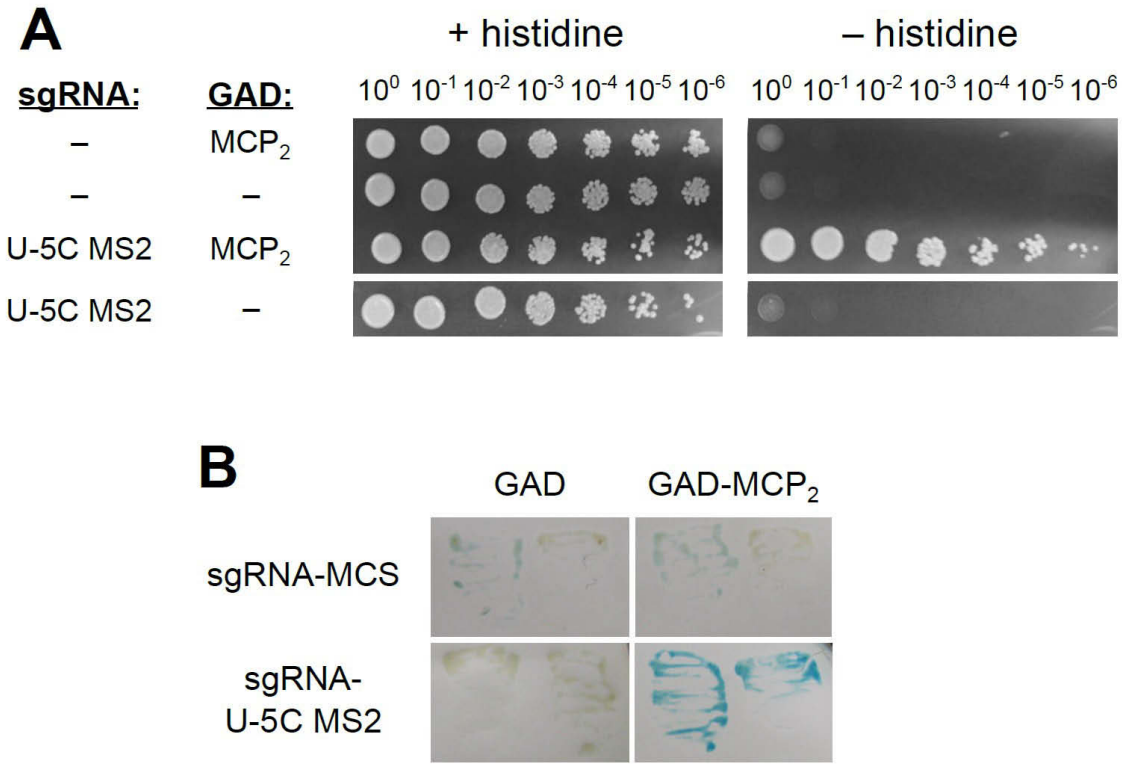

(**A**) The *HIS3* reporter gene in CARRYeast (1.0) is activated strongly and specifically by the MS2-MCP interaction. Yeast cells were grown to saturation in liquid culture. Cells from the undiluted culture and from six 10-fold serial dilutions (as indicated above the images) were spotted to, and grown on, medium with or without histidine. In the columns on the left, minus signs denote that the sgRNA or GAD were not fused to any RNA or protein, respectively. In the case of the sgRNA, this means that it contained the MCS sequence shown in Figure 4-1C. (**B**) The *LacZ* reporter gene in CARRYeast (1.0) is activated strongly and specifically by the MS2-MCP interaction. Yeast were grown overnight, lysed on a nitrocellulose filter with liquid nitrogen, and exposed to X-gal, as described in Materials and Methods. The filter was left at 30°C overnight for color to develop until the filter had dried out and the reaction had stopped. Pairs of yeast patches are biological replicate samples.

Figure 4-3: The sensitivity of the CARRY two-hybrid system: detection of RNA-protein binding interactions with near-micromolar dissociation constants.

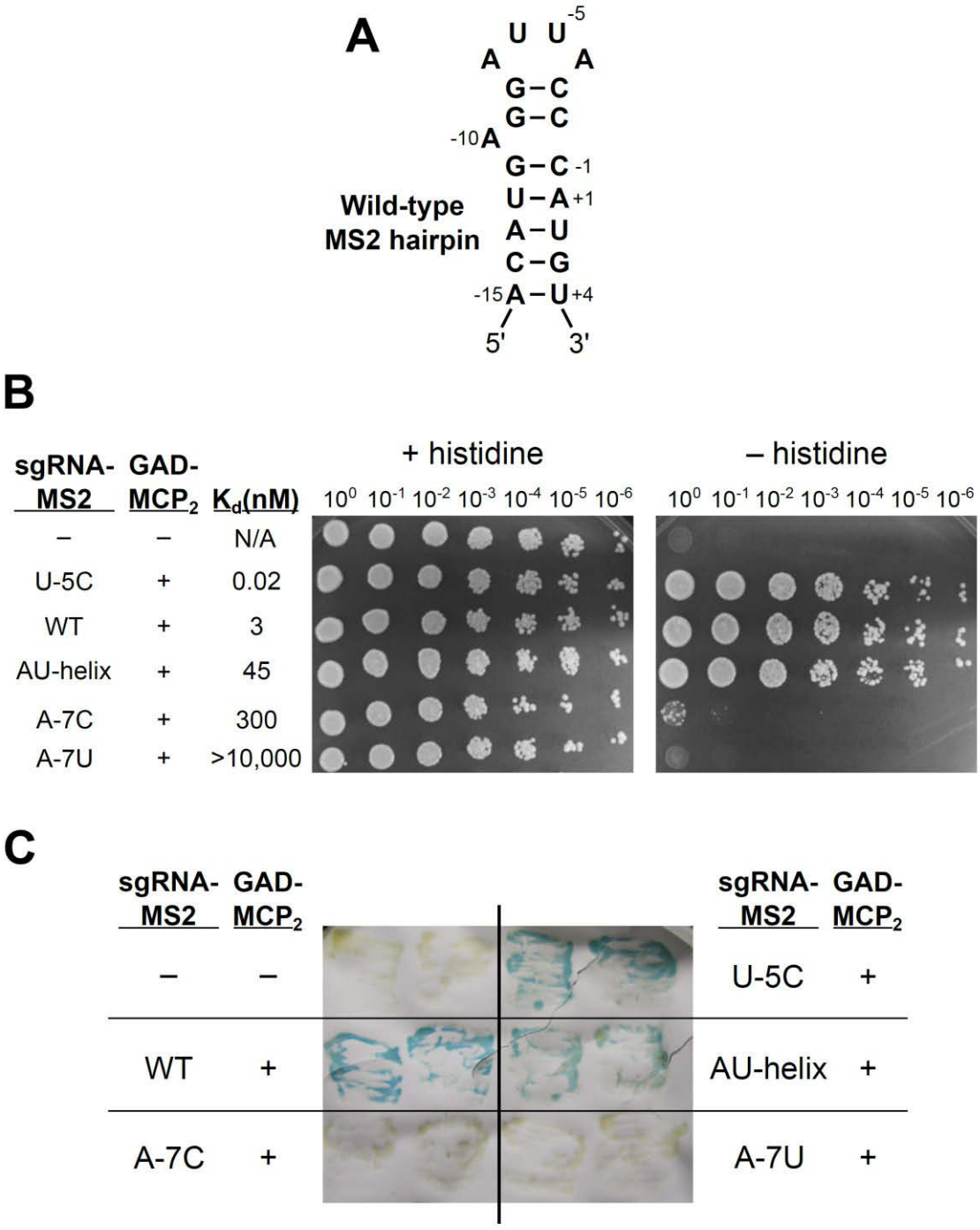

(**A**) The secondary structure of the wild-type MS2 RNA hairpin. Nucleotide numbering is based on the AUG start codon of the MS2 bacteriophage's replicase gene and serves as the basis for the

nomenclature of MS2 point mutants. (**B**) The *HIS3* reporter gene in CARRYeast (1.0) is activated robustly by MS2-MCP interactions with dissociation constants as high as 300 nM. Yeast were grown as in Figure 4-2A on solid media containing or lacking histidine. The dissociation constants reported here and in the text were calculated using association constants reported previously (Romaniuk et al., 1987). "AU-helix" refers to the C-14A/U-12A/A1U/G3U MS2 hairpin quadruple mutant. (**C**) The *LacZ* reporter gene in CARRYeast (1.0) is activated by MS2-MCP interactions with dissociation constants as high as 45 nM. Yeast were grown, lysed, and exposed to X-gal as in Figure 4-2B. Pairs of yeast patches are biological replicate samples. In Figures 4-3B and 4-3C, as in Figure 4-2A, minus signs denote that no RNA or protein was fused to the sgRNA or GAD, respectively. In this figure, an earlier design of the sgRNA MCS sequence, MCSv0.5, was used as a negative control (see Materials and Methods).

Figure 4-4: Expression of the hybrid sgRNA from a high-copy plasmid increases assay sensitivity.

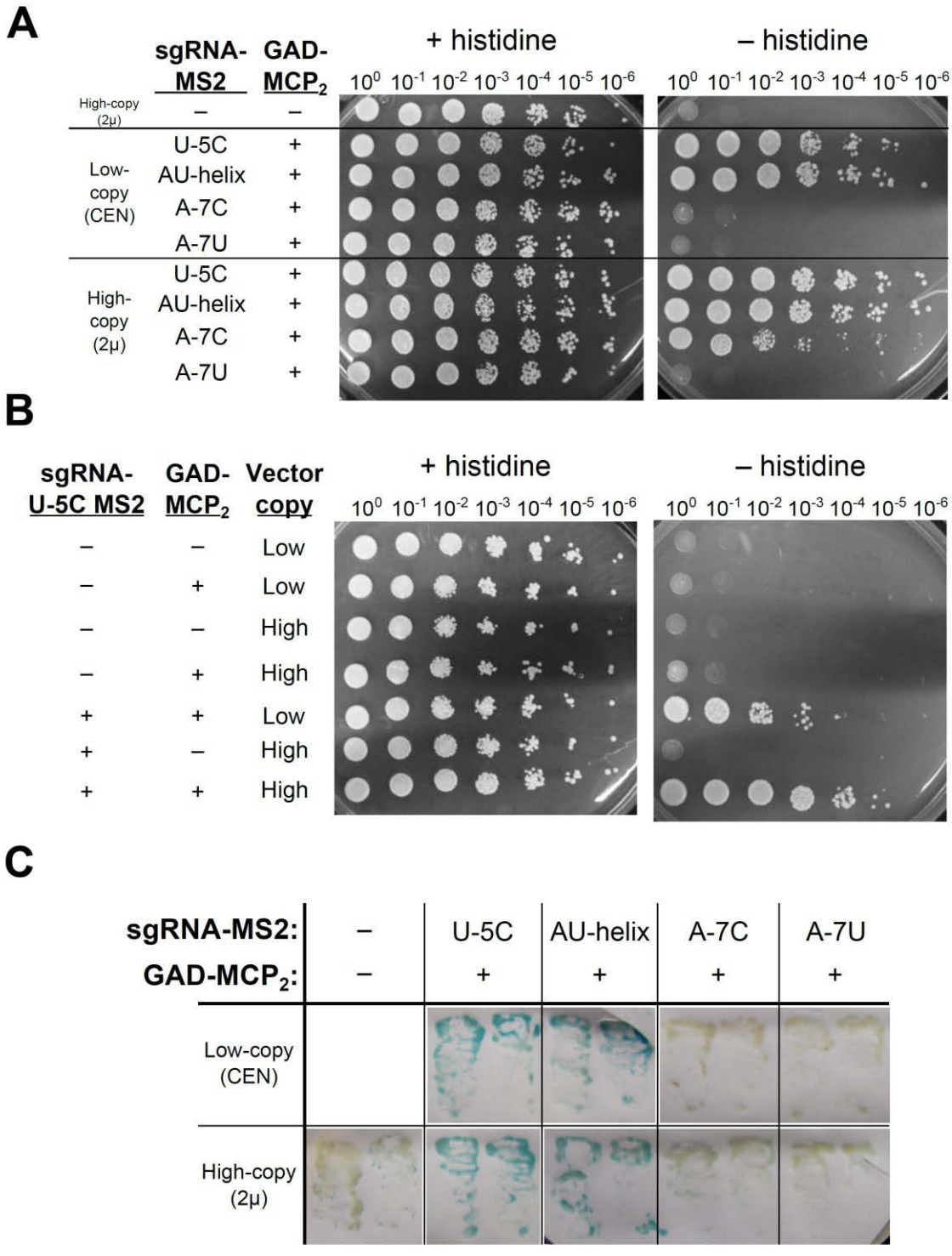

(**A** and **B**) Expression of the hybrid sgRNA from a high-copy plasmid increases *HIS3* reporter gene activation, allowing detection of low-affinity RNA-protein interactions. Yeast were grown as in Figure 4-2A on solid medium with or without histidine. Despite the increase in sensitivity of CARRY two-hybrid permitted by the increase in expression on 2μ plasmids, background signal was not increased. (**C**) Expression of the hybrid sgRNA from a high-copy (2μ) plasmid did not perceptibly increase activation strength of the *LacZ* reporter gene. Yeast were grown, lysed, and exposed to X-gal substrate for *LacZ*, as in Figure 4-2B. Pairs of yeast patches shown are biological-replicate samples. In Figure 4-4, as in the previous figures, a minus signs denote that no RNA or protein was fused to the sgRNA or GAD, respectively; i.e., pCARRY1, pCARRY2, and pGAD424 "vector-only" negative controls.

Figure 4-5: Junction 4 and the core-enclosing helix are required for Est2 to bind to the TLC1 core, while junction 1 is also important.

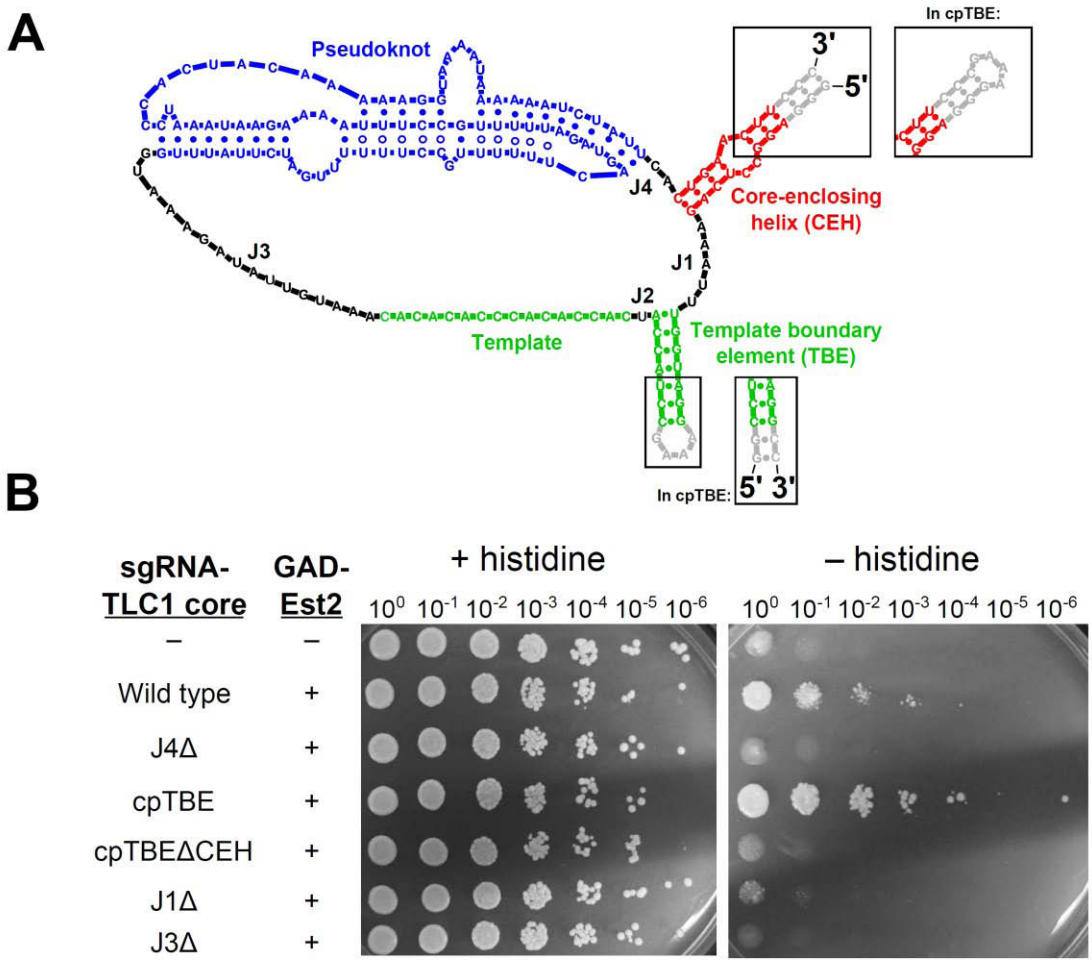

(**A**) Secondary structure of the minimal TLC1 RNA core. The four conserved secondary structure elements of telomerase RNA cores and the four junction regions are highlighted on the secondary-structure model of the minimal TLC1 RNA core (Niederer and Zappulla, 2015). As shown in the boxes, the 5′ and 3′ ends are moved to the distal tip of the template-boundary element helix in the cpTBE mutant, while the natural 5′ and 3′ ends are replaced with a GAAA tetraloop (Mefford et al., 2013). (**B**) Activation of the *HIS3* gene in CARRYeast(1.0) by the Est2-TLC1 interaction is abolished by deleting junction 3, junction 4, or the core-enclosing helix and decreased by deleting junction 1. All TLC1 hybrid sgRNAs were expressed from the high-copy

pCARRY2 plasmid, and yeast were grown with or without histidine as in Figure 4-2A. As in previous figures, minus signs denote that no RNA or protein were fused to the sgRNA or GAD, respectively.

Chapter 5: Conclusions

Telomerase and telomere-bound proteins work together to solve the end-replication problem and maintain genomic integrity in most eukaryotes. Due to the unique role that telomerase plays in maintaining telomere length, how telomerase is regulated has direct effects on the proliferative capacity of cells. Dysregulation of telomerase biogenesis and action at telomeres can both result in profound human pathologies (Shay and Bacchetti, 1997; Armanios and Blackburn, 2012), so research into how telomerase is made, assembled, and regulated is very important for understanding how these diseases arise. In my thesis, I focused my research on several different questions about the telomerase RNP in the yeast *Saccharomyces cerevisiae*.

5.1: Ku-mediated telomerase recruitment occurs through the Ku-Sir4 binding interaction and is negatively regulated by the telomere-length-sensing Rif proteins

The first and largest portion of my thesis research focused on the Ku-mediated pathway for recruitment of telomerase to telomeres. I found that Ku, which binds to the yeast telomerase RNA, TLC1 (Peterson et al., 2001; Dalby et al., 2013), requires the telomeric silent chromatin protein Sir4 to promote telomere lengthening and recruitment of telomerase to telomeres. Furthermore, point mutations in Sir4 that disrupt binding to Ku also cause telomere shortening and defects in telomerase recruitment that closely resemble the defects caused by complete deletion of *SIR4*. Lastly, I showed that when the interaction between Ku and TLC1 is abolished, telomeres can be restored to wild-type length by artificially tethering Sir4 directly to TLC1. Taken together, these data strongly support the conclusion that TLC1-bound Ku recruits telomerase to telomeres by binding to telomere-associated Sir4.

After characterizing the Ku-Sir4-mediated recruitment pathway, I next sought to elucidate the purpose of this pathway. The Ku-mediated telomerase-recruitment pathway is neither necessary nor sufficient for telomerase function, and the other telomerase-recruitment pathway in yeast — mediated by the proteins Est1 and Cdc13 — is both necessary and sufficient for telomerase function. However, the Ku binding site in TLC1 and the Ku-TLC1 interaction are

conserved in other yeast species (Zappulla and Cech, 2004; Dalby et al., 2013), and previous studies suggest that Ku-mediated recruitment in G1 makes subsequent Est1-mediated recruitment in S phase more efficient (Fisher et al., 2004; Williams et al., 2014). In investigating whether Ku-mediated telomere lengthening is regulated by other factors, I found that the proteins Rif1 and Rif2, long known to be negative regulators of telomere length (Hardy et al., 1992; Wotton and Shore, 1997), both inhibit Ku-mediated telomere lengthening. I also found that Rif1 and Rif2, which compete with Sir4 for binding to telomeres through the protein Rap1, inhibit Sir4 association with telomeres. These findings suggest that Rif1 and Rif2 inhibit Ku-mediated telomerase recruitment through competitive inhibition of Sir4 association with telomeres by binding to Rap1.

Telomere length in budding yeast is regulated by restricting telomerase action to only a few of the shortest telomeres in a given cell cycle, and the Rif1 and Rif2 proteins are known to be directly involved in this length-sensing process, likely by preventing telomerase from acting at longer telomeres (Levy and Blackburn, 2004; Teixeira et al., 2004; Bianchi and Shore, 2007; Sabourin et al., 2007; McGee et al., 2010). However, the molecular mechanism through which the Rif proteins communicate with telomerase has remained elusive. From my findings presented in Chapter 2, I propose that the Ku-Sir4-mediated telomerase recruitment pathway serves as a regulatory function that connects the telomere-length-sensing Rif proteins with the essential Est1-mediated telomerase recruitment pathway. This is the one of the first identified molecular mechanisms for how the Rif proteins inhibit telomerase action at telomeres. It is also clear, however, that this is not the only mechanism by which Rif1 and Rif2 negatively regulate telomerase. Though disrupting Ku-mediated telomere lengthening does reverse a large amount of the telomere hyper-lengthening that occurs in the absence of the Rif proteins, telomeres do not return all the way to wild-type length (see Figure 2-7), suggesting that there is at least one other telomere-lengthening pathway that remains uninhibited in the absence of the Rif proteins. Given this observation and the observations that Rif1 and Rif2 do not inhibit telomere lengthening in a

redundant manner (Wotton and Shore, 1997), it seems likely that these proteins inhibit telomerase both through the Ku-mediated recruitment pathway as well as other mechanisms.

It remains unclear whether this Ku-mediated telomerase recruitment pathway itself is conserved in humans, but published data show that telomerase recruitment has similar dynamics in yeast and human cells. Imaging telomerase in live yeast cells has revealed that the residence time of telomerase-telomere associations differs across the cell cycle (Gallardo et al., 2011). In G1 phase, when, according to chromatin immunoprecipitation experiments, only the Ku-mediated recruitment pathway is active (Fisher et al., 2004; Chan et al., 2008), telomerase-telomere associations are short-lived and dynamic. However, in S phase, when the Est1-mediated recruitment pathway is active (Taggart et al., 2002; Chan et al., 2008), telomerase recruitment events appear more stable. Intriguingly, human telomerase has also been shown to interact with telomeres through two different modes: short-lived "probing" interactions and longer-lived "stable" interactions (Schmidt et al., 2016). This striking similarity in telomerase recruitment dynamics between yeast and human suggests that human telomere length homeostasis and telomerase recruitment may be linked through mechanisms very similar to those present in yeast.

5.2: Sm_7 is an organizationally flexible module in the telomerase RNP and defines the 3′ end of poly(A)– TLC1.

The model that TLC1 acts as a flexible scaffold for the telomerase RNP is supported by a large body of experiments (Zappulla and Cech, 2006), but the most direct support for this model are the findings that Est1 and Ku retain their functions in the telomerase RNP even when their RNA binding sites are repositioned in TLC1 (Zappulla and Cech, 2004; Zappulla et al., 2011). In Chapter 3, I showed that this is also true of the Sm_7 complex, which is required for stabilization of the major, non-polyadenylated form of TLC1 (Seto et al., 1999). When I repositioned the Sm-binding site in full-length TLC1 along with the natural 5′ and 3′ ends of the RNA, Sm_7 remained at least partially functional in stabilizing poly(A)– TLC1 at all tested positions. This demonstrates

that Sm_7, like Est1 and Ku, is an organizationally flexible module that does not require a specific spatial position within the telomerase RNP in order to carry out its function. From these experiments and those repositioning Est1 and Ku I conclude that TLC1 acts as a flexible scaffold for all RNA-bound holoenzyme protein subunits of telomerase.

After having found that Sm_7 does not require a specific position in the telomerase RNP in order to perform its functions, I next used Sm-site repositioning to address unanswered questions regarding the role Sm_7 plays in TLC1 biogenesis. The prevailing model in the field for TLC1 biogenesis is that poly(A)+ TLC1 is exonucleolytically processed in a 3′-to-5′ manner, possibly by the nuclear exosome, and that this degradation is halted at position 1157 by the nearby Sm_7 complex, resulting in formation and stabilization of poly(A)– TLC1 (Chapon et al., 1997; Seto et al., 1999; Coy et al., 2013). However, the hypothesis that Sm_7 defines the poly(A)– 3′ end has not been thoroughly tested. When I repositioned the Sm-binding site further 5′ in TLC1 without circular permutation, I found that that the stabilized poly(A)– TLC1 RNAs were shorter than the wild-type RNA and that this difference in size was equivalent to the distance between the repositioned Sm site and the native Sm site. This suggests strongly that Sm_7 defines the mature 3′ end of poly(A)– TLC1.

Lastly, I sought to use Sm-site repositioning to test whether poly(A)+ TLC1 is the precursor of poly(A)– TLC1. Though the fact that Sm_7 defines the 3′ end of poly(A)– TLC1 suggests that it is processed from a longer transcript, poly(A)+ is not the only possible precursor since TLC1 transcription can also be terminated only ~50 nucleotides earlier by the Nrd1-Nab3-Sen1 (NNS) complex (Jamonnak et al., 2011; Noel et al., 2012). To test which of these transcripts is a precursor of poly(A)– TLC1, I repositioned the Sm-binding site downstream of the NNS termination signals but upstream of the polyadenylation signal such that only poly(A)+ TLC1, not NNS-terminated TLC1 transcripts, would include an Sm site. I found that an Sm site at this position is unable to stabilize poly(A)– TLC1 when the native Sm site has been mutated. This result is consistent with a model where poly(A)+ TLC1 does not undergo processing and

poly(A)– TLC1 is only derived from NNS-terminated transcripts. However, I cannot rule out the possibility that the Sm site I inserted at this non-native position is simply non-functional due to possible disrupted folding of and Sm-binding to the repositioned site.

This leaves three possible models for biogenesis of poly(A)– TLC1. The first possibility is that poly(A)+ TLC1 is the lone precursor of poly(A)– TLC1. If this is the case, NNS-terminated TLC1 transcripts may simply be spurious products of the TLC1 gene given that they are present at very low abundance and that the NNS complex is known to terminate transcription of many unstable transcripts in yeast (Arigo et al., 2006; Thiebaut et al., 2006; Schulz et al., 2013). The second possibility is that NNS-terminated TLC1 transcripts are the sole precursors of poly(A)– TLC1 and that poly(A)+ TLC1 is a completely separate isoform of TLC1 RNA. In this scenario, poly(A)+ TLC1 may serve a specific function that poly(A)– TLC1 does not, possibly in lengthening telomeres under specific environmental conditions. The third possibility is that poly(A)+ TLC1 and NNS-terminated TLC1 transcripts both undergo 3′-end processing to yield poly(A)– TLC1. Given the rapidly evolving nature of telomerase RNA genes, it does not seem unlikely that TLC1 would acquire two different transcription termination signals. It is unclear which of these possibilities is true, so more experiments are required to fully elucidate the nature of telomerase RNA biogenesis in budding yeast.

5.3: CARRY-two hybrid: a novel method for investigating RNA-protein interactions.

In the final portion of my thesis, I took a brief departure from research on telomerase to develop CRISPR-assisted RNA/RBP yeast (CARRY) two-hybrid, a new technique for studying RNA-protein interactions. CARRY two-hybrid builds on the widely used yeast two-hybrid system for studying protein-protein interactions (Fields and Song, 1989; Chien et al., 1991; Vidal and Fields, 2014) and makes use of a previously developed approach for tethering an RNA to a specific genomic locus using the nuclease-deactivated *S. pyogenes* Cas9 (dCas9) complex (Shechner et al., 2015; Zalatan et al., 2015). In this system, an RNA is tethered to the promoters

of the standard yeast two-hybrid reporter genes, *HIS3* and *LacZ*, by fusing it to the 3′ end of a CRISPR single guide RNA (sgRNA), and binding of the RNA to a given protein can be evaluated by measuring reporter-gene expression when said protein is fused to the Gal4 activation domain. In my tests of this system using the MS2 hairpin and MS2 coat protein, I found that CARRY two-hybrid can detect RNA-protein interactions with high specificity and sensitivity. Furthermore, the hybrid sgRNA in CARRY two-hybrid is transcribed by RNA polymerase II instead of RNA polymerase III, making it less likely that an RNA of interest will contain a premature termination signal, and the multiple-cloning site in the sgRNA is designed to form a hairpin when transcribed. Together, these design features make CARRY two-hybrid equipped to accommodate the study of a diverse array of RNAs.

I next used CARRY two-hybrid to study the interaction between Est2 and the TLC1 RNA core. I confirmed previous reports that the core-enclosing helix is an important binding site for TERT (Livengood et al., 2002; Chappell and Lundblad, 2004; Lin et al., 2004) and found that junctions J1 and J4 play important roles in the interaction as well. Given previous experiments showing that the length of these regions, not their sequences, are important for telomerase function (Mefford et al., 2013), I hypothesize that J1 and J4 are important for maintaining proper spacing between the TERT-binding sites in the TLC1 core. Together, these experiments suggest that CARRY two-hybrid will be a widely useful tool for studying the many RNA-protein interactions that play critical roles in diverse cellular processes.

References

Abdallah P, Luciano P, Runge KW, Lisby M, Geli V, Gilson E, Teixeira MT. 2009. A two-step model for senescence triggered by a single critically short telomere. *Nat Cell Biol* **11**: 988-993. doi:10.1038/ncb1911.

Allison DS, Hall BD. 1985. Effects of alterations in the 3' flanking sequence on in vivo and in vitro expression of the yeast SUP4-o tRNATyr gene. *The EMBO journal* **4**: 2657-2664.

Andrulis ED, Zappulla DC, Ansari A, Perrod S, Laiosa CV, Gartenberg MR, Sternglanz R. 2002. Esc1, a nuclear periphery protein required for Sir4-based plasmid anchoring and partitioning. *Molecular and cellular biology* **22**: 8292-8301.

Arigo JT, Eyler DE, Carroll KL, Corden JL. 2006. Termination of cryptic unstable transcripts is directed by yeast RNA-binding proteins Nrd1 and Nab3. *Molecular cell* **23**: 841-851. doi:10.1016/j.molcel.2006.07.024.

Armanios M, Blackburn EH. 2012. The telomere syndromes. *Nature reviews Genetics* **13**: 693-704. doi:10.1038/nrg3246.

Arnoult N, Van Beneden A, Decottignies A. 2012. Telomere length regulates TERRA levels through increased trimethylation of telomeric H3K9 and HP1alpha. *Nature structural & molecular biology* **19**: 948-956. doi:10.1038/nsmb.2364.

Askree SH, Yehuda T, Smolikov S, Gurevich R, Hawk J, Coker C, Krauskopf A, Kupiec M, McEachern MJ. 2004. A genome-wide screen for Saccharomyces cerevisiae deletion mutants that affect telomere length. *Proceedings of the National Academy of Sciences of the United States of America* **101**: 8658-8663. doi:10.1073/pnas.0401263101.

Bartel PL, Chien C-T, Sternglanz R, Fields S. 1993. Using the two-hybrid system to detect protein-protein interactions. in *Cellular Interactions in Development: A Practical Approach* (ed. DA Hartley), pp. 153-179. Oxford University Press, Oxford.

Baur JA, Zou Y, Shay JW, Wright WE. 2001. Telomere position effect in human cells. *Science* **292**: 2075-2077. doi:10.1126/science.1062329.

Bertuch AA, Lundblad V. 2004. EXO1 contributes to telomere maintenance in both telomerase-proficient and telomerase-deficient Saccharomyces cerevisiae. *Genetics* **166**: 1651-1659.

Bianchi A, Shore D. 2007. Increased association of telomerase with short telomeres in yeast. *Genes & development* **21**: 1726-1730. doi:10.1101/gad.438907.

Bonetti D, Clerici M, Anbalagan S, Martina M, Lucchini G, Longhese MP. 2010. Shelterin-like proteins and Yku inhibit nucleolytic processing of Saccharomyces cerevisiae telomeres. *PLoS genetics* **6**: e1000966. doi:10.1371/journal.pgen.1000966.

Bosoy D, Peng Y, Mian IS, Lue NF. 2003. Conserved N-terminal motifs of telomerase reverse transcriptase required for ribonucleoprotein assembly in vivo. *The Journal of biological chemistry* **278**: 3882-3890. doi:10.1074/jbc.M210645200.

Boulton SJ, Jackson SP. 1998. Components of the Ku-dependent non-homologous end-joining pathway are involved in telomeric length maintenance and telomeric silencing. *The EMBO journal* **17**: 1819-1828. doi:10.1093/emboj/17.6.1819.

Branlant C, Krol A, Ebel JP, Lazar E, Haendler B, Jacob M. 1982. U2 RNA shares a structural domain with U1, U4, and U5 RNAs. *The EMBO journal* **1**: 1259-1265.

Cervantes RB, Lundblad V. 2002. Mechanisms of chromosome-end protection. *Curr Opin Cell Biol* **14**: 351-356.

Chan A, Boule JB, Zakian VA. 2008. Two pathways recruit telomerase to Saccharomyces cerevisiae telomeres. *PLoS genetics* **4**: e1000236. doi:10.1371/journal.pgen.1000236.

Chapon C, Cech TR, Zaug AJ. 1997. Polyadenylation of telomerase RNA in budding yeast. *Rna* **3**: 1337-1351.

Chappell AS, Lundblad V. 2004. Structural elements required for association of the Saccharomyces cerevisiae telomerase RNA with the Est2 reverse transcriptase. *Molecular and cellular biology* **24**: 7720-7736. doi:10.1128/MCB.24.17.7720-7736.2004.

Chen JL, Greider CW. 2004. An emerging consensus for telomerase RNA structure. *Proceedings of the National Academy of Sciences of the United States of America* **101**: 14683-14684. doi:10.1073/pnas.0406204101.

Chien CT, Bartel PL, Sternglanz R, Fields S. 1991. The two-hybrid system: a method to identify and clone genes for proteins that interact with a protein of interest. *Proceedings of the National Academy of Sciences of the United States of America* **88**: 9578-9582.

Christianson TW, Sikorski RS, Dante M, Shero JH, Hieter P. 1992. Multifunctional yeast high-copy-number shuttle vectors. *Gene* **110**: 119-122.

Conrad MN, Wright JH, Wolf AJ, Zakian VA. 1990. RAP1 protein interacts with yeast telomeres in vivo: overproduction alters telomere structure and decreases chromosome stability. *Cell* **63**: 739-750.

Coy S, Volanakis A, Shah S, Vasiljeva L. 2013. The Sm complex is required for the processing of non-coding RNAs by the exosome. *PLoS One* **8**: e65606. doi:10.1371/journal.pone.0065606.

Dalby AB, Goodrich KJ, Pfingsten JS, Cech TR. 2013. RNA recognition by the DNA end-binding Ku heterodimer. *Rna* **19**: 841-851. doi:10.1261/rna.038703.113.

Dandjinou AT, Levesque N, Larose S, Lucier JF, Abou Elela S, Wellinger RJ. 2004. A phylogenetically based secondary structure for the yeast telomerase RNA. *Current biology : CB* **14**: 1148-1158. doi:10.1016/j.cub.2004.05.054.

DiCarlo JE, Norville JE, Mali P, Rios X, Aach J, Church GM. 2013. Genome engineering in Saccharomyces cerevisiae using CRISPR-Cas systems. *Nucleic acids research* **41**: 4336-4343. doi:10.1093/nar/gkt135.

Diede SJ, Gottschling DE. 1999. Telomerase-mediated telomere addition in vivo requires DNA primase and DNA polymerases alpha and delta. *Cell* **99**: 723-733.

Evans SK, Lundblad V. 1999. Est1 and Cdc13 as comediators of telomerase access. *Science* **286**: 117-120.

Feeser EA, Wolberger C. 2008. Structural and functional studies of the Rap1 C-terminus reveal novel separation-of-function mutants. *Journal of molecular biology* **380**: 520-531. doi:10.1016/j.jmb.2008.04.078.

Fields S, Song O. 1989. A novel genetic system to detect protein-protein interactions. *Nature* **340**: 245-246. doi:10.1038/340245a0.

Fisher TS, Taggart AK, Zakian VA. 2004. Cell cycle-dependent regulation of yeast telomerase by Ku. *Nature structural & molecular biology* **11**: 1198-1205. doi:10.1038/nsmb854.

Fisher TS, Zakian VA. 2005. Ku: a multifunctional protein involved in telomere maintenance. *DNA repair* **4**: 1215-1226. doi:10.1016/j.dnarep.2005.04.021.

Friedman KL, Cech TR. 1999. Essential functions of amino-terminal domains in the yeast telomerase catalytic subunit revealed by selection for viable mutants. *Genes & development* **13**: 2863-2874.

Friedman KL, Heit JJ, Long DM, Cech TR. 2003. N-terminal domain of yeast telomerase reverse transcriptase: recruitment of Est3p to the telomerase complex. *Mol Biol Cell* **14**: 1-13. doi:10.1091/mbc.E02-06-0327.

Gallardo F, Laterreur N, Cusanelli E, Ouenzar F, Querido E, Wellinger RJ, Chartrand P. 2011. Live cell imaging of telomerase RNA dynamics reveals cell cycle-dependent clustering of

telomerase at elongating telomeres. *Molecular cell* **44**: 819-827. doi:10.1016/j.molcel.2011.09.020.
Gallardo F, Olivier C, Dandjinou AT, Wellinger RJ, Chartrand P. 2008. TLC1 RNA nucleo-cytoplasmic trafficking links telomerase biogenesis to its recruitment to telomeres. *The EMBO journal* **27**: 748-757. doi:10.1038/emboj.2008.21.
Gao Y, Zhao Y. 2014. Self-processing of ribozyme-flanked RNAs into guide RNAs in vitro and in vivo for CRISPR-mediated genome editing. *J Integr Plant Biol* **56**: 343-349. doi:10.1111/jipb.12152.
Gatbonton T, Imbesi M, Nelson M, Akey JM, Ruderfer DM, Kruglyak L, Simon JA, Bedalov A. 2006. Telomere length as a quantitative trait: genome-wide survey and genetic mapping of telomere length-control genes in yeast. *PLoS genetics* **2**: e35. doi:10.1371/journal.pgen.0020035.
Gottschling DE, Aparicio OM, Billington BL, Zakian VA. 1990. Position effect at S. cerevisiae telomeres: reversible repression of Pol II transcription. *Cell* **63**: 751-762.
Gravel S, Larrivee M, Labrecque P, Wellinger RJ. 1998. Yeast Ku as a regulator of chromosomal DNA end structure. *Science* **280**: 741-744.
Greider CW, Blackburn EH. 1985. Identification of a specific telomere terminal transferase activity in Tetrahymena extracts. *Cell* **43**: 405-413.
-. 1989. A telomeric sequence in the RNA of Tetrahymena telomerase required for telomere repeat synthesis. *Nature* **337**: 331-337. doi:10.1038/337331a0.
Guertin MJ, Lis JT. 2013. Mechanisms by which transcription factors gain access to target sequence elements in chromatin. *Current opinion in genetics & development* **23**: 116-123. doi:10.1016/j.gde.2012.11.008.
Hamm J, Kazmaier M, Mattaj IW. 1987. In vitro assembly of U1 snRNPs. *The EMBO journal* **6**: 3479-3485.
Hardy CF, Sussel L, Shore D. 1992. A RAP1-interacting protein involved in transcriptional silencing and telomere length regulation. *Genes & development* **6**: 801-814.
Hass EP, Zappulla DC. 2015. The Ku subunit of telomerase binds Sir4 to recruit telomerase to lengthen telomeres in S. cerevisiae. *Elife* **4**. doi:10.7554/eLife.07750.
Hollenberg SM, Sternglanz R, Cheng PF, Weintraub H. 1995. Identification of a new family of tissue-specific basic helix-loop-helix proteins with a two-hybrid system. *Molecular and cellular biology* **15**: 3813-3822.
Hoppe GJ, Tanny JC, Rudner AD, Gerber SA, Danaie S, Gygi SP, Moazed D. 2002. Steps in assembly of silent chromatin in yeast: Sir3-independent binding of a Sir2/Sir4 complex to silencers and role for Sir2-dependent deacetylation. *Molecular and cellular biology* **22**: 4167-4180.
Hughes TR, Evans SK, Weilbaecher RG, Lundblad V. 2000. The Est3 protein is a subunit of yeast telomerase. *Current biology : CB* **10**: 809-812.
Jamonnak N, Creamer TJ, Darby MM, Schaughency P, Wheelan SJ, Corden JL. 2011. Yeast Nrd1, Nab3, and Sen1 transcriptome-wide binding maps suggest multiple roles in post-transcriptional RNA processing. *Rna* **17**: 2011-2025. doi:10.1261/rna.2840711.
Jones MH, Guthrie C. 1990. Unexpected flexibility in an evolutionarily conserved protein-RNA interaction: genetic analysis of the Sm binding site. *The EMBO journal* **9**: 2555-2561.
Koering CE, Pollice A, Zibella MP, Bauwens S, Puisieux A, Brunori M, Brun C, Martins L, Sabatier L, Pulitzer JF et al. 2002. Human telomeric position effect is determined by chromosomal context and telomeric chromatin integrity. *EMBO reports* **3**: 1055-1061. doi:10.1093/embo-reports/kvf215.

Kohrer K, Domdey H. 1991. Preparation of high molecular weight RNA. *Methods in enzymology* **194**: 398-405.

Kyrion G, Boakye KA, Lustig AJ. 1992. C-terminal truncation of RAP1 results in the deregulation of telomere size, stability, and function in Saccharomyces cerevisiae. *Molecular and cellular biology* **12**: 5159-5173.

Kyrion G, Liu K, Liu C, Lustig AJ. 1993. RAP1 and telomere structure regulate telomere position effects in Saccharomyces cerevisiae. *Genes & development* **7**: 1146-1159.

Laterreur N, Eschbach SH, Lafontaine DA, Wellinger RJ. 2013. A new telomerase RNA element that is critical for telomere elongation. *Nucleic acids research* **41**: 7713-7724. doi:10.1093/nar/gkt514.

Laughery MF, Hunter T, Brown A, Hoopes J, Ostbye T, Shumaker T, Wyrick JJ. 2015. New vectors for simple and streamlined CRISPR-Cas9 genome editing in Saccharomyces cerevisiae. *Yeast* **32**: 711-720. doi:10.1002/yea.3098.

Lebo KJ, Niederer RO, Zappulla DC. 2015. A second essential function of the Est1-binding arm of yeast telomerase RNA. *Rna*. doi:10.1261/rna.049379.114.

Lebo KJ, Zappulla DC. 2012. Stiffened yeast telomerase RNA supports RNP function in vitro and in vivo. *Rna* **18**: 1666-1678. doi:10.1261/rna.033555.112.

Lemieux B, Laterreur N, Perederina A, Noel JF, Dubois ML, Krasilnikov AS, Wellinger RJ. 2016. Active Yeast Telomerase Shares Subunits with Ribonucleoproteins RNase P and RNase MRP. *Cell* **165**: 1171-1181. doi:10.1016/j.cell.2016.04.018.

Lendvay TS, Morris DK, Sah J, Balasubramanian B, Lundblad V. 1996. Senescence mutants of Saccharomyces cerevisiae with a defect in telomere replication identify three additional EST genes. *Genetics* **144**: 1399-1412.

Levy DL, Blackburn EH. 2004. Counting of Rif1p and Rif2p on Saccharomyces cerevisiae telomeres regulates telomere length. *Molecular and cellular biology* **24**: 10857-10867. doi:10.1128/MCB.24.24.10857-10867.2004.

Levy MZ, Allsopp RC, Futcher AB, Greider CW, Harley CB. 1992. Telomere end-replication problem and cell aging. *Journal of molecular biology* **225**: 951-960.

Liautard JP, Sri-Widada J, Brunel C, Jeanteur P. 1982. Structural organization of ribonucleoproteins containing small nuclear RNAs from HeLa cells. Proteins interact closely with a similar structural domain of U1, U2, U4 and U5 small nuclear RNAs. *Journal of molecular biology* **162**: 623-643.

Lim F, Spingola M, Peabody DS. 1994. Altering the RNA binding specificity of a translational repressor. *The Journal of biological chemistry* **269**: 9006-9010.

Lin J, Ly H, Hussain A, Abraham M, Pearl S, Tzfati Y, Parslow TG, Blackburn EH. 2004. A universal telomerase RNA core structure includes structured motifs required for binding the telomerase reverse transcriptase protein. *Proceedings of the National Academy of Sciences of the United States of America* **101**: 14713-14718. doi:10.1073/pnas.0405879101.

Lin JJ, Zakian VA. 1996. The Saccharomyces CDC13 protein is a single-strand TG1-3 telomeric DNA-binding protein in vitro that affects telomere behavior in vivo. *Proceedings of the National Academy of Sciences of the United States of America* **93**: 13760-13765.

Lingner J, Hughes TR, Shevchenko A, Mann M, Lundblad V, Cech TR. 1997. Reverse transcriptase motifs in the catalytic subunit of telomerase. *Science* **276**: 561-567.

Livengood AJ, Zaug AJ, Cech TR. 2002. Essential regions of Saccharomyces cerevisiae telomerase RNA: separate elements for Est1p and Est2p interaction. *Molecular and cellular biology* **22**: 2366-2374.

Longtine MS, McKenzie A, 3rd, Demarini DJ, Shah NG, Wach A, Brachat A, Philippsen P, Pringle JR. 1998. Additional modules for versatile and economical PCR-based gene deletion and modification in Saccharomyces cerevisiae. *Yeast* **14**: 953-961. doi:10.1002/(SICI)1097-0061(199807)14:10<953::AID-YEA293>3.0.CO;2-U.

Lundblad V, Szostak JW. 1989. A mutant with a defect in telomere elongation leads to senescence in yeast. *Cell* **57**: 633-643.

Luo K, Vega-Palas MA, Grunstein M. 2002. Rap1-Sir4 binding independent of other Sir, yKu, or histone interactions initiates the assembly of telomeric heterochromatin in yeast. *Genes & development* **16**: 1528-1539. doi:10.1101/gad.988802.

Marcand S, Gilson E, Shore D. 1997. A protein-counting mechanism for telomere length regulation in yeast. *Science* **275**: 986-990.

Marcand S, Pardo B, Gratias A, Cahun S, Callebaut I. 2008. Multiple pathways inhibit NHEJ at telomeres. *Genes & development* **22**: 1153-1158. doi:10.1101/gad.455108.

Martin SG, Laroche T, Suka N, Grunstein M, Gasser SM. 1999. Relocalization of telomeric Ku and SIR proteins in response to DNA strand breaks in yeast. *Cell* **97**: 621-633.

Mattaj IW, De Robertis EM. 1985. Nuclear segregation of U2 snRNA requires binding of specific snRNP proteins. *Cell* **40**: 111-118.

McClintock B. 1942. The Fusion of Broken Ends of Chromosomes Following Nuclear Fusion. *Proceedings of the National Academy of Sciences of the United States of America* **28**: 458-463.

McGee JS, Phillips JA, Chan A, Sabourin M, Paeschke K, Zakian VA. 2010. Reduced Rif2 and lack of Mec1 target short telomeres for elongation rather than double-strand break repair. *Nature structural & molecular biology* **17**: 1438-1445. doi:10.1038/nsmb.1947.

McHugh CA, Russell P, Guttman M. 2014. Methods for comprehensive experimental identification of RNA-protein interactions. *Genome Biol* **15**: 203. doi:10.1186/gb4152.

Mefford MA, Rafiq Q, Zappulla DC. 2013. RNA connectivity requirements between conserved elements in the core of the yeast telomerase RNP. *The EMBO journal* **32**: 2980-2993. doi:10.1038/emboj.2013.227.

Mishra K, Shore D. 1999. Yeast Ku protein plays a direct role in telomeric silencing and counteracts inhibition by rif proteins. *Current biology : CB* **9**: 1123-1126.

Moretti P, Freeman K, Coodly L, Shore D. 1994. Evidence that a complex of SIR proteins interacts with the silencer and telomere-binding protein RAP1. *Genes & development* **8**: 2257-2269.

Mozdy AD, Cech TR. 2006. Low abundance of telomerase in yeast: implications for telomerase haploinsufficiency. *Rna* **12**: 1721-1737. doi:10.1261/rna.134706.

Mozdy AD, Podell ER, Cech TR. 2008. Multiple yeast genes, including Paf1 complex genes, affect telomere length via telomerase RNA abundance. *Molecular and cellular biology* **28**: 4152-4161. doi:10.1128/MCB.00512-08.

Muhlrad D, Decker CJ, Parker R. 1995. Turnover mechanisms of the stable yeast PGK1 mRNA. *Molecular and cellular biology* **15**: 2145-2156.

Nandakumar J, Cech TR. 2013. Finding the end: recruitment of telomerase to telomeres. *Nature reviews Molecular cell biology* **14**: 69-82. doi:10.1038/nrm3505.

Niederer RO, Zappulla DC. 2015. Refined secondary-structure models of the core of yeast and human telomerase RNAs directed by SHAPE. *Rna* **21**: 254-261. doi:10.1261/rna.048959.114.

Noel JF, Larose S, Abou Elela S, Wellinger RJ. 2012. Budding yeast telomerase RNA transcription termination is dictated by the Nrd1/Nab3 non-coding RNA termination pathway. *Nucleic acids research* **40**: 5625-5636. doi:10.1093/nar/gks200.

Nugent CI, Hughes TR, Lue NF, Lundblad V. 1996. Cdc13p: a single-strand telomeric DNA-binding protein with a dual role in yeast telomere maintenance. *Science* **274**: 249-252.

Olovnikov AM. 1973. A theory of marginotomy. The incomplete copying of template margin in enzymic synthesis of polynucleotides and biological significance of the phenomenon. *J Theor Biol* **41**: 181-190.

Palladino F, Laroche T, Gilson E, Axelrod A, Pillus L, Gasser SM. 1993. SIR3 and SIR4 proteins are required for the positioning and integrity of yeast telomeres. *Cell* **75**: 543-555.

Park Y, Lustig AJ. 2000. Telomere structure regulates the heritability of repressed subtelomeric chromatin in Saccharomyces cerevisiae. *Genetics* **154**: 587-598.

Peterson SE, Stellwagen AE, Diede SJ, Singer MS, Haimberger ZW, Johnson CO, Tzoneva M, Gottschling DE. 2001. The function of a stem-loop in telomerase RNA is linked to the DNA repair protein Ku. *Nature genetics* **27**: 64-67. doi:10.1038/83778.

Pfingsten JS, Goodrich KJ, Taabazuing C, Ouenzar F, Chartrand P, Cech TR. 2012. Mutually exclusive binding of telomerase RNA and DNA by Ku alters telomerase recruitment model. *Cell* **148**: 922-932. doi:10.1016/j.cell.2012.01.033.

Plaschka C, Lin PC, Nagai K. 2017. Structure of a pre-catalytic spliceosome. *Nature* **546**: 617-621. doi:10.1038/nature22799.

Polotnianka RM, Li J, Lustig AJ. 1998. The yeast Ku heterodimer is essential for protection of the telomere against nucleolytic and recombinational activities. *Current biology : CB* **8**: 831-834.

Porrua O, Libri D. 2015. Transcription termination and the control of the transcriptome: why, where and how to stop. *Nature reviews Molecular cell biology* **16**: 190-202. doi:10.1038/nrm3943.

Putz U, Skehel P, Kuhl D. 1996. A tri-hybrid system for the analysis and detection of RNA--protein interactions. *Nucleic acids research* **24**: 4838-4840.

Qi H, Zakian VA. 2000. The Saccharomyces telomere-binding protein Cdc13p interacts with both the catalytic subunit of DNA polymerase alpha and the telomerase-associated est1 protein. *Genes & development* **14**: 1777-1788.

Qiao F, Cech TR. 2008. Triple-helix structure in telomerase RNA contributes to catalysis. *Nature structural & molecular biology* **15**: 634-640. doi:10.1038/nsmb.1420.

Raker VA, Hartmuth K, Kastner B, Luhrmann R. 1999. Spliceosomal U snRNP core assembly: Sm proteins assemble onto an Sm site RNA nonanucleotide in a specific and thermodynamically stable manner. *Molecular and cellular biology* **19**: 6554-6565.

Ray A, Runge KW. 1998. The C terminus of the major yeast telomere binding protein Rap1p enhances telomere formation. *Molecular and cellular biology* **18**: 1284-1295.

Ribes-Zamora A, Mihalek I, Lichtarge O, Bertuch AA. 2007. Distinct faces of the Ku heterodimer mediate DNA repair and telomeric functions. *Nature structural & molecular biology* **14**: 301-307. doi:10.1038/nsmb1214.

Romaniuk PJ, Lowary P, Wu HN, Stormo G, Uhlenbeck OC. 1987. RNA binding site of R17 coat protein. *Biochemistry* **26**: 1563-1568.

Roy R, Meier B, McAinsh AD, Feldmann HM, Jackson SP. 2004. Separation-of-function mutants of yeast Ku80 reveal a Yku80p-Sir4p interaction involved in telomeric silencing. *The Journal of biological chemistry* **279**: 86-94. doi:10.1074/jbc.M306841200.

Sabourin M, Tuzon CT, Zakian VA. 2007. Telomerase and Tel1p preferentially associate with short telomeres in S. cerevisiae. *Molecular cell* **27**: 550-561. doi:10.1016/j.molcel.2007.07.016.

Schmidt JC, Dalby AB, Cech TR. 2014. Identification of human TERT elements necessary for telomerase recruitment to telomeres. *Elife* **3**. doi:10.7554/eLife.03563.

Schmidt JC, Zaug AJ, Cech TR. 2016. Live Cell Imaging Reveals the Dynamics of Telomerase Recruitment to Telomeres. *Cell* **166**: 1188-1197 e1189. doi:10.1016/j.cell.2016.07.033.

Schulz D, Schwalb B, Kiesel A, Baejen C, Torkler P, Gagneur J, Soeding J, Cramer P. 2013. Transcriptome surveillance by selective termination of noncoding RNA synthesis. *Cell* **155**: 1075-1087. doi:10.1016/j.cell.2013.10.024.

SenGupta DJ, Zhang B, Kraemer B, Pochart P, Fields S, Wickens M. 1996. A three-hybrid system to detect RNA-protein interactions in vivo. *Proceedings of the National Academy of Sciences of the United States of America* **93**: 8496-8501.

Seto AG, Zaug AJ, Sobel SG, Wolin SL, Cech TR. 1999. Saccharomyces cerevisiae telomerase is an Sm small nuclear ribonucleoprotein particle. *Nature* **401**: 177-180. doi:10.1038/43694.

Shampay J, Blackburn EH. 1988. Generation of telomere-length heterogeneity in Saccharomyces cerevisiae. *Proceedings of the National Academy of Sciences of the United States of America* **85**: 534-538.

Shampay J, Szostak JW, Blackburn EH. 1984. DNA sequences of telomeres maintained in yeast. *Nature* **310**: 154-157.

Shay JW, Bacchetti S. 1997. A survey of telomerase activity in human cancer. *European journal of cancer* **33**: 787-791. doi:10.1016/S0959-8049(97)00062-2.

Shechner DM, Hacisuleyman E, Younger ST, Rinn JL. 2015. Multiplexable, locus-specific targeting of long RNAs with CRISPR-Display. *Nat Methods* **12**: 664-670. doi:10.1038/nmeth.3433.

Shi T, Bunker RD, Mattarocci S, Ribeyre C, Faty M, Gut H, Scrima A, Rass U, Rubin SM, Shore D et al. 2013. Rif1 and Rif2 shape telomere function and architecture through multivalent Rap1 interactions. *Cell* **153**: 1340-1353. doi:10.1016/j.cell.2013.05.007.

Shippen-Lentz D, Blackburn EH. 1990. Functional evidence for an RNA template in telomerase. *Science* **247**: 546-552.

Sikorski RS, Hieter P. 1989. A system of shuttle vectors and yeast host strains designed for efficient manipulation of DNA in Saccharomyces cerevisiae. *Genetics* **122**: 19-27.

Singer MS, Gottschling DE. 1994. TLC1: template RNA component of Saccharomyces cerevisiae telomerase. *Science* **266**: 404-409.

Song K, Jung Y, Jung D, Lee I. 2001. Human Ku70 interacts with heterochromatin protein 1alpha. *The Journal of biological chemistry* **276**: 8321-8327. doi:10.1074/jbc.M008779200.

Stellwagen AE, Haimberger ZW, Veatch JR, Gottschling DE. 2003. Ku interacts with telomerase RNA to promote telomere addition at native and broken chromosome ends. *Genes & development* **17**: 2384-2395. doi:10.1101/gad.1125903.

Taggart AK, Teng SC, Zakian VA. 2002. Est1p as a cell cycle-regulated activator of telomere-bound telomerase. *Science* **297**: 1023-1026. doi:10.1126/science.1074968.

Talley JM, DeZwaan DC, Maness LD, Freeman BC, Friedman KL. 2011. Stimulation of yeast telomerase activity by the ever shorter telomere 3 (Est3) subunit is dependent on direct interaction with the catalytic protein Est2. *The Journal of biological chemistry* **286**: 26431-26439. doi:10.1074/jbc.M111.228635.

Teixeira MT, Arneric M, Sperisen P, Lingner J. 2004. Telomere length homeostasis is achieved via a switch between telomerase- extendible and -nonextendible states. *Cell* **117**: 323-335.

Teng SC, Chang J, McCowan B, Zakian VA. 2000. Telomerase-independent lengthening of yeast telomeres occurs by an abrupt Rad50p-dependent, Rif-inhibited recombinational process. *Molecular cell* **6**: 947-952.

Thiebaut M, Kisseleva-Romanova E, Rougemaille M, Boulay J, Libri D. 2006. Transcription termination and nuclear degradation of cryptic unstable transcripts: a role for the nrd1-nab3 pathway in genome surveillance. *Molecular cell* **23**: 853-864. doi:10.1016/j.molcel.2006.07.029.

Tian B, Graber JH. 2012. Signals for pre-mRNA cleavage and polyadenylation. *Wiley Interdiscip Rev RNA* **3**: 385-396. doi:10.1002/wrna.116.

Ting NS, Yu Y, Pohorelic B, Lees-Miller SP, Beattie TL. 2005. Human Ku70/80 interacts directly with hTR, the RNA component of human telomerase. *Nucleic acids research* **33**: 2090-2098. doi:10.1093/nar/gki342.

Tsukamoto Y, Kato J, Ikeda H. 1997. Silencing factors participate in DNA repair and recombination in Saccharomyces cerevisiae. *Nature* **388**: 900-903. doi:10.1038/42288.

Tuzon CT, Wu Y, Chan A, Zakian VA. 2011. The Saccharomyces cerevisiae telomerase subunit Est3 binds telomeres in a cell cycle- and Est1-dependent manner and interacts directly with Est1 in vitro. *PLoS genetics* **7**: e1002060. doi:10.1371/journal.pgen.1002060.

Tzfati Y, Fulton TB, Roy J, Blackburn EH. 2000. Template boundary in a yeast telomerase specified by RNA structure. *Science* **288**: 863-867.

Tzfati Y, Knight Z, Roy J, Blackburn EH. 2003. A novel pseudoknot element is essential for the action of a yeast telomerase. *Genes & development* **17**: 1779-1788. doi:10.1101/gad.1099403.

Vidal M, Fields S. 2014. The yeast two-hybrid assay: still finding connections after 25 years. *Nat Methods* **11**: 1203-1206.

Walker JR, Corpina RA, Goldberg J. 2001. Structure of the Ku heterodimer bound to DNA and its implications for double-strand break repair. *Nature* **412**: 607-614. doi:10.1038/35088000.

Watson JD. 1972. Origin of concatemeric T7 DNA. *Nat New Biol* **239**: 197-201.

Weinert TA, Hartwell LH. 1988. The RAD9 gene controls the cell cycle response to DNA damage in Saccharomyces cerevisiae. *Science* **241**: 317-322.

Will CL, Luhrmann R. 2001. Spliceosomal UsnRNP biogenesis, structure and function. *Curr Opin Cell Biol* **13**: 290-301.

Williams JM, Ouenzar F, Lemon LD, Chartrand P, Bertuch AA. 2014. The principal role of ku in telomere length maintenance is promotion of est1 association with telomeres. *Genetics* **197**: 1123-1136. doi:10.1534/genetics.114.164707.

Wotton D, Shore D. 1997. A novel Rap1p-interacting factor, Rif2p, cooperates with Rif1p to regulate telomere length in Saccharomyces cerevisiae. *Genes & development* **11**: 748-760.

Wright JH, Gottschling DE, Zakian VA. 1992. Saccharomyces telomeres assume a non-nucleosomal chromatin structure. *Genes & development* **6**: 197-210.

Zalatan JG, Lee ME, Almeida R, Gilbert LA, Whitehead EH, La Russa M, Tsai JC, Weissman JS, Dueber JE, Qi LS et al. 2015. Engineering complex synthetic transcriptional programs with CRISPR RNA scaffolds. *Cell* **160**: 339-350. doi:10.1016/j.cell.2014.11.052.

Zappulla DC, Cech TR. 2004. Yeast telomerase RNA: a flexible scaffold for protein subunits. *Proceedings of the National Academy of Sciences of the United States of America* **101**: 10024-10029. doi:10.1073/pnas.0403641101.

-. 2006. RNA as a flexible scaffold for proteins: yeast telomerase and beyond. *Cold Spring Harb Symp Quant Biol* **71**: 217-224. doi:10.1101/sqb.2006.71.011.

Zappulla DC, Goodrich K, Cech TR. 2005. A miniature yeast telomerase RNA functions in vivo and reconstitutes activity in vitro. *Nature structural & molecular biology* **12**: 1072-1077. doi:10.1038/nsmb1019.

Zappulla DC, Goodrich KJ, Arthur JR, Gurski LA, Denham EM, Stellwagen AE, Cech TR. 2011. Ku can contribute to telomere lengthening in yeast at multiple positions in the telomerase RNP. *Rna* **17**: 298-311. doi:10.1261/rna.2483611.

Zappulla DC, Maharaj AS, Connelly JJ, Jockusch RA, Sternglanz R. 2006. Rtt107/Esc4 binds silent chromatin and DNA repair proteins using different BRCT motifs. *BMC Mol Biol* **7**: 40. doi:10.1186/1471-2199-7-40.

Zhang F, Wen Y, Guo X. 2014. CRISPR/Cas9 for genome editing: progress, implications and challenges. *Hum Mol Genet* **23**: R40-46. doi:10.1093/hmg/ddu125.

Zhong FL, Batista LF, Freund A, Pech MF, Venteicher AS, Artandi SE. 2012. TPP1 OB-fold domain controls telomere maintenance by recruiting telomerase to chromosome ends. *Cell* **150**: 481-494. doi:10.1016/j.cell.2012.07.012.

Zuker M, Jacobson AB. 1998. Using reliability information to annotate RNA secondary structures. *Rna* **4**: 669-679.

Curriculum Vitae

Education

Johns Hopkins University – Baltimore, MD 2011-Present

- Doctoral program in Cell, Molecular, Developmental Biology, and Biophysics (CMDB)

University of Rochester – Rochester, NY 2007-2011

- B.S. Biochemistry, Minor: Music

Research Experience

Zappulla Laboratory (Johns Hopkins University) Jun 2012-Present

PhD student; research focuses:

- Studying telomere-length regulation by the Ku-mediated telomerase recruitment pathway in *Saccharomyces cerevisiae*
- Studying the function of the Sm_7 complex in stabilization and 3′-end formation of *S. cerevisiae* telomerase RNA
- Developing "CARRY two-hybrid", a CRISPR-based yeast two-hybrid assay for RNA-protein interactions

Phizicky Laboratory (University of Rochester School of Medicine) Jan-Dec 2010

Undergraduate student; research focus:

- Identification of molecular determinants for modification of tRNA by Trm7 in S. cerevisiae

Pochapsky Laboratory (Brandeis University) Jun-Aug 2009

Summer undergraduate researcher; research focus:

- Improving yields of cytochrome P450 3A4 for NMR structural studies

Publications

1. **Hass, E.P.** and Zappulla, D.C. (2015). The Ku subunit of telomerase binds Sir4 to recruit telomerase to lengthen telomeres in *S. cerevisiae*. *ELife*. 4:e07750.
2. Niederer, R.O., **Hass, E.P.**, and Zappulla, D.C. (2017). Long noncoding RNAs in the yeast *S. cerevisiae*. *Adv Exp Med Biol*. 1008: 119-132.

In press

3. Chen, H., Xue, J., Churikov, D., **Hass, E.P.**, Lemon, L.D., Luciano, P., Bertuch, A.A., Zappulla, D.C., Geli, V., Wu, J., and Lei, M. Structural insights into yeast telomerase recruitment to telomeres. (accepted for publication at *Cell*)

Under revision

4. **Hass, E.P.** and Zappulla, D.C. (2017). Repositioning the Sm-binding site in *S. cerevisiae* telomerase RNA reveals organizational flexibility and Sm-directed 3′-end formation. (prepublished at *bioRxiv*, under revision at *RNA*)

Prepublication manuscripts

5. **Hass, E.P.** and Zappulla, D.C. (2017). A CRISPR-based yeast two-hybrid system for investigating RNA-protein interactions. *bioRxiv*. 139600.

In preparation

6. **Hass, E.P.** and Zappulla, D.C. The "reach" model: a new model for how telomerase recruitment regulates telomere length in *S. cerevisiae*. (minireview)

Awards and Honors

- GRO Travel Grant for attending the 2016 RNA Society Meeting, Graduate Representative Organization, Johns Hopkins University, 2016
- Owen Scholars Fellowship, CMDB Program, Johns Hopkins University, 2011
- deKiewiet Summer Research Fellowship, Undergraduate Program in Biology and Medicine, University of Rochester, 2010

Scientific Meetings

- 2017 Cold Spring Harbor Laboratory meeting on Telomeres and Telomerase (oral presentation) – Cold Spring Harbor, NY
- 2017 NCI Symposium on RNA Biology – Bethesda, MD
- 2016 RNA Society Meeting (poster presentation) – Kyoto, Japan
- 2015 Cold Spring Harbor Laboratory meeting on Telomeres and Telomerase (poster presentation) – Cold Spring Harbor, NY
- 2015 NIH Symposium on RNA Biology (poster presentation) – Bethesda, MD
- 2014 Cold Spring Harbor Laboratory meeting on Epigenetics and Chromatin (poster presentation) – Cold Spring Harbor, NY

Local Presentations

- RNA Club, Johns Hopkins University (oral presentation) – Spring 2016

Courses/Workshops

- 2016 Practical Genomics Workshop, Center for Computational Genomics at Johns Hopkins

Peer-Reviewing Experience

- 2016 – *The EMBO Journal* (assisted advisor with review)
- 2016 – *PLoS Genetics* (assisted advisor with review)
- 2017 – *Scientific Reports* (assisted advisor with review)
- 2017 – *PLoS Genetics* (assisted advisor with review)

Teaching Experience

Seven semesters as Teaching Assistant at Johns Hopkins for the following courses:

- Fall 2016 – Molecular Biology (lecture)
- Spring 2016 – Cell Biology (lecture)
- Fall 2015 – Biochemistry (lecture)
- Spring 2015 – Advanced Molecular Biology (lecture)
- Fall 2014 – Eukaryotic Molecular Biology (lecture)

- Spring 2013 – Cell Biology (lab and lecture)
- Fall 2012 – Biochemistry (lab and lecture)

Students Mentored

- Undergraduate students (Johns Hopkins Univeristy)
    - Alex Rittenhouse (Fall 2016 and Spring 2017)
    - Yae Eun Yang (Spring 2016, Fall 2016, and Spring 2017)
    - Timothy Kistner (Fall 2014, Spring 2015, and Fall 2015)
    - Benjamin Ford (Fall 2013, Spring 2014, and Spring 2015)
    - Jorge Zhingre Sanchez (Summer 2014)
    - Tom Huaitao Zhang (Spring 2013)
- Graduate rotation students (CMDB Program, Johns Hopkins University)
    - Robert Levendosky (Spring 2014)